

DETERMINATION OF MINIMUM DOUBLER LENGTH FOR TAPERED  
SANDWICH STRUCTURES

A THESIS SUBMITTED TO  
THE GRADUATE SCHOOL OF NATURAL AND APPLIED SCIENCES  
OF  
MIDDLE EAST TECHNICAL UNIVERSITY

BY

ASLIHAN ALTUN

IN PARTIAL FULFILLMENT OF THE REQUIREMENTS  
FOR  
THE DEGREE OF MASTER OF SCIENCE  
IN  
AEROSPACE ENGINEERING

AUGUST 2019



Approval of the thesis:

**DETERMINATION OF MINIMUM DOUBLER LENGTH FOR TAPERED SANDWICH STRUCTURES**

submitted by **ASLIHAN ALTUN** in partial fulfillment of the requirements for the degree of **Master of Science in Aerospace Engineering Department, Middle East Technical University** by,

Prof. Dr. Halil Kalıpçılar  
Dean, Graduate School of **Natural and Applied Sciences**

\_\_\_\_\_

Prof. Dr. İsmail Hakkı Tuncer  
Head of Department, **Aerospace Engineering**

\_\_\_\_\_

Prof. Dr. YavuzYaman  
Supervisor, **Aerospace Engineering, METU**

\_\_\_\_\_

**Examining Committee Members:**

Assist. Prof. Dr. Tuncay Yalçınkaya  
Aerospace Engineering, METU

\_\_\_\_\_

Prof. Dr. YavuzYaman  
Aerospace Engineering, METU

\_\_\_\_\_

Assist. Prof. Dr. Mustafa Perçin  
Aerospace Engineering, METU

\_\_\_\_\_

Assist. Prof. Dr. Mustafa Kaya  
Aerospace Engineering, Ankara Yıldırım Beyazıt U.

\_\_\_\_\_

Assist. Prof. Dr. Munir Elfarra  
Aerospace Engineering, Ankara Yıldırım Beyazıt U.

\_\_\_\_\_

Date: 29.08.2019

**I hereby declare that all information in this document has been obtained and presented in accordance with academic rules and ethical conduct. I also declare that, as required by these rules and conduct, I have fully cited and referenced all material and results that are not original to this work.**

Name, Surname: Aslıhan Altun

Signature:

## **ABSTRACT**

### **DETERMINATION OF MINIMUM DOUBLER LENGTH FOR TAPERED SANDWICH STRUCTURES**

Altun, Aslihan  
Master of Science, Aerospace Engineering  
Supervisor: Prof. Dr. Yavuz Yaman

August 2019, 108 pages

Sandwich structures are widely used in aerospace industry due to their structural efficiency. In order to connect the sandwich structures to the adjacent parts, monolithic region is necessary. Because of the design requirements and strength necessities, this monolithic region must be strengthened. This reinforcement is provided by doublers [26]. In order to retain the weight advantage of sandwich structures, doubler span length must be minimum that keeps the core flatwise tension stress below the core allowable. In this thesis sandwich structures with different materials and different geometries under bending load are analyzed and the geometry of the doubler is designated such that minimum weight of the sandwich structure is obtained. ABAQUS Standard solver is used for the analyses. In the first part of the study after the determination of the mesh size, the effects of the friction coefficient between the parts in contact and the value of tightening torque of the bolts that connects the sandwich structure to adjacent parts are investigated. The effects of geometric and material nonlinearity are also examined in this part. Second part of the thesis covers the finite element model verification done by using tests and analytical approaches. At the final phase of the thesis, failure types of the sandwich structures are investigated and minimum failure load among these failure criteria is determined. The effect of doubler geometry on the failure mechanism is studied for several

sandwich structures with specified geometry and materials. Doubler geometry is specified by doing a parametric study. This parametric study is performed by running Python scripts in ABAQUS Standard.

Keywords: Sandwich Structures, Tapered Sandwich Structures, Honeycomb, Finite Element Analysis, Sandwich Panel Local Reinforcements

## ÖZ

### KONİK UÇLU SANDVIÇ YAPILARIN MİNİMUM DUBLİN PARÇASI UZUNLUĞUNUN BELİRLENMESİ

Altun, Aslıhan  
Yüksek Lisans, Havacılık ve Uzay Mühendisliği  
Tez Danışmanı: Prof. Dr. Yavuz Yaman

Ağustos 2019, 108 sayfa

Sandviç yapılar yapısal etkinliklerinden dolayı havacılık endüstrisinde yaygın olarak kullanılmaktadır. Sandviç yapılarda monolitik bölge, komşu parçalar ile bağlantının yapılabilmesi için gereklidir. Tasarım gereksinimleri ve mukavemet ihtiyaçları, monolitik bölgenin güçlendirilmesini gerekli hale getirmektedir. Bu güçlendirme dublin parçası ile sağlanmaktadır [26]. Sandviç yapıların ağırlık kazanımlarını sürdürebilmek için dublin parçalarının geometrilerinin balpeteği çekme gerilimini balpeteğinin müsaade edilen geriliminden düşük tutacak şekilde olması gerekmektedir. Bu tezde, bükülme yükü altındaki farklı malzeme ve geometrik özelliklere sahip sandviç yapıların analizleri yapılacak ve dublin parçasının geometrisi, asgari ağırlık sağlanacak şekilde elde edilecektir. Sonlu elemanlar analizleri ABAQUS sonlu elemanlar programında yapılmıştır. Çalışmanın ilk bölümünde, çözüm ağı boyutuna karar verilmesinin ardından, birbiri ile konuşan yüzeyler arasındaki sürtünme katsayıları ile sandviç yapıyı komşu parçalara bağlayan bağlayıcılar üzerindeki sıkma momentinin etkileri incelenmiştir. Tezin ikinci aşaması testler ve çözümsel yaklaşımlar kullanılarak sonlu elemanlar modelinin doğrulanmasını içermektedir. Tezin son bölümünde sandviç yapıların kırılma tipleri incelenmiş ve bu kırılma tipleri için asgari kırılma yükü belirlenmiştir. Dublin yapısının geometrik karakteristiğinin kırılma mekanizmasına olan etkisi, farklı

geometrik ve mekanik özelliklere sahip çeşitli sandviç yapıları üzerinde çalışılmıştır. Dublin yapısının geometrisi deęiştirgesel bir çalışma ile belirlenmiştir. Bu deęiştirgesel çalışmalar ABAQUS sonlu elemanlar programında Python komut dosyasının çalıştırılması ile yapılmıştır.

Anahtar Kelimeler: Sandviç yapılar, Konik Uçlu Sandviç Yapılar, Balpeteęi Malzeme, Sonlu Elemanlar Analizi, Bölgesel Sandviç Panel Güçlendirmeleri



To My Family

## **ACKNOWLEDGEMENTS**

I would like to express my special thanks of gratitude to Prof. Dr. Yavuz Yaman for his advice, criticism, and excellent guidance throughout the study.

My heartfelt thanks also to my dear parents and my little brother not just during finishing this thesis but also during my all studies. Without their constructive comments and warm encouragements, this study would not have been possible.

My deepest appreciation goes to my beloved husband, Akif. His support, patience, unconditional love and hand-made fruit soda have been the greatest contributors in the completion of the thesis.

Finally, grateful acknowledgment to all my friends for their understanding. Although I could not have enough time for them during studying this thesis, I felt their support all this time. I am very lucky to have such friends.

## TABLE OF CONTENTS

ABSTRACT .....	v
ÖZ.....	vii
ACKNOWLEDGEMENTS .....	x
TABLE OF CONTENTS .....	xi
LIST OF TABLES .....	xiv
LIST OF FIGURES .....	xv
LIST OF ABBREVIATIONS .....	xix
LIST OF SYMBOLS .....	xx
CHAPTERS	
1. INTRODUCTION .....	1
1.1. Scope of the Study.....	3
1.2. Summary of Thesis Plan.....	3
2. LITERATURE SURVEY AND THEORETICAL BACKGROUND .....	5
2.1. Sandwich Structures and Failure Types .....	6
2.1.1. Intracell Buckling .....	10
2.1.2. Facesheet Wrinkling .....	11
2.1.3. Facesheet Tension Failure .....	12
2.1.4. Core Shear Failure .....	12
2.1.5. Core Flatwise Tension Failure .....	14
2.1.6. Shear Crimping .....	15
2.2. Ramp-down Region of the Sandwich Structures.....	15
2.3. Beam Theory for Sandwich Structures .....	17

2.4. ABAQUS Finite Element Model .....	21
2.4.1. Sandwich Panel Modelling Techniques and Equivalent Modeling.....	21
2.4.2. Tie Constraint .....	25
3. METHODOLOGY .....	27
3.1. Finite Element Model Validation.....	27
3.1.1. Test 1: Finite Element Model Correlation with Three Point Bending Test of Sandwich Panels with Aluminum Skins and Nomex Honeycomb Core .....	27
3.1.1.1. Finite Element Model Description.....	28
3.1.1.2. Results.....	31
3.1.2. Test 2: Three Point Bending Test of Tapered Sandwich Panels with Aluminum Skins and Aluminum Honeycomb Core .....	33
3.1.2.1. Finite Element Description .....	33
3.1.2.2. Simplified Finite Element Model .....	42
4. FINITE ELEMENT MODEL .....	45
4.1. Material Properties .....	46
4.2. Geometric Description .....	46
4.3. Loads and Boundary Conditions.....	47
4.4. Python Script.....	47
4.5. Design of Experiment .....	48
4.6. Results.....	51
4.6.1. Simply Supported Boundary Condition .....	51
4.6.2. Fixed Boundary Condition .....	56
4.6.3. Minimum Doubler Length of Design of Experiment Sets for Fixed Boundary Conditions.....	64
5. DISCUSSION AND CONCLUSION .....	65

REFERENCES.....	69
APPENDICES	
A. RESULTS OF PARAMETRIC STUDY .....	73
B. SCRIPT FOR FIXED BOUNDARY CONDITION .....	85
C. SCRIPT FOR SIMPLY SUPPORTED BOUNDARY CONDITION.....	97

## LIST OF TABLES

### TABLES

Table 2.1. Coefficients for Facesheet Wrinkling Calculation [28].....	12
Table 2.2. Geometric Constants for Sandwich Beam Theory [32].....	21
Table 2.3. Orthotropic Material Definitions for Equivalent Modeling [4].....	24
Table 3.1. Equivalent Mechanical Properties of HRH 10-3/16-2 [16].....	29
Table 3.2. Geometrical and mechanical properties of the tested sandwich panels and of their components [14].....	29
Table 3.3. Literature Correction Mesh Sets.....	31
Table 3.4. Equivalent Mechanical Properties of HRH 10-3/16-2 [16].....	33
Table 3.5. Geometrical and mechanical properties of the tested sandwich panels and of their components [33].....	34
Table 3.6. Mesh Size Sets for First Mesh Sensitivity Study (Glass is Included) .....	36
Table 3.7. Element Type and Total Element Number of Mesh Sets (Glass is Included) .....	36
Table 3.8. Results of the First Mesh Sensitivity Study (Glass is Included) .....	36
Table 3.9. Mesh Size Sets for Second Mesh Sensitivity Study (Glass is Excluded). 37	
Table 3.10. Element Type and Total Element Number of Mesh Sets (Glass is Excluded).....	38
Table 3.11. Results of the Second Mesh Sensitivity Study (Glass is Excluded).....	38
Table 4.1. Equivalent Mechanical Properties of 1/8-5056-3.1 and 1/8-5052-4.5 [16] .....	46
Table 4.2. Mechanical Properties of Al2024-T3 [24].....	46
Table 4.3. Design of Experiment of Parametric Study.....	49
Table 4.4. Minimum Doubler Length of Sets for Fixed Boundary Condition .....	64

## LIST OF FIGURES

### FIGURES

Figure 2.1. Taper Configurations of Sandwich Constructions Tested under Tensile Load [27].....	5
Figure 2.2. Sandwich Construction [26].....	7
Figure 2.3. Core Forms [6].....	7
Figure 2.4. Corrugation Fabrication Process [5].....	8
Figure 2.5. Ribbon and Transverse Directions of Honeycomb Cores [11].....	8
Figure 2.6. Analogy between the Sandwich Structure and I-beam [17].....	9
Figure 2.7. Intracell Buckling [28].....	10
Figure 2.8. Facesheet Wrinkling [28].....	11
Figure 2.9. Facesheet Tension Failure [28].....	12
Figure 2.10. Core Shear Failure [28].....	13
Figure 2.11. Core Shear Strength Correction Factor [26].....	13
Figure 2.12. Flatwise Tension Test Setup [5].....	14
Figure 2.13. Shear Crimping [6].....	15
Figure 2.14. Ramp-down Region of the Sandwich Structure [19].....	16
Figure 2.15. Doublers in the Ramp-down Region [26].....	16
Figure 2.16. Core Flatwise Tension Failure [33].....	17
Figure 2.17. Sandwich Beam Definition [4].....	18
Figure 2.18. Actual and Approximate Stress Distribution [32].....	20
Figure 2.19. Full 2D Modeling [4].....	22
Figure 2.20. Mixed Modeling [4].....	22
Figure 2.21. Equivalent Model Simplifications [4].....	23
Figure 3.1. Test Set-up for TPBT [14].....	30
Figure 3.2. Load and Boundary Condition of Test-1.....	31
Figure 3.3. Load & Displacement Curve of Test Adapted from [14].....	32

Figure 3.4. Load & Displacement Curve –Test-1.....	32
Figure 3.5. Test Set-up for Tapered Sandwich Structure [33].....	34
Figure 3.6. Load and Boundary Condition of Test-2.....	35
Figure 3.7. Change in Core Flatwise Tension Stress According to Mesh Size (Glass is Included).....	37
Figure 3.8. Change in Core Flatwise Tension Stress According to Mesh Size (Glass is Excluded).....	38
Figure 3.9. Effect of Glass on Load vs Displacement Results .....	39
Figure 3.10. Effect of Friction Coefficient .....	40
Figure 3.11. Bolt Preload Simulation in FEM [18] .....	41
Figure 3.12. Effect of Bolt Preload.....	41
Figure 3.13. Fixed Boundary Condition .....	42
Figure 3.14. Simply Supported Boundary Condition .....	43
Figure 4.1. Python Script Scheme .....	47
Figure 4.2. Numbering Methodology of the Sets .....	49
Figure 4.3. Displacement Plot of Set-00010 With 60 mm Doubler Length for Simply Supported Boundary Condition .....	52
Figure 4.4. Core Normal Stress Plot of Set-00010 With 60 mm Doubler Length for Simply Supported Boundary Condition.....	52
Figure 4.5. Core Flatwise Tension Stress vs Doubler Length Graphs for Set-00000 and Set-00010 with Simply Supported Boundary Condition .....	53
Figure 4.6. Core Flatwise Tension Stress vs Doubler Length Graphs for Set-00011 and Set-00110 with Simply Supported Boundary Condition .....	53
Figure 4.7. Core Flatwise Tension Stress vs Doubler Length Graphs for Set-01010 and Set-10010 with Simply Supported Boundary Condition .....	53
Figure 4.8. Effect of Doubler Thickness for Simply Supported Boundary Conditions .....	54
Figure 4.9. Effect of Core Material for Simply Supported Boundary Conditions ....	54
Figure 4.10. Effect of Facing Thickness for Simply Supported Boundary Conditions .....	55



Figure 4.11. Effect of Ramp Angle for Simply Supported Boundary Conditions.....	55
Figure 4.12. Effect of Core Thickness for Simply Supported Boundary Conditions	56
Figure 4.13. Displacement Plot of Set-00010 With 60 mm Doubler Length for Simply Supported Boundary Condition.....	57
Figure 4.14. Core Normal Stress Plot of Set-00010 With 60 mm Doubler Length for Simply Supported Boundary Condition.....	57
Figure 4.15. Core Flatwise Tension Stress vs Doubler Length Graphs for Set-00000 and Set-00001 with Fixed Boundary Condition .....	58
Figure 4.16. Core Flatwise Tension Stress vs Doubler Length Graphs for Set-00010 and Set-00100 with Fixed Boundary Condition .....	58
Figure 4.17. Core Flatwise Tension Stress vs Doubler Length Graphs for Set-01000 and Set-10000 with Fixed Boundary Condition .....	58
Figure 4.18. Effect of Ramp Angle for Fixed Boundary Conditions.....	59
Figure 4.19. Effect of Core Thickness for Fixed Boundary Conditions .....	59
Figure 4.20. Effect of Facing Thickness for Fixed Boundary Conditions.....	60
Figure 4.21. Effect of Doubler Thickness for Fixed Boundary Conditions.....	60
Figure 4.22. Effect of Core Material for Fixed Boundary Conditions.....	61
Figure 4.23. Core Flatwise Tension Stress Change According to Sandwich Structure's Zone.....	62
Figure 4.24. Comparison of Fixed and Simply Supported Boundary Conditions .....	63
Figure A.1. Core Flatwise Stress vs Doubler Length of Set-00000.....	73
Figure A.2. Core Flatwise Stress vs Doubler Length of Set-00001.....	73
Figure A.3. Core Flatwise Stress vs Doubler Length of Set-00010.....	74
Figure A.4. Core Flatwise Stress vs Doubler Length of Set-00011.....	74
Figure A.5. Core Flatwise Stress vs Doubler Length of Set-00100.....	74
Figure A.6. Core Flatwise Stress vs Doubler Length of Set-00101.....	75
Figure A.7. Core Flatwise Stress vs Doubler Length of Set-00110.....	75
Figure A.8. Core Flatwise Stress vs Doubler Length of Set-00111.....	75
Figure A.9. Core Flatwise Stress vs Doubler Length of Set-01000.....	76
Figure A.10. Core Flatwise Stress vs Doubler Length of Set-01001.....	76

Figure A.11. Core Flatwise Stress vs Doubler Length of Set-01010 .....	76
Figure A.12. Core Flatwise Stress vs Doubler Length of Set-01011 .....	77
Figure A.13. Core Flatwise Stress vs Doubler Length of Set-01100 .....	77
Figure A.14. Core Flatwise Stress vs Doubler Length of Set-01101 .....	77
Figure A.15. Core Flatwise Stress vs Doubler Length of Set-01110 .....	78
Figure A.16. Core Flatwise Stress vs Doubler Length of Set-01111 .....	78
Figure A.17. Core Flatwise Stress vs Doubler Length of Set-10000 .....	78
Figure A.18. Core Flatwise Stress vs Doubler Length of Set-10001 .....	79
Figure A.19. Core Flatwise Stress vs Doubler Length of Set-10010 .....	79
Figure A.20. Core Flatwise Stress vs Doubler Length of Set-10011 .....	79
Figure A.21. Core Flatwise Stress vs Doubler Length of Set-10100 .....	80
Figure A.22. Core Flatwise Stress vs Doubler Length of Set-10101 .....	80
Figure A.23. Core Flatwise Stress vs Doubler Length of Set-10110 .....	80
Figure A.24. Core Flatwise Stress vs Doubler Length of Set-10111 .....	81
Figure A.25. Core Flatwise Stress vs Doubler Length of Set-11000 .....	81
Figure A.26. Core Flatwise Stress vs Doubler Length of Set-11001 .....	81
Figure A.27. Core Flatwise Stress vs Doubler Length of Set-11010 .....	82
Figure A.28. Core Flatwise Stress vs Doubler Length of Set-11011 .....	82
Figure A.29. Core Flatwise Stress vs Doubler Length of Set-11100 .....	82
Figure A.30. Core Flatwise Stress vs Doubler Length of Set-11101 .....	83
Figure A.31. Core Flatwise Stress vs Doubler Length of Set-11110 .....	83
Figure A.32. Core Flatwise Stress vs Doubler Length of Set-11111 .....	83

## LIST OF ABBREVIATIONS

FE	Finite Element
FEM	Finite Element Model
R	Core Ribbon Direction
W	Core Transverse Direction
UX, U1	Translational Displacement in X-Direction
UY, U2	Translational Displacement in Y-Direction
UZ, U3	Translational Displacement in Z-Direction

## LIST OF SYMBOLS

$A$	Deformed Area
$A_0$	Initial Area
$b$	Beam Width
$D$	Flexural Rigidity of Sandwich Construction
$E_c$	Core Compressive Modulus of Elasticity
$E_f$	Modulus of Elasticity of Facing and Doubler
$G_c$	Minimum of Core Shear Modulus in Ribbon and Transverse Directions
$G_{13}$	Core Shear Modulus in Ribbon Direction
$G_{23}$	Core Shear Modulus in Transverse Direction
$h$	Distance between Facing Skin Centers
$I$	Second Moment of Area of Sandwich Beam
$I_f$	Second Moment of Area of the Skins with respect to Their own Centroidal
$L$	Span of the Sandwich Beam
$L_d$	Doubler Span
$l$	Deformed Length
$l_0$	Initial Length
$M$	Maximum Bending Moment
$P$	Applied Load
$s$	Cell Size
$t_c$	Core Thickness
$t_d$	Doubler Thickness
$t_f$	Facing Thickness
$t'$	Foil Thickness
$Q$	Applied Load per Unit Width
$\alpha$	Core Ramp Angle
$\varepsilon_{nom}$	Nominal Strain
$\varepsilon_{tr}$	True Strain
$\sigma_{ct}$	Core Flatwise Tension Stress
$\sigma_{ft}$	Facing Tension Stress
$\sigma_{nom}$	Nominal Stress
$\sigma_{scr}$	Critical Shear Crimping Stress
$\sigma_{tr}$	True Stress

$\sigma_{tu}$	Tensile Ultimate Allowable Stress
$\sigma_{wr}$	Critical Wrinkling Stress
$\sigma_{33}$	Core Flatwise Tension Allowable Stress
$\tau_{c,ribbon}$	Core Shear Stress in Ribbon Direction
$\tau_{c,transverse}$	Core Shear Stress in Transverse Direction
$\tau_{13}$	Core Shear Allowable in Ribbon Direction
$\tau_{23}$	Core Shear Allowable in Transverse Direction
$\nu$	Poisson's Ratio of Facing and Doubler



## CHAPTER 1

### INTRODUCTION

Sandwich structures are widely used in aerospace field due to their good flexural stiffness, strength, smooth skins, excellent fatigue resistance and low weight [5]. By increasing the weight in 6%, 37 times more rigid and 9.25 times stronger structures can be designed by using the thickness of the honeycomb in sandwich constructions compared to the solid metal sheet [7]. Together with its benefits, that sandwich constructions cannot be manufactured in every shape is the one of the disadvantages of these constructions. A sandwich structure is mainly composed of facings, core and core-to-face bonding materials. The function of sandwich construction is very similar to an “I-beam” structure. Facings of the sandwich structure carry axial loads while core carries the shear loads and increases the stiffness of the structure by holding the facing skins apart [16]. In this manner, facings of the sandwich panel correspond to the flanges while core corresponds to the web of the I-beam in terms of their functions under loading [26].

In general, materials of the facings can be selected as metal sheet or reinforced plastic laminate. Also, metallic or non-metallic materials can be used for core. Non-metallic cores have, in general, low strength compared to the metallic cores. However due to their high thermal insulation capabilities non-metallic cores are also very useful in certain applications. Other than the material, cores are grouped in terms of their forms. The most widely used core type is honeycomb which is divided into two groups according to core cell shape: square and hexagonal cells. The corrugated or truss core is another type which is also used in aircraft design [6].

It is a necessity to connect sandwich structures to the adjacent parts with reduced grip length for the fasteners and increased clamp-up in the aircraft structure [19]. To do

so, tapered transition type of sandwich ending is widely used. Tapered transition region is required to fasten sandwich structures to other parts because sandwich constructions are difficult to fasten support structures due to their low transverse compression strength [34]. This tapered area must be designed to:

- resist the shear loads caused by static, dynamic or sonic loads
- meet the tension allowable strength for the fastener pull-through failure that connects the sandwich structure to adjacent parts
- prevent the knife-edge condition in case of the usage of countersunk fasteners to joint the sandwich structure to adjacent parts

To meet these requirements without unnecessary weight increase, doublers are used in the ramp-down region of the sandwich structures [26].

Failure mechanism and prediction of the failure load of the sandwich structure is more complex compared to the isotropic materials. Other than the material failures such as facesheet tension failure, core tension, shear and compression failures; local instability failures are also faced with in the sandwich structures which are facesheet wrinkling, intracell buckling and shear crimping [34]. These failure mechanisms are formulated for the constant thickness region in the literature and the failure load of the sandwich structure can be calculated by only considering the constant thickness region [19],[26]. However, experiences have shown that, the ramp-down region is the weakest part of the sandwich structure [19]. Improper geometrical design of the ramp-down region causes the local stress concentrations [34]. Therefore, to prevent an early-failure under a load less than the failure load calculated for the constant thickness region, failure load for the ramp-down region must also be investigated.

Three-point bending tests of sandwich structures show that the design of the doublers has a remarkable effect on the failure load of the sandwich structures [33].



## **1.1. Scope of the Study**

The experiences show that the sandwich structures with shorter doubler length face with the core net tension failure around the tapering region below the expected failure load.

The objective of this thesis is to find the effect of the doubler geometry on the core flatwise tension stress for specified sandwich panel designs under bending. The main point is that the minimum doubler length that prevents the core net tension failure around the tapering region must be selected to keep the weight as low as possible.

In the first part of the study the finite element model is verified by two different test results.

Within the frame of the modelling methodology used in the verified model, a parametric finite element model is prepared in ABAQUS by using Python.

Sandwich panel allowable load for the constant-thickness region is specified as the applied load.

For each run, while keeping all the geometrical and material parameters constant, doubler span length is slightly increased until the core net tension stress becomes stable.

The calculations conducted in this study has no safety factor.

## **1.2. Summary of Thesis Plan**

Chapter 1 of the thesis includes the introduction part. In the introduction, a general information about sandwich structures is presented and problem is defined. In Chapter 2, theoretical background and literature survey are given. In this part, analysis techniques of sandwich structures, beam theory and sandwich panel finite element modeling techniques are described. Finite element model verification and simplification are done in Chapter 3. Verification is done by using two different test results. One of these test results is obtained from a study in literature and the other test

is conducted in Turkish Aerospace. Mesh sensitivity study is also conducted in this chapter. According to the results of the studies presented in this chapter, a new modeling strategy is created for the rest of the thesis. In Chapter 4, analysis sets used in this study are defined. To create and analyze these sets automatically, a Python code is developed. This Python code and the results of these analyses are also explained and interpreted in this chapter. Finally, Chapter 7 is devoted to discussion, conclusion remarks and possible future work.

## CHAPTER 2

### LITERATURE SURVEY AND THEORETICAL BACKGROUND

In [2], the ramp-down region is specified as the most critical region of the sandwich structures. According to [22], tapered area causes significant stress distribution changes. In this tapered region, core shear stress, axial forces in facesheets, and local bending shows a significant increase. Kassapoglou [19] examines the stress distribution of ramp-down region under bending moments or transverse shear loads. In this study, facesheets are selected as three fabric plies. The aim of this study is to predict the applied load at which core will fail. According to [19], core thickness and ramp angle have a significant effect on this failure load.

Ramp-down failure analysis under tensile loading is discussed in [27]. In this study, sandwich specimens are tested under tensile loading. These test results show that core ramp reinforcing manufacturing scenarios and smaller ramp radius reduce the ramp failure load. Taper configurations tested in the scope of this paper are presented in Figure 2.1.

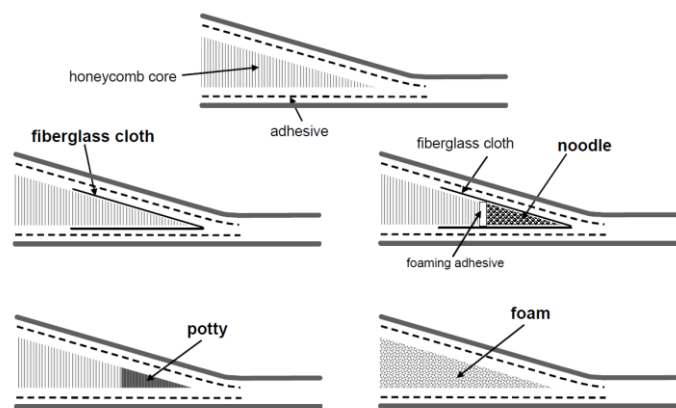


Figure 2.1. Taper Configurations of Sandwich Constructions Tested under Tensile Load [27]

Other than the ramp down failure analysis, constant thickness failure types of sandwich constructions are investigated in [27] and [17] in detail. These failure modes are expressed in the following sub-titles of this chapter.

In [27] and [6] core flatwise tension failure mode and honeycomb flatwise tensile strength property is not published. In [5], flatwise tensile strengths of some of the core types obtained by conduction flatwise tension test are presented.

In [14], three point bending test results and numerical investigation of sandwich construction with aluminum skins and Nomex honeycomb is studied. By this study, a finite element model with high accuracy and capability of local behavior of cell crushing is developed.

Finite element modeling of sandwich constructions and mechanical property definitions of core are examined in detail by Ilke [4]. Details of this study are explicated in the next sub-titles of this chapter.

In this study, minimum doubler length for specified sandwich construction geometries are determined to prevent any unnecessary weight increase.

## **2.1. Sandwich Structures and Failure Types**

Sandwich structures are mainly composed of two facings and a core between these facings. The bonding between the facings and the core is provided by adhesives. A symbolic presentation of sandwich structures is illustrated in Figure 2.2.

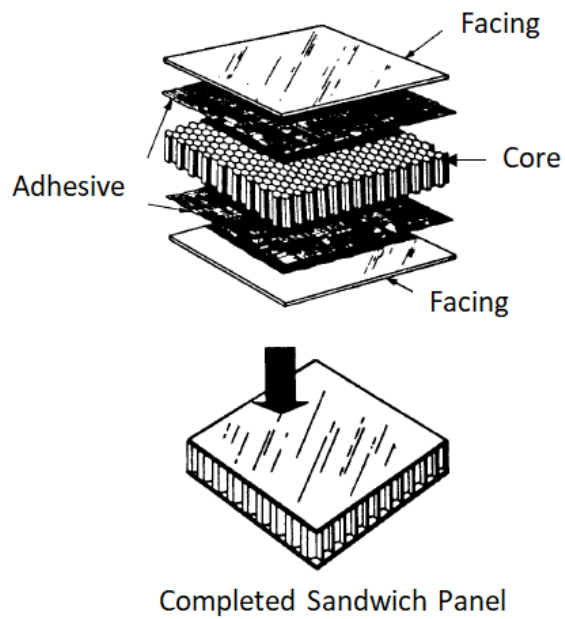


Figure 2.2. Sandwich Construction [26]

Facing materials can be selected as metal sheet or reinforced plastic laminate and core materials may be metallic or non-metallic. Cores are also classified according to their forms. The most commonly used core types are: Honeycomb Core (square and hexagonal cells) and Corrugated Core [8]. Geometry of these two types of core is illustrated in the Figure 2.3.

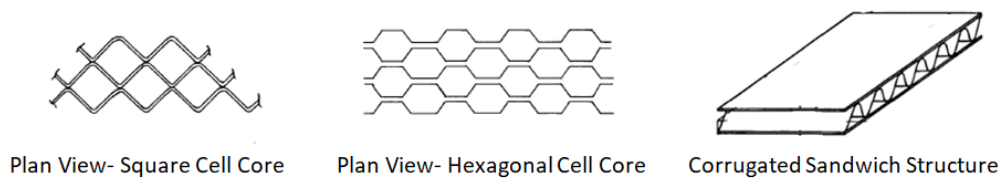


Figure 2.3. Core Forms [6]

The original fabrication method for the honeycombs is the corrugation method. In this method after the sheets are corrugated, they are bonded together with adhesives and cured in an oven. This fabrication procedure is illustrated in Figure 2.4 [5].

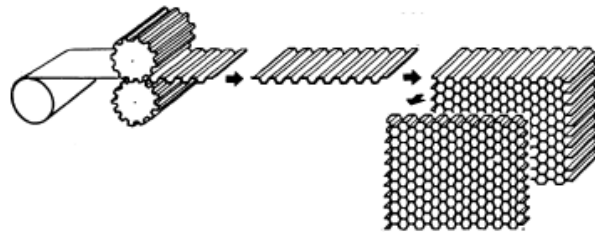


Figure 2.4. Corrugation Fabrication Process [5]

Thickness of the cell walls, in the direction in which corrugated face sheets are bonded, is twice of the thickness of other cell walls. This mentioned direction is called as the “Ribbon Direction” and the strength of the core is higher in this direction. Ribbon and transverse directions are illustrated in Figure 2.5.

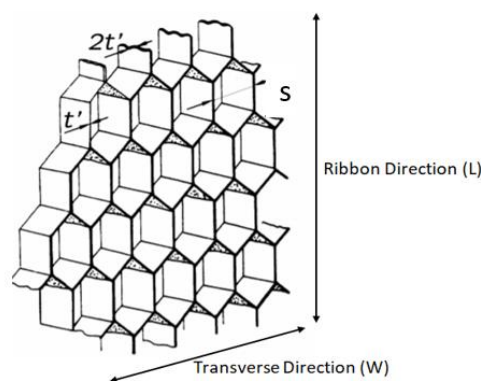


Figure 2.5. Ribbon and Transverse Directions of Honeycomb Cores [11]

The working principle of sandwich structures is very similar to the working principle of an “I-beam”. Facings and core of sandwich structures correspond to the flanges and

web of the I beam, respectively. Both flange of an I beam and facing of a sandwich construction carry the bending stresses while both core and the web carry the shear loads and increase the stiffness of the structure by holding facings apart [17].

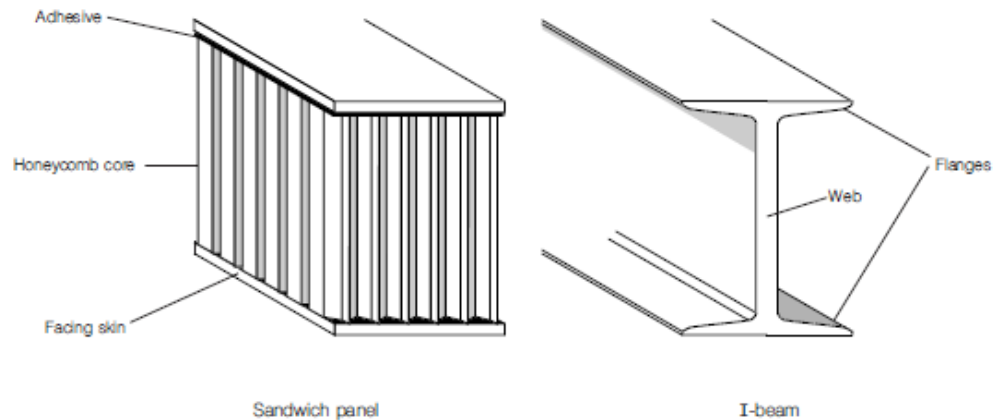


Figure 2.6. Analogy between the Sandwich Structure and I-beam [17]

Design requirements of the sandwich structures are as listed [26]:

- Thickness of the facings shall be thick enough to withstand the tensile and compressive loads
- Thickness of the core shall be thick enough to prevent global buckling, face sheet wrinkling, shear crimping and intracell buckling failure modes under edge wise loading
- Core strength must be sufficient to resist the shear and compressive loads
- Honeycomb structure must have sufficient flexural and shear rigidity to prevent excessive deflections
- The adhesive used to bond facings and the core shall be strong enough to resist flatwise tensile and shear loads
- Since core and facings are in contact, their materials shall be selected by considering thermal expansion coefficients

The allowable loads of a sandwich panel designed in the frame of these requirements can be calculated for the specified failure modes in the literature. These failure modes can be grouped as skin and core failures [28].

Skin failures are:

- intracell buckling
- face sheet wrinkling
- face sheet tension failure

Core failures are:

- core flatwise tension failure
- core shear failure

In addition to core and skin failures, shear crimping which is a global instability failure is also observed in the sandwich structures.

For the constant core thickness region of the sandwich structures, theory of the calculation of critical stress levels for these failure modes are described under the following sub-chapters.

### **2.1.1. Intracell Buckling**

This type of the skin failure is defined as the buckling of the facings where it is unsupported by the walls of the honeycomb [28].

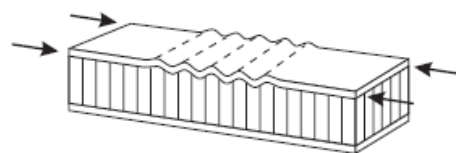


*Figure 2.7. Intracell Buckling [28]*



The stress at which intracell buckling occurs in the skins are calculated by using the following relation [28]:

$$\sigma_{ib} = \frac{2E_f}{1 - \nu_f^2} \left(\frac{t}{s}\right)^2 \quad (2.1)$$

### 2.1.2. Facesheet Wrinkling

In this failure mode, facings buckle with a wavelength greater than the cell size of the honeycomb. Depending on the core compression stiffness and the adhesive strength, buckling may occur either towards the core or outwards [28].



Figure 2.8. Facesheet Wrinkling [28]

Facesheet wrinkling stress is calculated for two different relations according to core relative thickness. Firstly, whether the core is thick or thin must be checked, then wrinkling stress must be calculated.

Core is said to be thick if [28]:

$$t_c \geq 1.82t_f \sqrt[3]{\frac{E_f E_c}{G_c^2}} \quad (2.2)$$

For thick cores [28]:

$$\sigma_{wr} = C_1 (E_f E_c G_c)^{\frac{1}{3}} + C_2 G_c \frac{t_c}{t_f} \quad (2.3)$$

For thin cores [28]:

$$\sigma_{wr} = C_3 \sqrt{\frac{t_f}{t_c} E_c E_f} + C_4 G_c \frac{t_c}{t_f} \quad (2.4)$$

The coefficients can be conservatively selected as:

Table 2.1. *Coefficients for Facesheet Wrinkling Calculation [28]*

$C_1$	$C_2$	$C_3$	$C_4$
0.247	0.078	0.330	0.00

### 2.1.3. Facesheet Tension Failure

This type of failure occurs when the axial stress on the skin reaches the in plane tension allowable of the facing material [28]

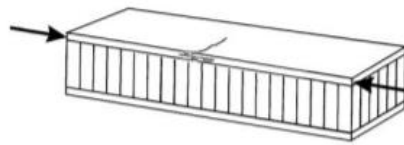


Figure 2.9. Facesheet Tension Failure [28]

Failure stress is simply defined as [28]:

$$\sigma_{ft} = \sigma_{tu} \quad (2.5)$$

### 2.1.4. Core Shear Failure

Core shear failure occurs when the transverse shear stress on the core reaches the core out-of-plane shear allowable values [28].

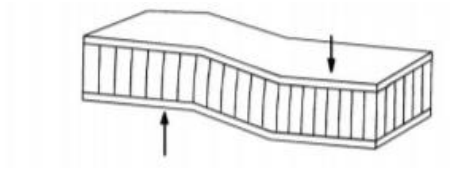


Figure 2.10. Core Shear Failure [28]

This failure mode shall be checked for both ribbon and transverse directions. Critical stress values are calculated as [28]:

$$\tau_{c,ribbon} = \tau_{13} \quad (2.6)$$

$$\tau_{c,transverse} = \tau_{23} \quad (2.7)$$

It is an important point that, as the core thickness increases, shear strength of the core must be reduced by a correction factor given in Figure 2.11. The reason is that, core shear allowable values are obtained from the tests practiced with the metallic honeycombs with 15.9 mm thickness and nonmetallic cores with 12.7 mm thickness.

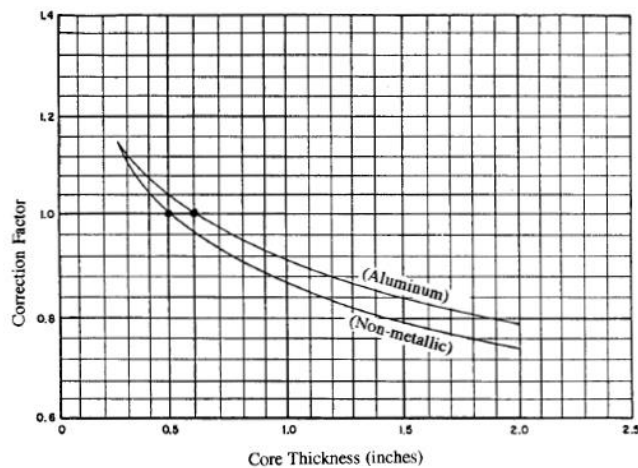
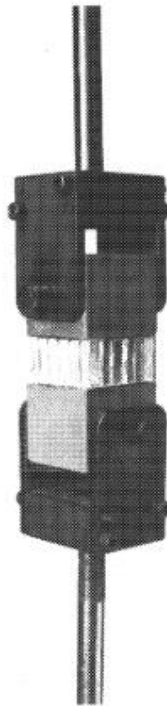


Figure 2.11. Core Shear Strength Correction Factor [26]

### 2.1.5. Core Flatwise Tension Failure

Like core shear failure, core flatwise tension failure occurs when the flatwise tension stress on the core reaches the core flatwise tension allowable value.

Flatwise tension allowable of honeycombs are not often published. This property of honeycombs is obtained by attaching the core between two blocks and then pulling the one of the blocks. In [5] honeycomb flatwise tension allowable values which are tested in room temperature is given.



*Figure 2.12.* Flatwise Tension Test Setup [5]

The critical stress at which core flatwise tension failure occurs can be calculated by using the relation [5]:

$$\sigma_{ct} = \sigma_{33} \quad (2.8)$$

### 2.1.6. Shear Crimping

In this type of failure due to low core shear modulus wavelength of the buckle becomes very small and core suddenly fails in shear at the crimping [6].

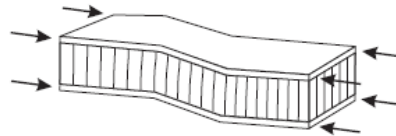


Figure 2.13. Shear Crimping [6]

The relation for the stress at which shear crimping occurs is calculated by the following equation [6]:

$$\sigma_{scr} = \frac{h^2 G_c}{2t_f t_c} \quad (2.9)$$

### 2.2. Ramp-down Region of the Sandwich Structures

To enable the connection of the sandwich structures to adjacent parts, tapered type sandwich ending is a common practice. By using this application, sandwich structure connection to another part is provided with reduced grip length for the fasteners and increased clamp-up in the aircraft structure [19].

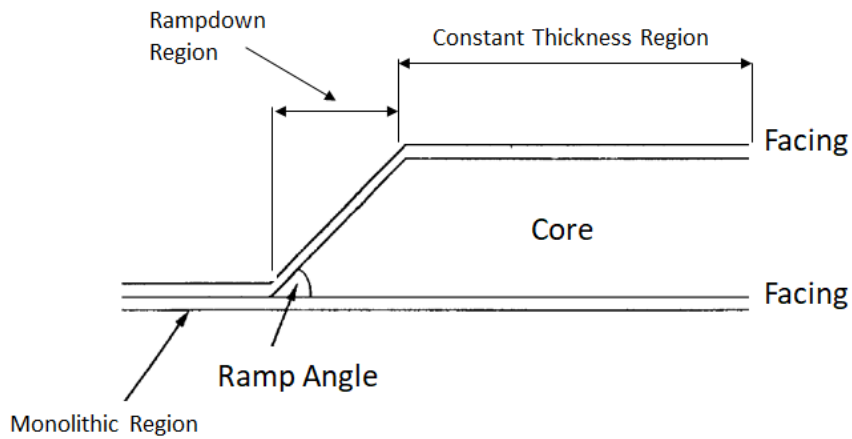


Figure 2.14. Ramp-down Region of the Sandwich Structure [19]

Ramp-down region is the weakest part of the sandwich structure and failure loads around this zone cannot be calculated by using the relations given for the constant-thickness core region. Geometrical design of this part of the sandwich construction is critical because improper geometry may cause the local stress concentrations and early unexpected failure [34].

In order to meet the ramp-down and monolithic region design requirements and to prevent unnecessary weight increase, use of doubler in this zone is a very useful practice [26].

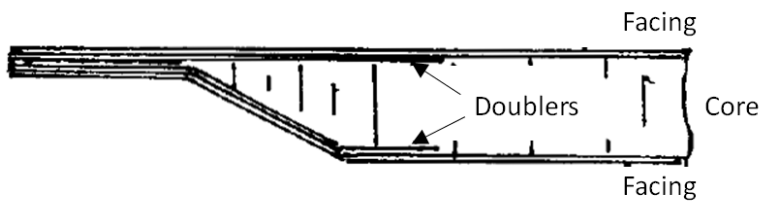
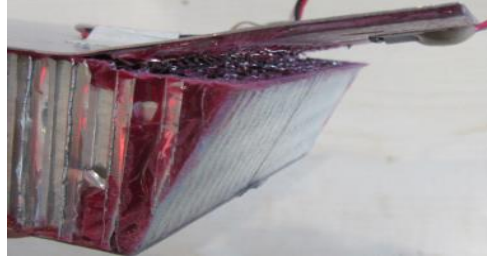


Figure 2.15. Doublers in the Ramp-down Region [26]

Following figure is an example of unexpected failure in the ramp-down region of the structure. In this example, specimen is under three point bending and core flatwise tension stress is higher than the core allowable. [33]



*Figure 2.16. Core Flatwise Tension Failure [33]*

### **2.3. Beam Theory for Sandwich Structures**

Elastic calculation of a sandwich structure under three-point bending can be done by assuming the sandwich structure as a beam with isotropic materials and perfectly bonded core and facings. Another approximation during these calculations is the ordinary theory of bending. Ordinary theory of bending assumes that cross-sections, which are plane and perpendicular to the longitudinal axis of unloaded beam, remain in this state when the bending takes place [28], [4].

The geometry, load and the boundary conditions of the sandwich beam are given in Figure 2.17. A simply supported sandwich beam with span length  $L$  and width  $b$  is loaded in three point bending with a central load  $Q$  per unit width.

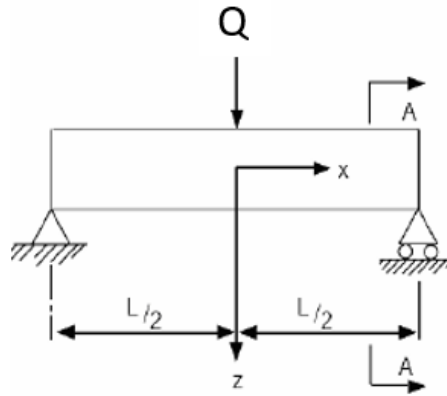


Figure 2.17. Sandwich Beam Definition [4]

In order to analyze a sandwich structure in the aspect of the behavior of the beam, following relation must be satisfied. If this relation is not satisfied or the panel is supported by more than two edges, it must be analyzed as a panel [29].

$$\frac{b}{L} \leq 0.3 \quad (2.10)$$

The flexural rigidity of the sandwich beam is given by the following equation [29].

$$D = \frac{E_f b t_f^3}{6} + \frac{E_f b t_f h^2}{2} + \frac{E_c b t_c^3}{12} \quad (2.11)$$

Axial stresses occur at the facings under maximum bending moment,  $M$ , is given by the following relation [29].

$$\sigma_f = \frac{M E_f h}{2D} = \frac{Q L}{4 h t_f} \quad (2.12)$$



This formulation of the facing axial stress under the bending moment,  $M$ , neglects the effect of shear deflection of the core. This is a significant issue if the core density is low.

For the sandwich beams with low density cores, facing stresses must be calculated by using the relation given below [29].

$$\sigma_f = \frac{QbL}{4} \left( \frac{t_c + 2t_f}{2I} + \frac{QL}{4} \frac{t_f}{2I_f} \frac{1}{\theta} \right) \quad (2.13)$$

Where;

$$\theta = \frac{L}{t_c} \left[ \frac{G_{13} t_c}{2E_f t_f} \left( 1 + \frac{3h^2}{t_f^2} \right) \right]^{\frac{1}{2}} \quad (2.14)$$

$$I = \frac{bt_f^3}{6} + \frac{bt_f h^2}{2} \quad (2.15)$$

$$I_f = \frac{bt_f^3}{6} \quad (2.16)$$

For different boundary conditions and loading types, other than the simply supported beam loaded in three point bending with a central load  $P$ , facing and core stresses can be calculated by using the following relations [32]. Stress distribution approximation used in these relations are illustrated in Figure 2.18.

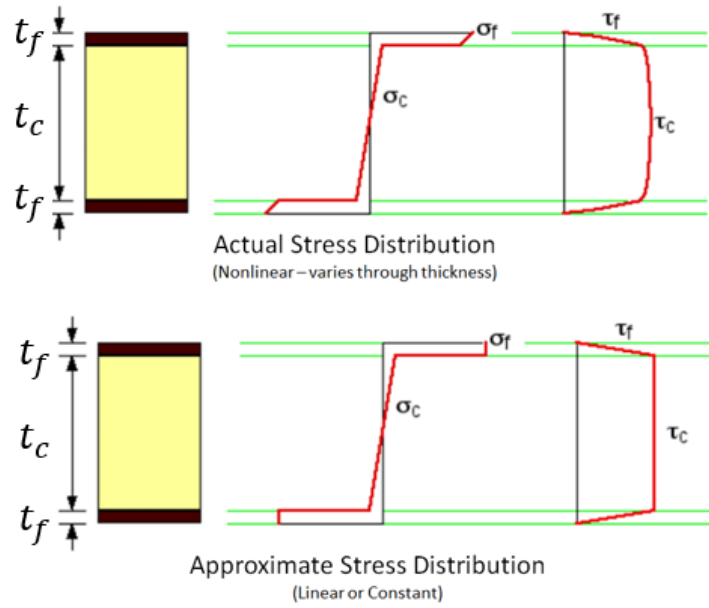


Figure 2.18. Actual and Approximate Stress Distribution [32]

$$\sigma_{ft} = \frac{PL}{B_3 b t_f t_c} \quad (2.17)$$

$$\tau_{c,ribbon} = \frac{P}{B_4 b t_c} \quad (2.18)$$

$$\tau_{c,transverse} = \frac{P}{B_4 L t_c} \quad (2.19)$$

In these equations,  $B_3$  and  $B_4$  are geometrical constants depend on the mode of loading. Table 2.2 illustrates these constants for different loadings and boundary conditions [32].

Table 2.2. Geometric Constants for Sandwich Beam Theory [32]

Mode of Loading	$B_3$	$B_4$
Cantilever, end load (P)	1	1
Cantilever, uniformly distributed load (P/L)	2	1
Three point bending, central load (P)	4	2
Three point bending, uniformly distributed load (P/L)	8	2
Ends built in, central load (P)	8	2
Ends built in, uniformly distributed load (P/L)	12	2

## 2.4. ABAQUS Finite Element Model

### 2.4.1. Sandwich Panel Modelling Techniques and Equivalent Modeling

Finite element model of a sandwich structure can be created in several ways. These methods are listed below [4]:

#### 1- Full 2D modeling with a Single Shell Geometry

In this technique, sandwich panel is defined by a single shell and property of the sandwich structure is assigned to this shell geometry via “Composite Lay-up” tool in ABAQUS.

#### 2- Full 2D modeling

In this modelling technique, both faces and core are modeled as shell geometries. This technique differs from the first one in that core structure is modeled in detail with its hexagonal cell type. Properties of core and facings are created and assigned separately.

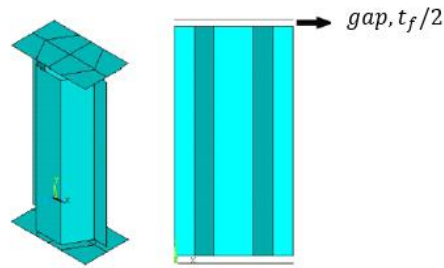


Figure 2.19. Full 2D Modeling [4]

### 3- Mixed Modeling

Mixed modeling is a mixture of 3D and shell modeling. In this technique, facings are modeled in 3D and the core is modeled as shell with a hexagonal geometry. Like the second method, properties of core and facings are created and assigned separately.

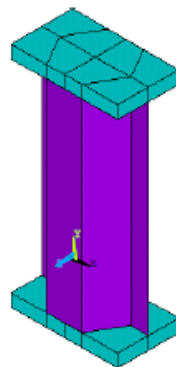
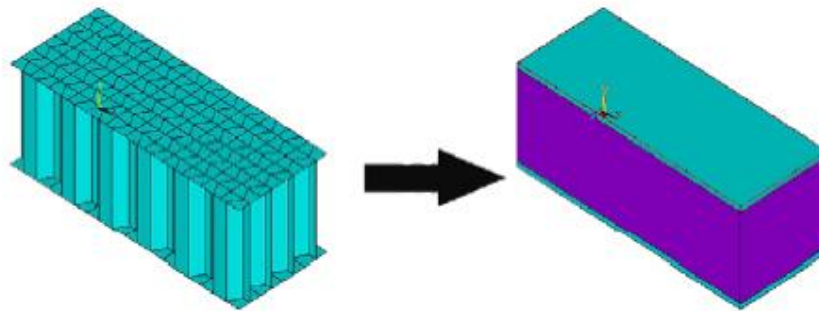


Figure 2.20. Mixed Modeling [4]

According to [10], sandwich construction is modeled by using the third modelling technique. In this model, the connection between the facings and the core is provided by the “tie constraints” without allowing any adjustments. Node-based slave surfaces of the tie constraint are defined as the core cell edges and master surfaces are specified as the facings’ inner surfaces.

In [4], in addition to these three methods, equivalent models are created, and their accuracies are investigated. During these studies, results of the second and the third modeling techniques are accepted as reference. In equivalent modeling, core is not intended to be modeled in detail. By modeling the core of the sandwich structure as an orthotropic bulk material, modelling is tried to be made simpler and faster.



*Figure 2.21.* Equivalent Model Simplifications [4]

Orthotropic material properties for the equivalent core is defined by using ten different methods. The difference between these models are the formulations of the orthotropic material constants.

The methodology used to calculate these constants are summarized in Table 2.3.

Table 2.3. Orthotropic Material Definitions for Equivalent Modeling [4]

<i>MODELS</i>					
	1	2	3	4	5
E1	Masters[23]	Nast[25]	-	-	-
E3					
E2	Masters[23]	Nast[25]	-	-	-
v13	-	Nast[25]	-	-	Ashby[35]
v23	-	Nast[25]	-	-	Ashby[35]
v12	Master[23]	Nast[25]	-	-	-
G13	-	Nast[25]	Quin Liu [21]	Shi[30]	Ashby[35]
G23	-	Nast[25]	Quin Liu [21]	Shi[30]	Ashby[35]
G12	Master[23]	Nast[25]	-	-	-
	6	7	8	9	10
E1	Grediac[15]	Grediac[15]	-	Nast[25]	Nast[25]
E3	Universally Agreed On	HEXCEL[17]	HEXCEL[17]	Universally Agreed On	-
E2	Grediac[15]	Grediac[15]	-	Master[23]	Nast[25]
v13	-	-	-	Nast[25]	Ashby[35]
v23	-	-	-	Nast[25]	Ashby[35]
v12	Grediac[15]	Grediac[15]	-	Nast[25]	-
G13	Grediac[15]	Grediac[15]	HEXCEL[17]	HEXCEL[17]	Nast[25]
G23	Grediac[15]	Grediac[15]	HEXCEL[17]	HEXCEL[17]	Nast[25]
G12	-	-	-	Masters[23]	Nast[25]

In the finite element analysis, it is not possible to leave blank elastic and shear moduli values. Therefore, if these values are missing for any of these models, these parameters are taken as a very small number such as 0.1 and 0.01.

These modeling techniques are used for four different core materials and nine different loadings in [4] and these results are compared to the results of the reference model. Among these nine different load cases, bending conditions are significant for this thesis scope. Therefore, for only these load cases, results are investigated, and it is

seen that the maximum difference between the Model-8 and the reference model is 15.86%.

Since 15.86% is a reasonable error for this study, core of the sandwich construction model suggested in the [10] is modeled as orthotropic bulk material with HEXCEL properties. Slave surfaces of the tie constraint are defined as the core surfaces instead of edges of the core cells.

#### **2.4.2. Tie Constraint**

Tie constraint are used to connect two different surfaces such that no relative motion is allowed between them. Tie constraints can be used even though the meshes of the connected surfaces are dissimilar. Also, between the edges of a surface or between the faces of solids or shells tie constraints can also be defined.

In the tie constraint definition, master and slave surfaces are expected to be specified.

In order to carry all the nodes of the slave surfaces on the master surface in the beginning of the analysis, there is an “Adjust slave surface initial position” option available in the tie constraint dialog box [13].





## CHAPTER 3

### METHODOLOGY

In this chapter, finite element modeling technique which is going to be used in this thesis is validated by using two different test results. According to the verification results, it is aimed to simplify finite element model to reduce the computation time. Moreover, mesh convergence study is also done in this chapter and mesh sizes of each instance in the model is determined.

#### **3.1. Finite Element Model Validation**

To be able to correlate finite element model used in this study, results of the finite element analyses are compared to the results of a test conducted by another study [14] and a test conducted by Turkish Aerospace. The sandwich structure tested in [14] has no ramp-down region and the structure is under three-point bending. However, a tapered sandwich structure fastened to adjacent parts with fasteners is tested under bending load in the test conducted by Turkish Aerospace. The reason why two different tests are used to validate the model is that, the first test does not cover the ramp-down region of the finite element model. The second test covers the ramp-down region but there are some uncertainties in this test such as friction coefficient between the parts in contact, bolt preload and manufacturing uncertainties.

##### **3.1.1. Test 1: Finite Element Model Correlation with Three Point Bending Test of Sandwich Panels with Aluminum Skins and Nomex Honeycomb Core**

In this chapter of the study, description of the finite element model created to validate the test and the results of the analyses are given.

### **3.1.1.1. Finite Element Model Description**

Finite element model created in ABAQUS by using equivalent modeling is intended to be validated by comparing the deflection results of the model and the test data. Test data for this study is taken from another research. Therefore, to be able to do the comparison, a finite element model is created for the validation purpose only by using the same modeling methodology defined in Chapter 2.4. Cylindrical supports and the indenter are modelled in 3D and steel is assumed as the material.

To be able to simulate the test properly, numerical contact definition is required between the upper face of the sandwich structure and indenter, and also between the lower face of the sandwich structure and roller supports. To define the surface-to-surface contact in ABAQUS “Penalty” tangential behavior and “Hard Contact” normal behavior is preferred. Friction coefficient in the Penalty definition is specified approximately as 0.5 for the aluminum on mild steel combination [13].

All parts in the model (cylindrical supports, indenter, core and facings) are modelled in 3D with linear element. 8-node brick, C3D8.

The test data given in [14] is referred as the reference to validate the methodology of finite element model in this thesis. Test is, generally, conducted according to ASTM C393 [3]. The difference between the test and the standard is that, this test has been carried out until the failure of the sandwich structure, to be able to understand the non-linear behavior after the fraction.

### **Material Properties**

Materials used in this test are:

Core: HRH 10-3/16-2

Facings: Al2024-T3

Core mechanical properties for equivalent model, recommended by [16], and facing mechanical properties are given in Table 3.1 and Table 3.2.

Table 3.1. *Equivalent Mechanical Properties of HRH 10-3/16-2 [16]*

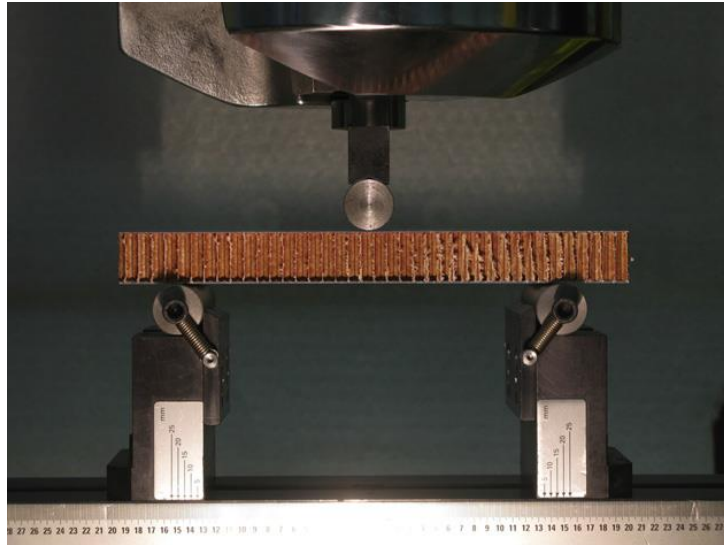
	<i>Modulus, Normal Direction [MPa]</i>	<i>Modulus, L Direction [MPa]</i>	<i>Modulus, W Direction [MPa]</i>
HRH 10-3/16-2	75.84	29.65	14.48

Table 3.2. *Geometrical and mechanical properties of the tested sandwich panels and of their components [14]*

<b>Metallic Skins</b>	
Material	Al2024-T3
Up skin thickness [mm]	0.25
Down skin thickness [mm]	0.447
Volumic mass [kg/m <sup>3</sup> ]	2700
Elastic Modulus [MPa]	72400
Poisson's Coefficient	0.3

### **Geometric Description and Imperfections**

The geometry of the test specimen is in a rectangular shape with the sizes 70x200 mm. Honeycomb ribbon direction of the test specimen is parallel to the axis of the cylindrical indenter. The supports are also in a cylindrical shape and both the supports and the indenter have the same diameter of 20 mm. Distance between the supports is 150 mm. Test setup is illustrated in Figure 3.1. The output of this test is the load displacement curve of the specimen.



*Figure 3.1.* Test Set-up for TPBT [14]

There are some defects, cracks and manufacturing errors in real specimen different than the FEM. Also, the core shape of the real specimen is hexagonal and solid mass core assumption is done for this part of the study. There could be differences between the model and the test results because of these dissimilarities.

### **Load and Boundary Condition**

Flat regions of the cylindrical supports are fixed in all degrees of freedom and the surfaces of the indenter which lay in XZ plane are fixed in X and Z directions. Uniform pressure is applied on the flat surface of the indenter. Applied load is slightly increased until the ultimate load is achieved.

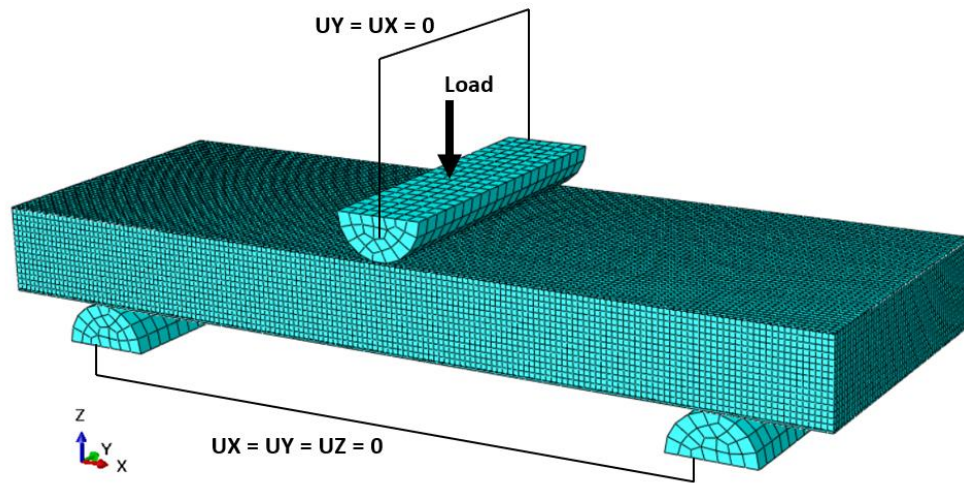


Figure 3.2. Load and Boundary Condition of Test-1

### 3.1.1.2. Results

Three different models with three different mesh sizes given in Table 3.3 are created and Load vs. Displacement data of these models are compared to each other and the literature data in Figure 3.4 [14].

Table 3.3. Literature Correction Mesh Sets

Set Name	Core Mesh Size [mm]	Facings Mesh Size [mm]	Indenter Mesh Size [mm]	Support Mesh Size [mm]
Mesh 1	2.5	2.75	6	6
Mesh 2	2	2.2	6	6
Mesh 3	1.5	1.75	6	6

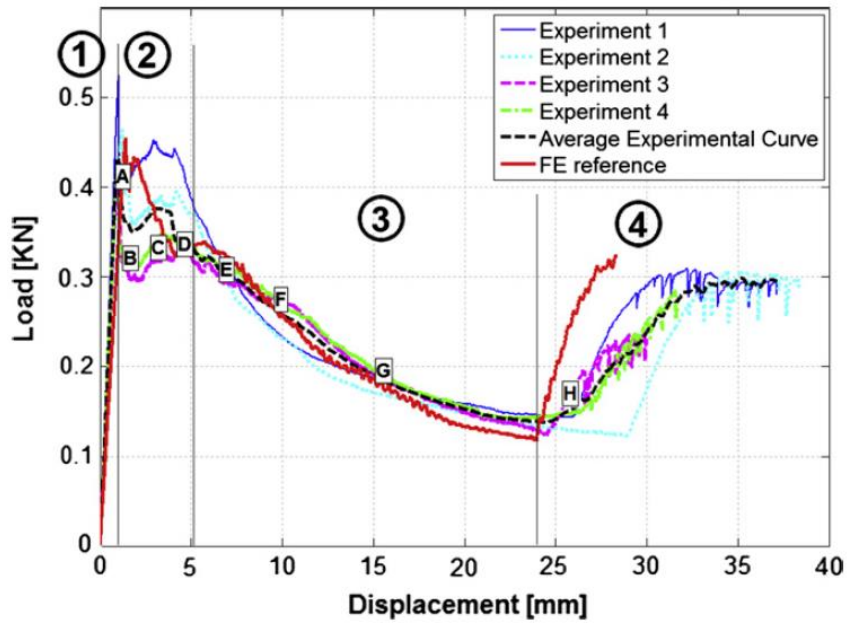


Figure 3.3. Load & Displacement Curve of Test Adapted from [14]

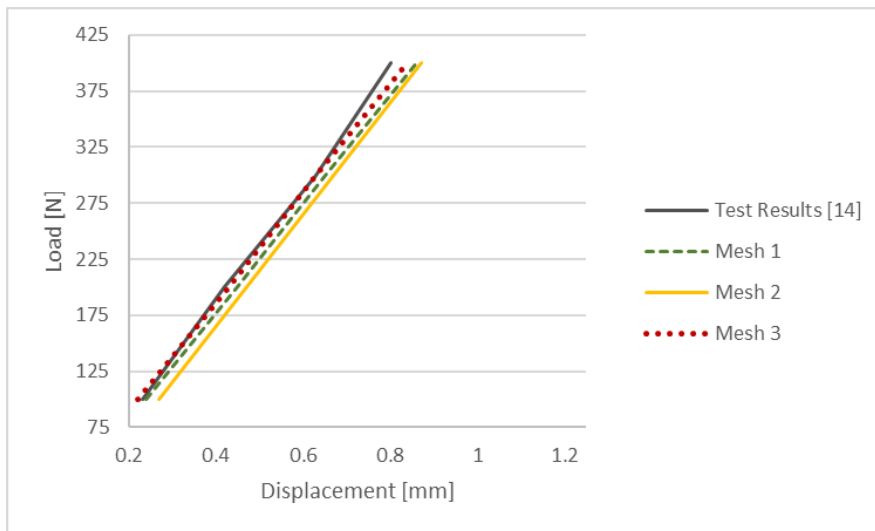


Figure 3.4. Load & Displacement Curve – Test-1

The difference between the results of “Finite Element Model: Mesh 3” and the test conducted in [14] is around 5%.

### 3.1.2. Test 2: Three Point Bending Test of Tapered Sandwich Panels with Aluminum Skins and Aluminum Honeycomb Core

Ramp-down region of the finite element model with equivalent modeling technique is correlated by using the test conducted by Turkish Aerospace [33].

#### 3.1.2.1. Finite Element Description

Finite element model that simulates the “Test 2” is created by using equivalent modelling technique.

In order to simulate the test correctly, contact is defined between the parts in contact. Bolt-nut and nut-angle connections are provided by tie constraint.

All parts in the model (cylindrical supports, indenter, core and facings) are modelled in 3D with linear element. 8-node brick, C3D8.

#### Material Properties

Materials used in this test are:

Core: CR-III – 1/8 – 5056 – 4.5

Facing: Al2024-T3

Core mechanical properties for equivalent model and facing mechanical properties are given as:

Table 3.4. *Equivalent Mechanical Properties of HRH 10-3/16-2 [16]*

	<i>Modulus, Normal Direction [MPa]</i>	<i>Modulus, L Direction [MPa]</i>	<i>Modulus, W Direction [MPa]</i>
CR-III – 1/8 – 5056 – 4.5	75.84	29.65	14.48

Table 3.5. Geometrical and mechanical properties of the tested sandwich panels and of their components [33]

Metallic Skins	
Material	Al2024-T3
Up skin thickness [mm]	0.25
Down skin thickness [mm]	0.447
Volumic mass [ $\text{kg/m}^3$ ]	2700
Elastic Modulus [MPa]	72400
Poisson's Coefficient	0.3

### Geometric Description and Imperfections

The test specimen is fastened to two angles with four fasteners. Load is applied by a rectangular shape indenter. Test set-up is illustrated in Figure 3.5. The test is displacement controlled and applied load for each displacement is measured by using load cells. Therefore, the output of this test is “Load vs Displacement” data of the specimen.

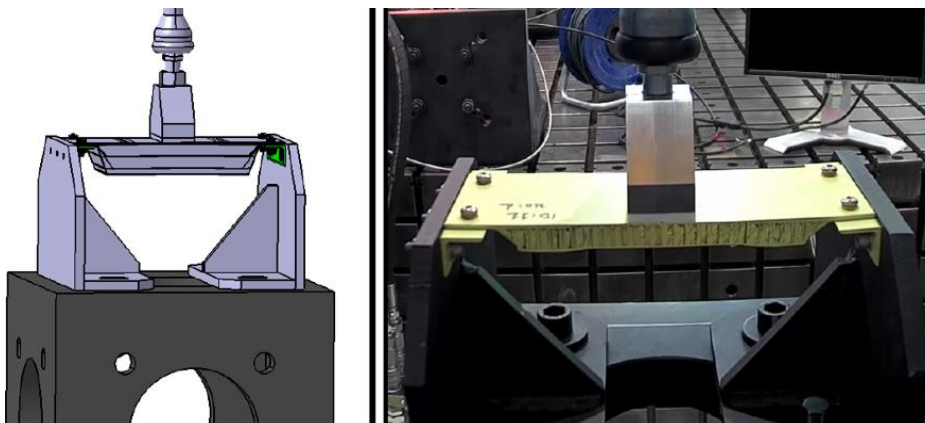


Figure 3.5. Test Set-up for Tapered Sandwich Structure [33]

Due to the existence of defects, cracks, manufacturing errors and uncertainties in real specimen, there could be differences between model and test results. For this test, the



friction coefficient between the parts and the tightening torque of the bolt that connects the angles and the sandwich structure to each other are uncertain. To understand the effect of the preload and the friction coefficient on the analysis and to determine the values of these two parameters, a parametric study is carried out after the mesh sensitivity part.

### Loads and Boundary Conditions

Surfaces of the indenter in XZ plane are fixed in X and Z directions. Angle surfaces in ZY plane are fixed in all degrees of freedom. Uniform pressure is applied on the upper surface of the indenter.

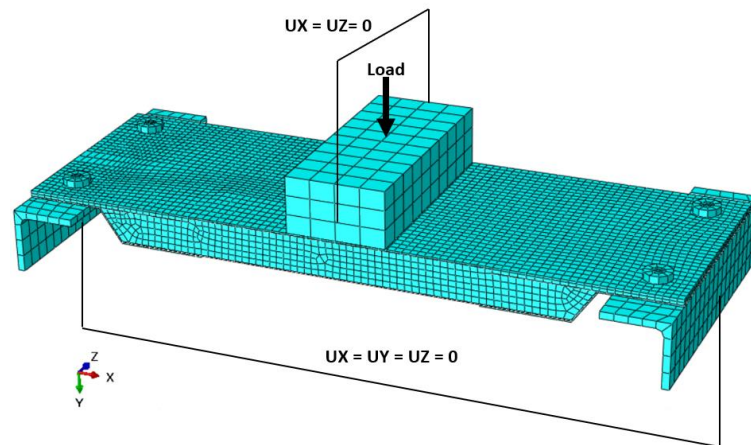


Figure 3.6. Load and Boundary Condition of Test-2

### Mesh Sensitivity Study and Results

In order to correlate the finite element model, glass that covers the tapered edges of the sandwich structure is also modeled. The first mesh sensitivity study is computed by including the glass. Four different mesh size sets shown in Table 3.6 are selected for this study. According to this mesh sensitivity study, the glass has a considerable effect on the core flatwise tension stress distribution around the ramp starting region

and on the convergence. Convergence of the finite element model with glass cannot be ensured and the results of this optimization study is given in Table 3.7. Change in core flatwise tension stress according to mesh size for this sensitivity analysis is illustrated in Figure 3.7. In this figure, core flatwise tension stress does not become stable with increasing element number in the sandwich construction assembly.

Table 3.6. Mesh Size Sets for First Mesh Sensitivity Study (Glass is Included)

Set Name	Core Mesh Size [mm]	Facings Mesh Size [mm]	Indenter Mesh Size [mm]	Angle Mesh Size [mm]	Bolts Mesh Size [mm]	Nuts Mesh Size [mm]
Mesh 1	2.5	2.75	8	3.5	3.5	3.5
Mesh 2	2	2.2	8	3.5	3.5	3.5
Mesh 3	1.5	1.75	8	3.5	3.5	3.5
Mesh 4	1.25	1.375	8	3.5	3.5	3.5

Table 3.7. Element Type and Total Element Number of Mesh Sets (Glass is Included)

Set Name	Element Type & Element Number of Sandwich Construction (Facings & Core)
Mesh 1	C3D8R & 16958
Mesh 2	C3D8R & 30140
Mesh 3	C3D8R & 63221
Mesh 4	C3D8R & 107621

Table 3.8. Results of the First Mesh Sensitivity Study (Glass is Included)

Set Name	Core Flatwise Tension Stress [MPa]	Change in Core Flatwise Tension Stress [%]
Mesh 1	1.82	-
Mesh 2	2.16	18.68
Mesh 3	2.60	20.37
Mesh 4	3.08	18.46

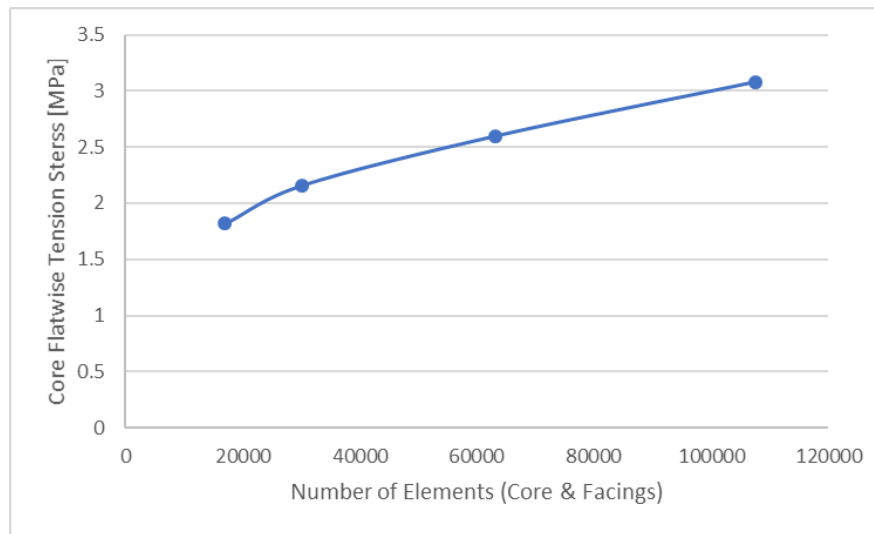


Figure 3.7. Change in Core Flatwise Tension Stress According to Mesh Size (Glass is Included)

Therefore, glass is excluded from the model and mesh sensitivity study is repeated. For the second study, five different mesh size sets are created and shown in Table 3.9. According to the results of the second mesh sensitivity study, mesh sizes of core and facings are determined as 1.5 and 1.75, respectively. Change in core flatwise tension stress according to mesh size for this sensitivity analysis is illustrated in Figure 3.8.

Table 3.9. Mesh Size Sets for Second Mesh Sensitivity Study (Glass is Excluded)

Set Name	Core Mesh Size [mm]	Facings Mesh Size [mm]	Indenter Mesh Size [mm]	Angle Mesh Size [mm]	Bolts Mesh Size [mm]	Nuts Mesh Size [mm]
Mesh 1	2.5	2.75	8	3.5	3.5	3.5
Mesh 2	2	2.2	8	3.5	3.5	3.5
Mesh 3	1.5	1.75	8	3.5	3.5	3.5
Mesh 4	1.25	1.375	8	3.5	3.5	3.5
Mesh 5	1	1.1	8	3.5	3.5	3.5

Table 3.10. *Element Type and Total Element Number of Mesh Sets (Glass is Excluded)*

Set Name	<i>Element Type &amp; Element Number of Sandwich Construction (Facings &amp; Core)</i>
Mesh 1	C3D8R & 16958
Mesh 2	C3D8R & 30140
Mesh 3	C3D8R & 63221
Mesh 4	C3D8R & 107621
Mesh 5	C3D8R & 208652

Table 3.11. *Results of the Second Mesh Sensitivity Study (Glass is Excluded)*

Set Name	<i>Core Flatwise Tension Stress [MPa]</i>	<i>Change in Core Flatwise Tension Stress [%]</i>
Mesh 1	2.15	-
Mesh 2	1.71	20.47
Mesh 3	1.91	11.70
Mesh 4	1.99	4.19
Mesh 5	1.97	1.01

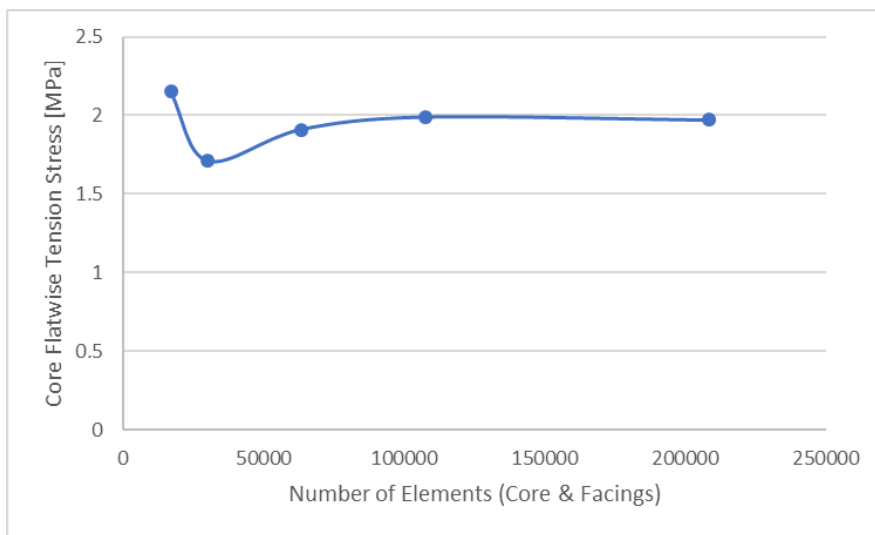


Figure 3.8. *Change in Core Flatwise Tension Stress According to Mesh Size (Glass is Excluded)*

Mesh sensitivity analyses show that glass must be excluded from the model to achieve the convergence. However as can be seen in the Figure 3.9 including the glass into the model reduces the difference between the test and the finite element model. The results given in Figure 3.9 are obtained for the “Mesh 3”.

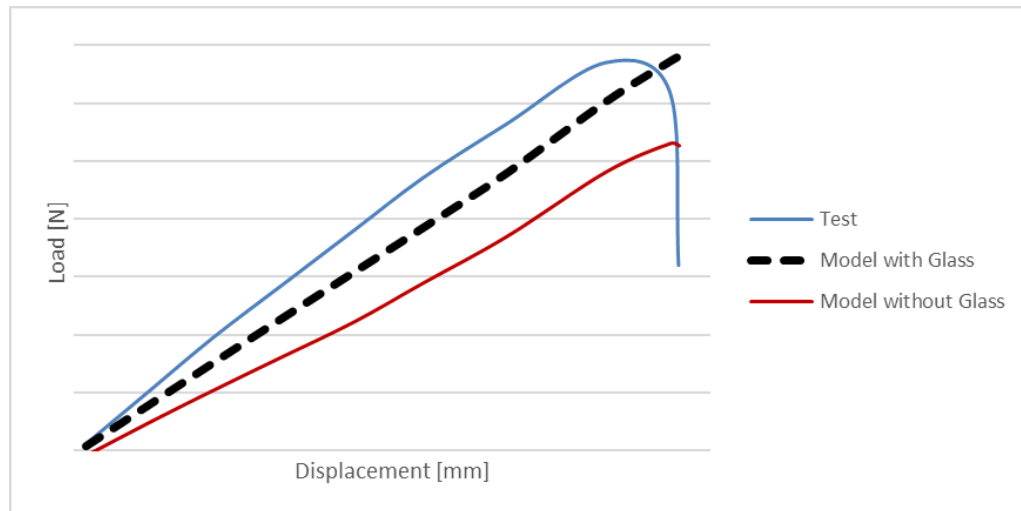


Figure 3.9. Effect of Glass on Load vs Displacement Results

According to the Load vs Displacement results, the difference between the “Finite Element Model with Glass (Mesh 3)” and the test is around 8% at the ultimate load. In order to understand the reason of this inconsistency, effects of the friction coefficient and bolt preload are investigated.

### Effect of Friction Coefficient

According to [13], the dynamic friction coefficient between steel and aluminum is 0.5. However, one of the reasons of the inconsistency between the finite element model and the test data may be that the friction coefficient between the parts is not equal to the theoretical value. Therefore, the effect of the 20% deviation in the friction coefficient on the analysis results is investigated. During the investigation of the effect

of friction coefficient, “Finite Element Model with Glass (Mesh 3)” is used as a base model and bolt preload is specified as 5000 N.

Results of the friction coefficient change are illustrated in Figure 3.10. According to these results, the effect of the change in the friction coefficient is negligible. Therefore, in the rest of the study friction coefficient is going to be defined as 0.5.

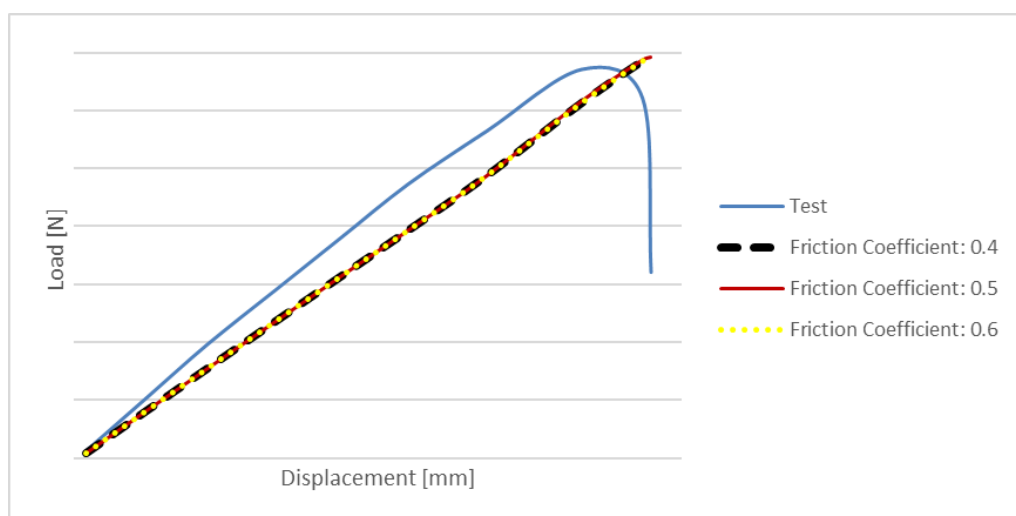


Figure 3.10. Effect of Friction Coefficient

### Effect of Bolt Preload

Bolt preload is determined such that neither separation nor bolt tension failure occur under loading. Bolt preload is selected as 5000 N during the mesh sensitivity study. In order to see how the bolt preload change affects the results, bolt preload in the finite element model is changed in 20% and results are compared. Preload applied on the bolts is simulated by applying equal and opposite forces on the bolt and nut [18]. Results of the change in bolt preload are illustrated in Figure 3.12. During these sensitivity analyses of bolt preload, the friction coefficient between the parts in contact is specified as 0.5 and “Finite Element Model with Glass (Mesh 3)” is used as a base model.

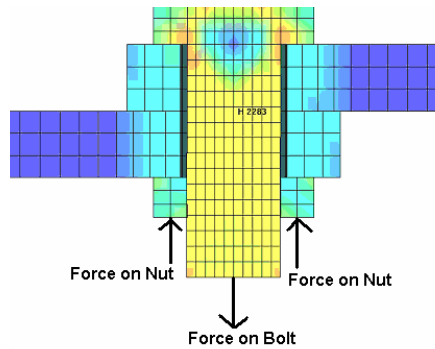


Figure 3.11. Bolt Preload Simulation in FEM [18]

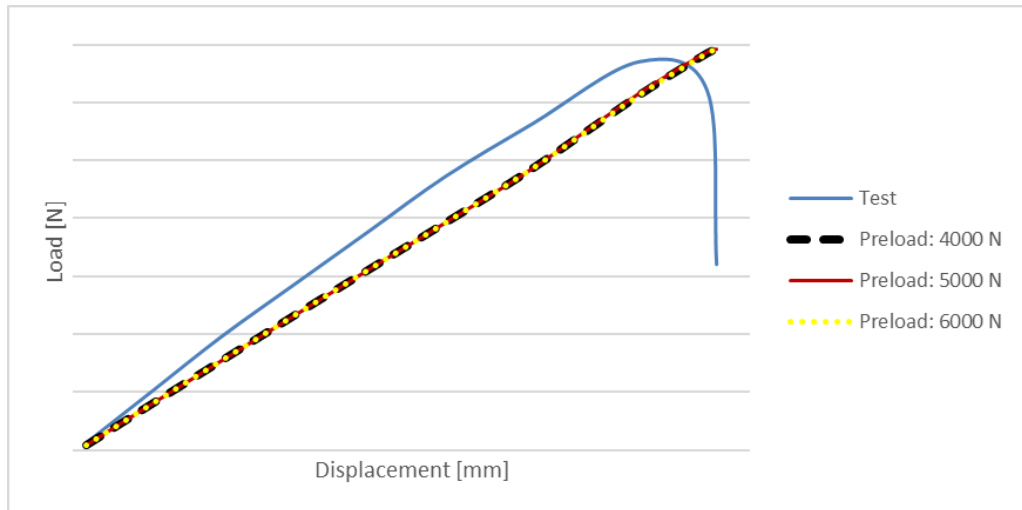


Figure 3.12. Effect of Bolt Preload

In Figure 3.10, the effect of friction coefficient is investigated. In this study, bolt preload is defined as 5000 N for all cases. According to Figure 3.10, effect of friction coefficient can be said to be negligible.

In Figure 3.12, friction coefficient between the parts in contact is specified as 0.5 and 3 different loads are applied on the bolt to understand the effect of bolt preload. According to the results of these analyses, effect of bolt preload on the “Load vs Displacement” curve of the test specimen is seemed to be negligible.

Therefore, the reason of 8% difference between the FEM and test can be explained as manufacturing defects, cracks and specified core stiffness in FEM.

### 3.1.2.2. Simplified Finite Element Model

According to the analysis results, following simplifications can be applied to the model:

- 1- Core is modelled according to equivalent modelling techniques.
- 2- Glass must be excluded from the model to be able to ensure the model convergence.

Boundary conditions must be simplified as fixed or simply supported, in order to create a more generic model. Definitions of these boundary conditions in the FEM is given below.

Fixed Edge Boundary Condition: Encastrate boundary condition is applied to the specified surface of the monolithic region of the sandwich structure.

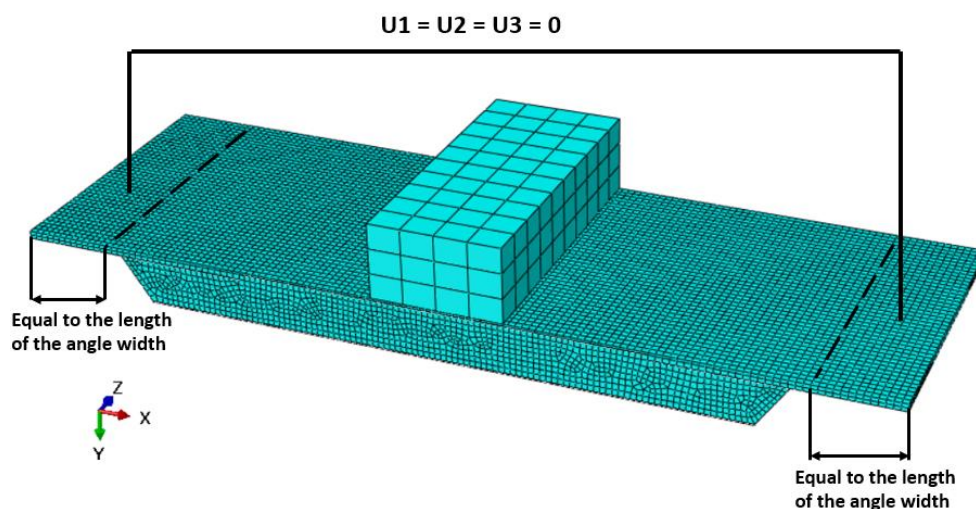


Figure 3.13. Fixed Boundary Condition



Simply Supported Boundary Condition: Boundary conditions are defined to simulate simply supported case.

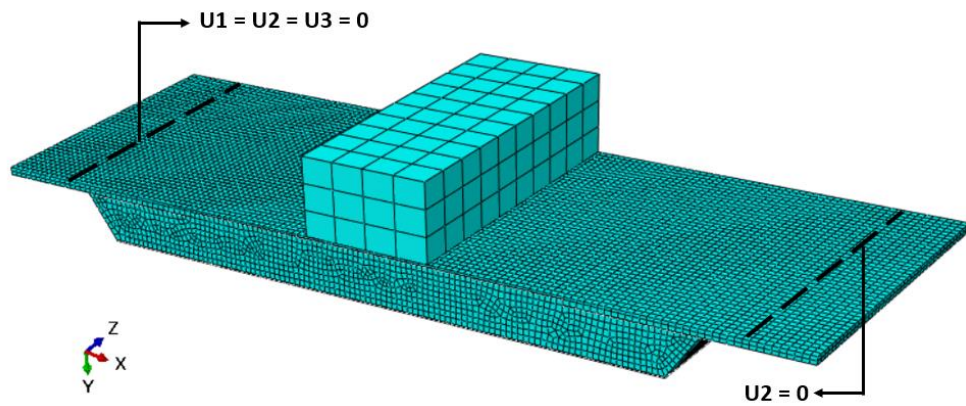


Figure 3.14. Simply Supported Boundary Condition



## CHAPTER 4

### FINITE ELEMENT MODEL

In this study a simplified model is created in order to understand the effects of the doubler geometry on the core flatwise tension stress. Following simplifications were found to be applicable in previous chapters:

- Equivalent core modeling technique is used.
- Fixed edge boundary condition is applied. To be able to compare the effects of doubler span on core flatwise tension stress with different boundary conditions, simply supported boundary condition is also modeled for limited analysis sets.
- Load is applied by a cylindrical indenter to simulate the central load correctly.
- Materials of doubler and facings are the same.
- Core material is aluminum.

All parts in the model (indenter, core and facings) are modelled in 3D with linear elements 8-node brick, C3D8. According to mesh sensitivity study, mesh sizes of the parts are specified as:

Core mesh size: 1.5 mm

Facing mesh size: 1.75 mm

Indenter mesh size: 8 mm

Then, finite element model of this assembly is created in ABAQUS via a Python script. Geometric and material properties of the assembly can automatically be modified by using the Python script. To find the effect of the doubler span on the core flatwise tension failure defined in Chapter 2.1.

#### 4.1. Material Properties

Materials used in this models are:

Core Material # 1: 1/8-5056-3.1

Core Material # 2: 1/8-5052-4.5

Facings and Doubler: Al2024-T3

Mechanical properties of the materials are given below.

Table 4.1. *Equivalent Mechanical Properties of 1/8-5056-3.1 and 1/8-5052-4.5 [16]*

	$E_c$ [MPa]	$G_{13}$ [MPa]	$G_{23}$ [MPa]	$\sigma_{33}$ [MPa]	$\tau_{13}$ [MPa]	$\tau_{23}$ [MPa]
1/8-5056-3.1	668.8	310.3	137.9	6.41	1.38	0.76
1/8-5052-4.5	1034.2	482.6	213.7	8.41	1.97	1.16

Table 4.2. *Mechanical Properties of Al2024-T3 [24]*

	$E_f$ [MPa]	$\nu$
Al 2024-T3	72395	0.3

#### 4.2. Geometric Description

Finite element model consists of facings, doubler, core and indenter. Span length and width of the sandwich structure is specified such that the beam theory can be applicable. During the parametric analyses defined in this chapter, span length and width are specified as 210 mm and 70 mm, respectively. Radius of the cylindrical indenter is 10 mm [3]. Length of the monolithic region of the sandwich beam is specified as 27 mm which is equal to the length of the monolithic region of the specimen used in the test conducted by Turkish Aerospace.

### 4.3. Loads and Boundary Conditions

Loads and boundary conditions are applied as described in Chapter 3.1.2.2. Two different boundary conditions are defined for this thesis: Fixed and Simply Supported. Central load is applied for both boundary conditions. To distribute the load accordingly, load is applied by a cylindrical support.

### 4.4. Python Script

Python script is run in ABAQUS to be able to do followings in order:

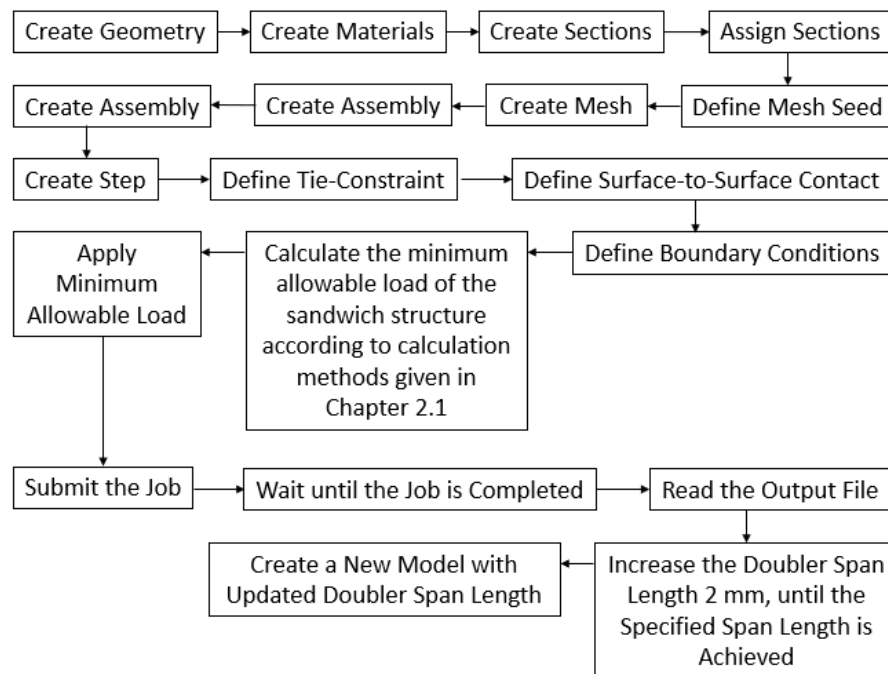


Figure 4.1. Python Script Scheme

Parameters that can be modified in the scripts are listed below:

#### Geometric Parameters:

- Span length of the specimen
- Width of the specimen

- Length of the monolithic region
- Upper face thickness
- Lower face thickness
- Doubler thickness
- Core thickness
- Indenter radius
- Doubler span length
- Core ramp angle
- Core cell size

Mechanical Properties:

- Young's modulus of the metallic parts (facings, doubler, indenter)
- Poisson's ratio of the metallic parts (facings, doubler, indenter)
- Core flatwise modulus
- Core shear modulus in ribbon and transverse directions
- Core shear strength in ribbon and transverse directions
- Core flatwise tension allowable
- Compressive yield strength of the facings
- Tensile ultimate strength of the facings

Thirty-two different combinations of these parameters are created. These sets are described in Table 4.3.

#### **4.5. Design of Experiment**

The logic behind the numbering of each set given in Table 4.3 is explained in Figure 4.2.

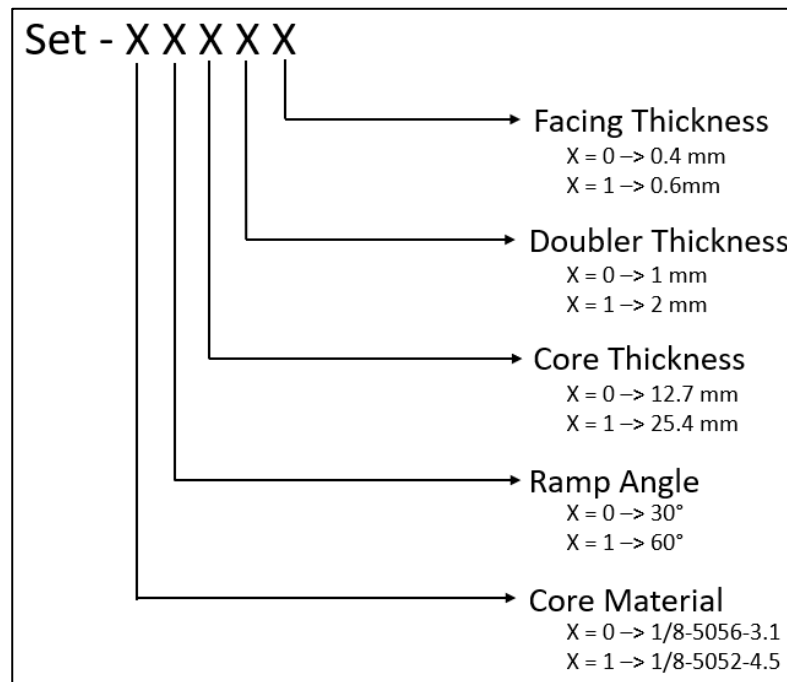


Figure 4.2. Numbering Methodology of the Sets

Table 4.3. Design of Experiment of Parametric Study

	SET-00000	SET-00010	SET-00100	SET-00110
Core Thickness	12.7	12.7	25.4	25.4
Facing Thickness	0.4	0.4	0.4	0.4
Doubler Thickness	1	1	1	1
Core Ramp Angle	30	60	30	60
Core Material	1/8-5056-3.1	1/8-5056-3.1	1/8-5056-3.1	1/8-5056-3.1
Facing Material	Al2024-T3	Al2024-T3	Al2024-T3	Al2024-T3
	SET-10000	SET-10010	SET-10100	SET-10110
Core Thickness	12.7	12.7	25.4	25.4
Facing Thickness	0.6	0.6	0.6	0.6
Doubler Thickness	1	1	1	1
Core Ramp Angle	30	60	30	60
Core Material	1/8-5056-3.1	1/8-5056-3.1	1/8-5056-3.1	1/8-5056-3.1
Facing Material	Al2024-T3	Al2024-T3	Al2024-T3	Al2024-T3

Table 4.3. *continued*

	SET-01000	SET-01010	SET-01100	SET-01110
Core Thickness	12.7	12.7	25.4	25.4
Facing Thickness	0.4	0.4	0.4	0.4
Doubler Thickness	2	2	2	2
Core Ramp Angle	30	60	30	60
Core Material	1/8-5056-3.1	1/8-5056-3.1	1/8-5056-3.1	1/8-5056-3.1
Facing Material	Al2024-T3	Al2024-T3	Al2024-T3	Al2024-T3
	SET-11000	SET-11010	SET-11100	SET-11110
Core Thickness	12.7	12.7	25.4	25.4
Facing Thickness	0.6	0.6	0.6	0.6
Doubler Thickness	2	2	2	2
Core Ramp Angle	30	60	30	60
Core Material	1/8-5056-3.1	1/8-5056-3.1	1/8-5056-3.1	1/8-5056-3.1
Facing Material	Al2024-T3	Al2024-T3	Al2024-T3	Al2024-T3
	SET-00001	SET-00011	SET-00101	SET-00111
Core Thickness	12.7	12.7	25.4	25.4
Facing Thickness	0.4	0.4	0.4	0.4
Doubler Thickness	1	1	1	1
Core Ramp Angle	30	60	30	60
Core Material	1/8-5052-4.5	1/8-5052-4.5	1/8-5052-4.5	1/8-5052-4.5
Facing Material	Al2024-T3	Al2024-T3	Al2024-T3	Al2024-T3
	SET-10001	SET-10011	SET-10101	SET-10111
Core Thickness	12.7	12.7	25.4	25.4
Facing Thickness	0.6	0.6	0.6	0.6
Doubler Thickness	1	1	1	1
Core Ramp Angle	30	60	30	60
Core Material	1/8-5052-4.5	1/8-5052-4.5	1/8-5052-4.5	1/8-5052-4.5
Facing Material	Al2024-T3	Al2024-T3	Al2024-T3	Al2024-T3
	SET-01001	SET-01011	SET-01101	SET-01111
Core Thickness	12.7	12.7	25.4	25.4
Facing Thickness	0.4	0.4	0.4	0.4



Table 4.3. *continued*

Doubler Thickness	2	2	2	2
Core Ramp Angle	30	60	30	60
Core Material	1/8-5052-4.5	1/8-5052-4.5	1/8-5052-4.5	1/8-5052-4.5
Facing Material	Al2024-T3	Al2024-T3	Al2024-T3	Al2024-T3
	SET-11001	SET-11011	SET-11101	SET-11111
Core Thickness	12.7	12.7	25.4	25.4
Facing Thickness	0.6	0.6	0.6	0.6
Doubler Thickness	2	2	2	2
Core Ramp Angle	30	60	30	60
Core Material	1/8-5052-4.5	1/8-5052-4.5	1/8-5052-4.5	1/8-5052-4.5
Facing Material	Al2024-T3	Al2024-T3	Al2024-T3	Al2024-T3

For fixed boundary condition, design of experiment given in Table 4.3 are analyzed. For simply supported case, following sets are chosen to be able to compare the effects of facing thickness, core thickness, ramp angle, core material and doubler thickness on core flatwise tension stress.

- Set-00000
- Set-00010
- Set-00011
- Set-00110
- Set-01010
- Set-10010

## 4.6. Results

Results of simply supported and fixed boundary condition analyses are given in the following sub-chapters.

### 4.6.1. Simply Supported Boundary Condition

For simply supported boundary condition, five different finite element models are created and core flatwise tension stress change with increasing doubler length is investigated. The effects of facing thickness, core thickness, core material, doubler

thickness and ramp angle on core flatwise tension stress is compared. Core flatwise tension stress vs doubler length graphs are given from Figure 4.5 to Figure 4.7. In Figure 4.3 and Figure 4.4, displacement and core normal stress plots of Set-00010 with 60 mm doubler length is illustrated.

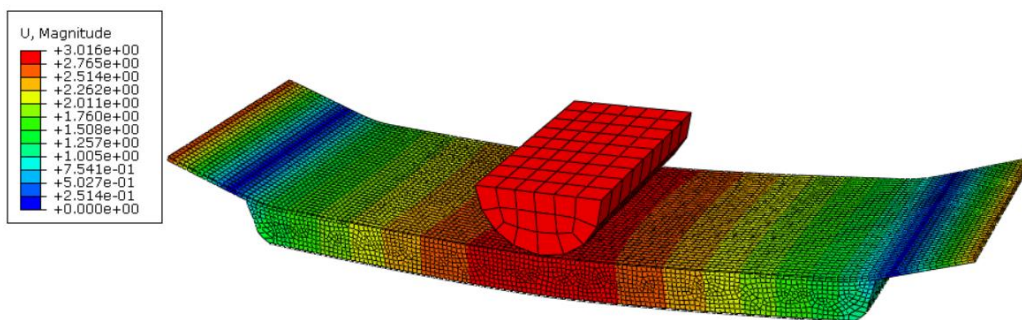


Figure 4.3. Displacement Plot of Set-00010 With 60 mm Doubler Length for Simply Supported Boundary Condition

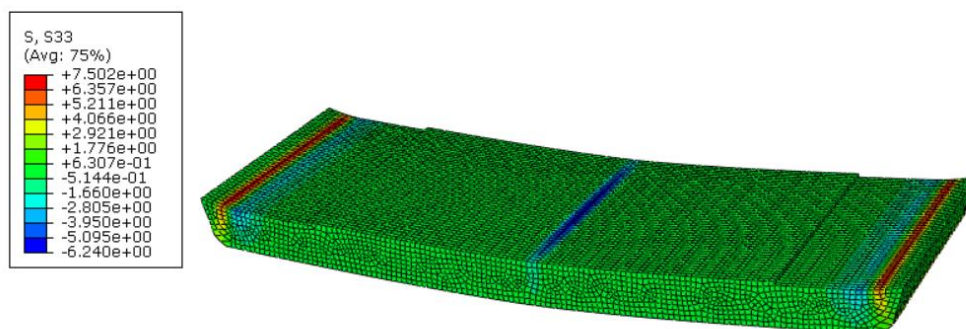


Figure 4.4. Core Normal Stress Plot of Set-00010 With 60 mm Doubler Length for Simply Supported Boundary Condition

In Figure 4.4, it is clearly seen that maximum core tension stress occurs around the ramp starting region.

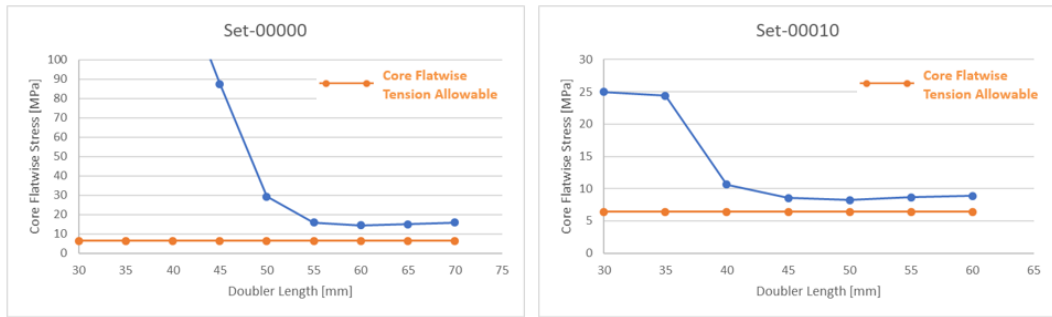


Figure 4.5. Core Flatwise Tension Stress vs Doubler Length Graphs for Set-00000 and Set-00010 with Simply Supported Boundary Condition

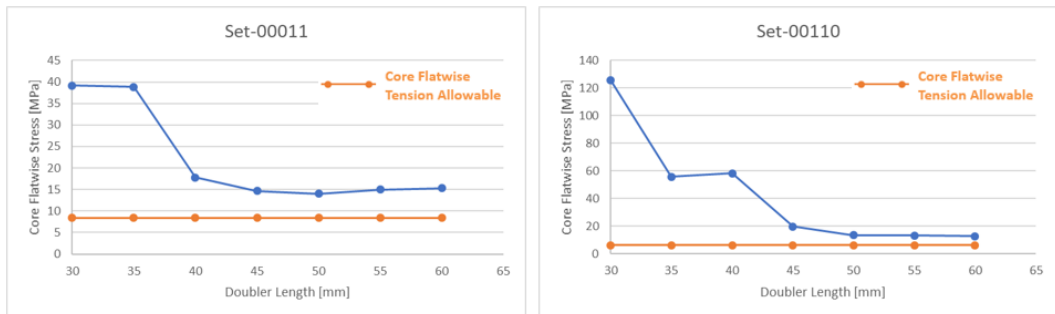


Figure 4.6. Core Flatwise Tension Stress vs Doubler Length Graphs for Set-00011 and Set-00110 with Simply Supported Boundary Condition

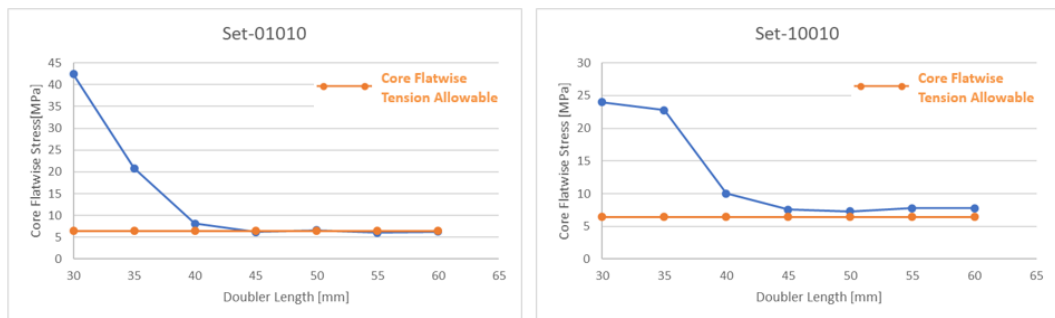


Figure 4.7. Core Flatwise Tension Stress vs Doubler Length Graphs for Set-01010 and Set-10010 with Simply Supported Boundary Condition

According to the results presented in Figures Figure 4.5 to Figure 4.7, core flatwise tension stress is mostly higher than the core flatwise tension allowable for selected geometries.

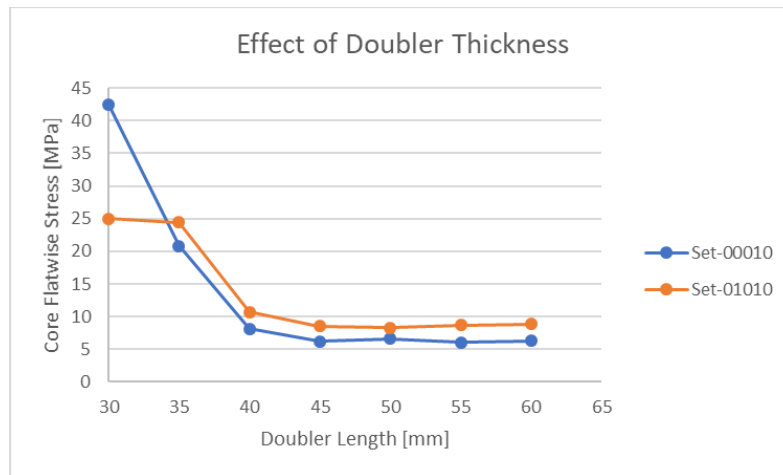


Figure 4.8. Effect of Doubler Thickness for Simply Supported Boundary Conditions

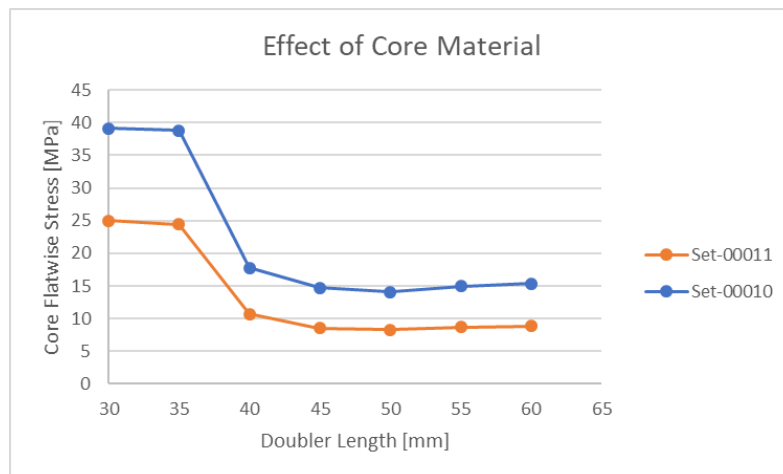


Figure 4.9. Effect of Core Material for Simply Supported Boundary Conditions

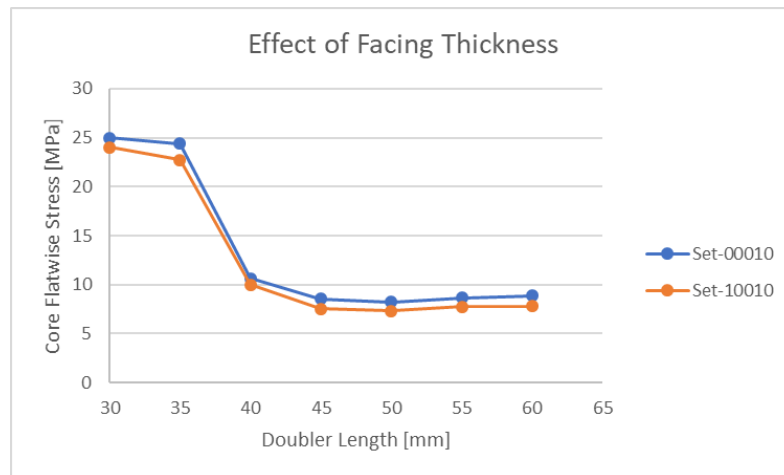


Figure 4.10. Effect of Facing Thickness for Simply Supported Boundary Conditions

The trend of the change in core flatwise tension stress with doubler span length does not considerably change with changing facing thickness, doubler thickness or core material. Increasing doubler thickness causes an increase in core flatwise tension stress. For thicker facings and stiffer core material core flatwise tension stress shows a decrease.

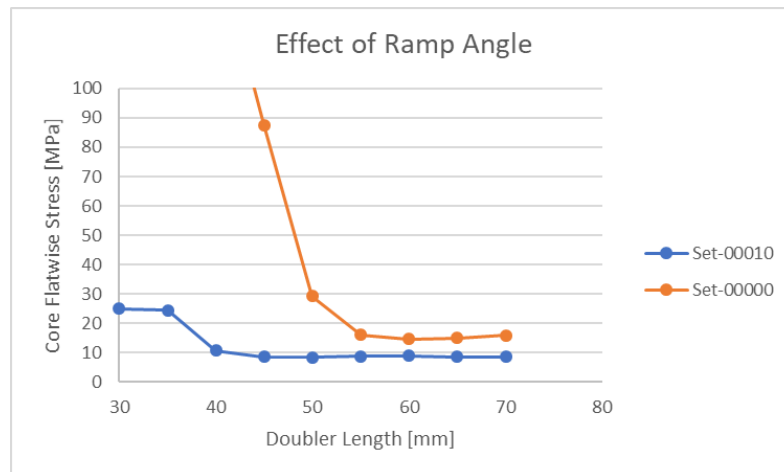


Figure 4.11. Effect of Ramp Angle for Simply Supported Boundary Conditions

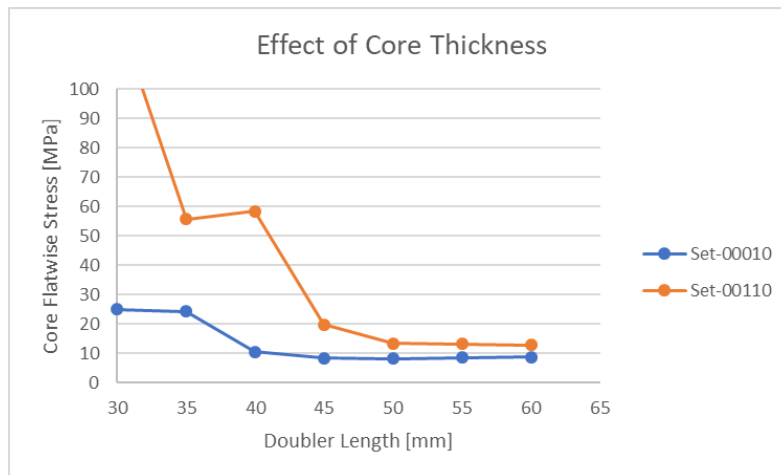


Figure 4.12. Effect of Core Thickness for Simply Supported Boundary Conditions

Compared to the other parameters, ramp angle and core thickness have an observable effect on core flatwise tension stress. For the sandwich structure with 30 degrees ramp angle, doubler length must be at least 37.5% longer than the sandwich structure with 60 degrees ramp angle for the geometry specified in this study. For thicker cores, to achieve the core flatwise tension stress stability, higher doubler span length is required compared to the sandwich structures with thinner core.

#### 4.6.2. Fixed Boundary Condition

Fixed boundary condition is applied as described in Chapter 3.1.2.1. Thirty-two different geometrical and material combinations with fixed boundary condition are created. This study claims to understand the effects of doubler length, ramp angle, core thickness, doubler thickness, facing thickness and core material individually and combined. In Figure 4.13 and Figure 4.14, displacement and core normal stress plots of Set-00010 with 60 mm doubler length is illustrated.

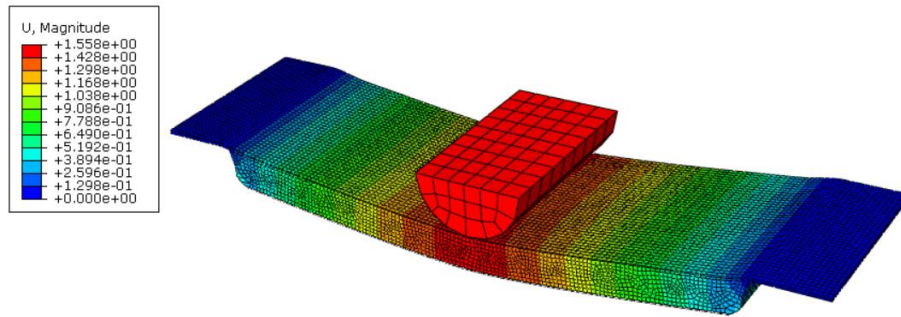


Figure 4.13. Displacement Plot of Set-00010 With 60 mm Doubler Length for Simply Supported Boundary Condition

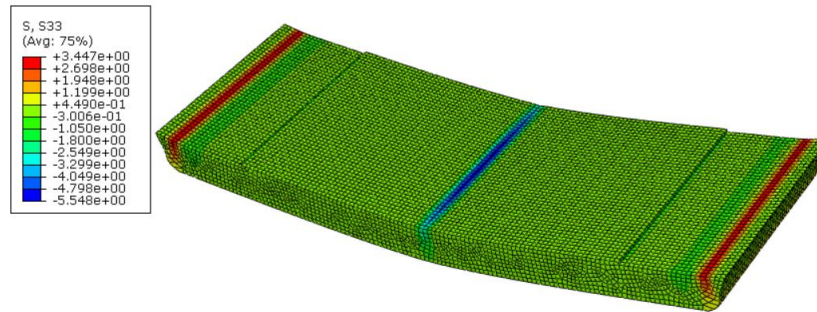


Figure 4.14. Core Normal Stress Plot of Set-00010 With 60 mm Doubler Length for Simply Supported Boundary Condition

Like the simply supported case, core flatwise tension stress is around ramp starting region. Maximum compression occurs due to the interaction between the sandwich structure and cylindrical indenter.

From Figure 4.15 to Figure 4.17 core flatwise tension stress vs doubler length graphs are given for the sets listed below. All analysis results are presented in Appendix A.

- Set-00000
- Set-00001
- Set-00010
- Set-00011
- Set-00100
- Set-01000
- Set-10000

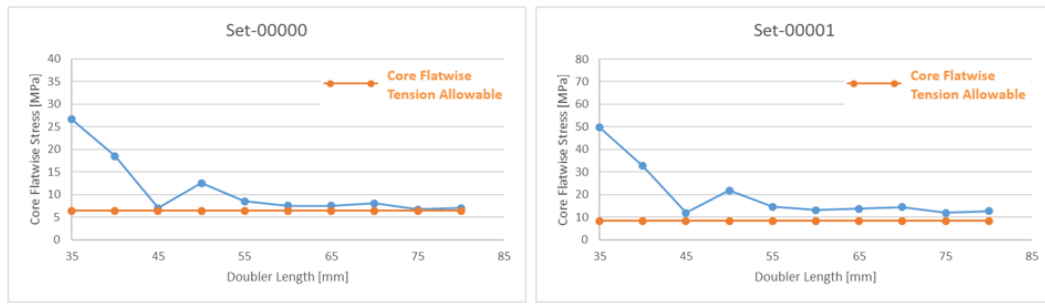


Figure 4.15. Core Flatwise Tension Stress vs Doubler Length Graphs for Set-00000 and Set-00001 with Fixed Boundary Condition

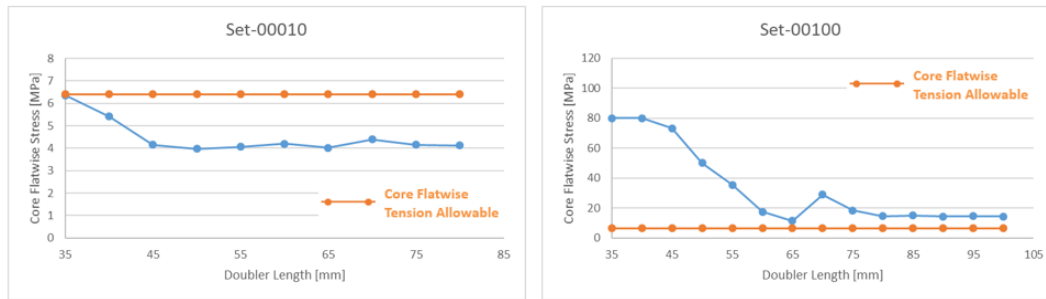


Figure 4.16. Core Flatwise Tension Stress vs Doubler Length Graphs for Set-00010 and Set-00100 with Fixed Boundary Condition

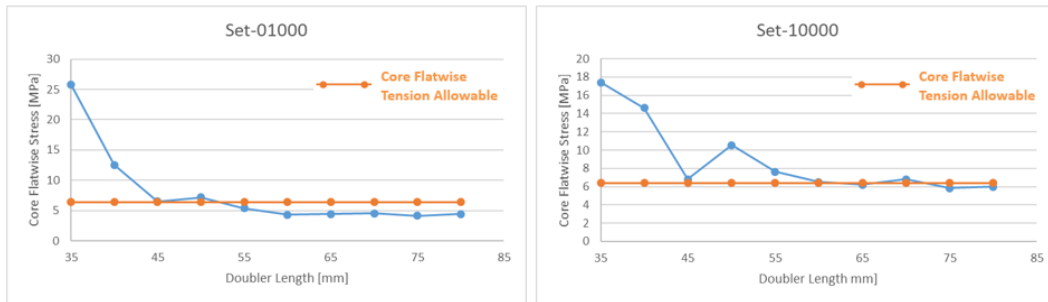


Figure 4.17. Core Flatwise Tension Stress vs Doubler Length Graphs for Set-01000 and Set-10000 with Fixed Boundary Condition

According to the analysis results presented in Figures from Figure 4.15 to Figure 4.17 for some designs core flatwise tension stress is lower than the core flatwise tension allowable. To bring down the core flatwise tension stress below the core flatwise



tension allowable for the rest of the designs, geometric and material changes must be done in these structures. These changes are necessary for the sandwich design in order to prevent an unpredictable failure in the structure.

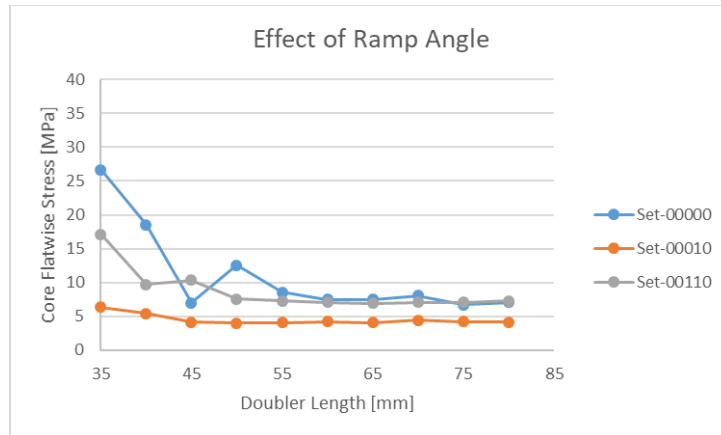


Figure 4.18. Effect of Ramp Angle for Fixed Boundary Conditions

In the graph presented in the Figure 4.18 it is seen that the core flatwise tension stress becomes stable at higher doubler span length with lower ramp angle configurations. For higher ramp angle with lower core thickness case, core flatwise tension stress is lower and more stable.

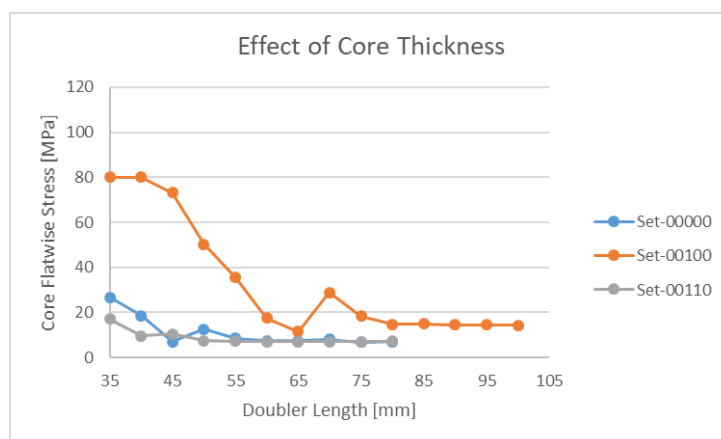


Figure 4.19. Effect of Core Thickness for Fixed Boundary Conditions

The effect of increase in core thickness becomes more significant at lower ramp angle levels. For the configurations with the same ramp angle and different core thickness values, core flatwise tension stress behavior with increasing doubler length does not show a remarkable change.

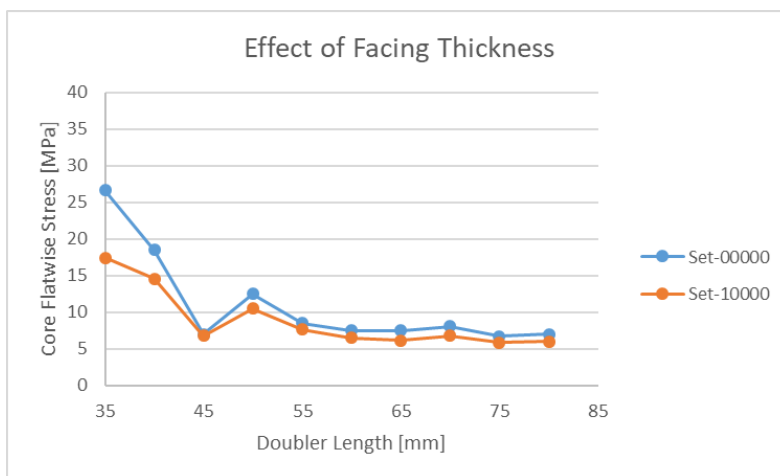


Figure 4.20. Effect of Facing Thickness for Fixed Boundary Conditions

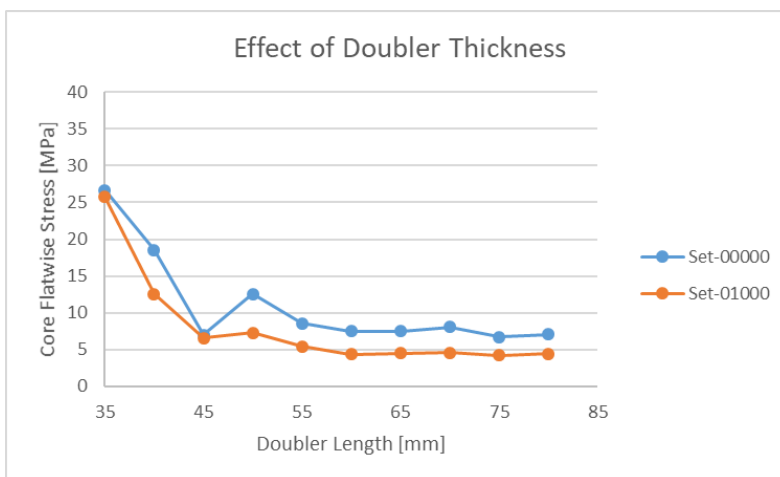


Figure 4.21. Effect of Doubler Thickness for Fixed Boundary Conditions

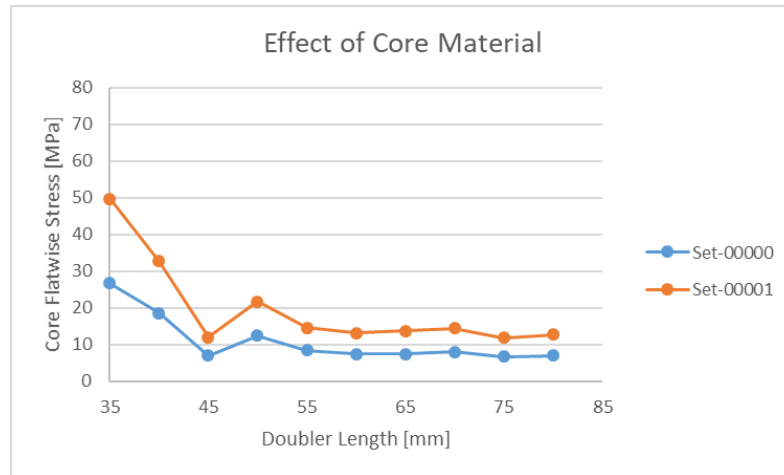


Figure 4.22. Effect of Core Material for Fixed Boundary Conditions

According to the comparison results, compared to the ramp angle and core thickness, effects of core material, doubler thickness and facing thickness on core flatwise tension stress level for different doubler span length values are less significant. Like the simply supported boundary condition, thicker doublers cause an increase in the core flatwise tension stress. However, for the sandwich structures with stiffer cores and higher facing thickness, required doubler length to stabilize the core flatwise tension stress is lower.

In Figure 4.23 core flatwise tension change with increasing doubler length is investigated according to sandwich construction zones for different ramp angle and core thickness values.

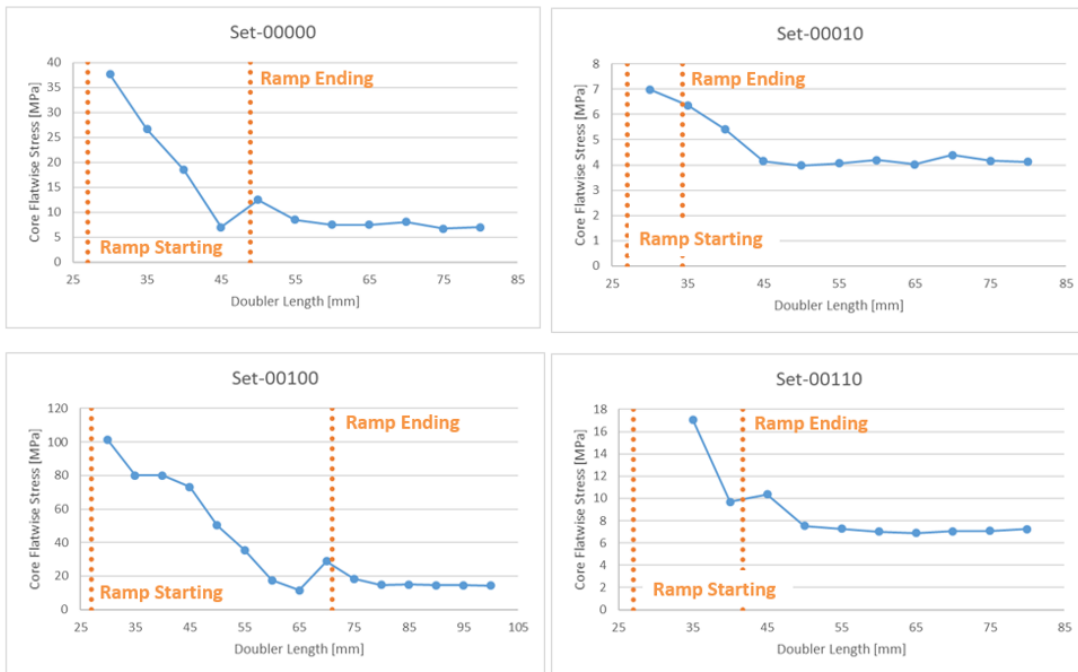


Figure 4.23. Core Flatwise Tension Stress Change According to Sandwich Structure's Zone

In Figure 4.23, it is seen that for the sandwich structures with 30 degrees ramp angle, core flatwise tension stress becomes stable around the ramp ending region. For the structures with 60 degrees ramp angle, the doubler span length where core flatwise tension stress becomes stable is higher than the doubler length at ramp ending point.

However, for the sandwich structures whose core thickness are equal, doubler span length at the ramp ending region is higher for the structures with lower ramp angle.

In Figure 4.24, simply supported and fixed boundary conditions are compared for the sets listed below:

- Set-00000
- Set-00010
- Set-00011
- Set-00110
- Set-01010
- Set-10010

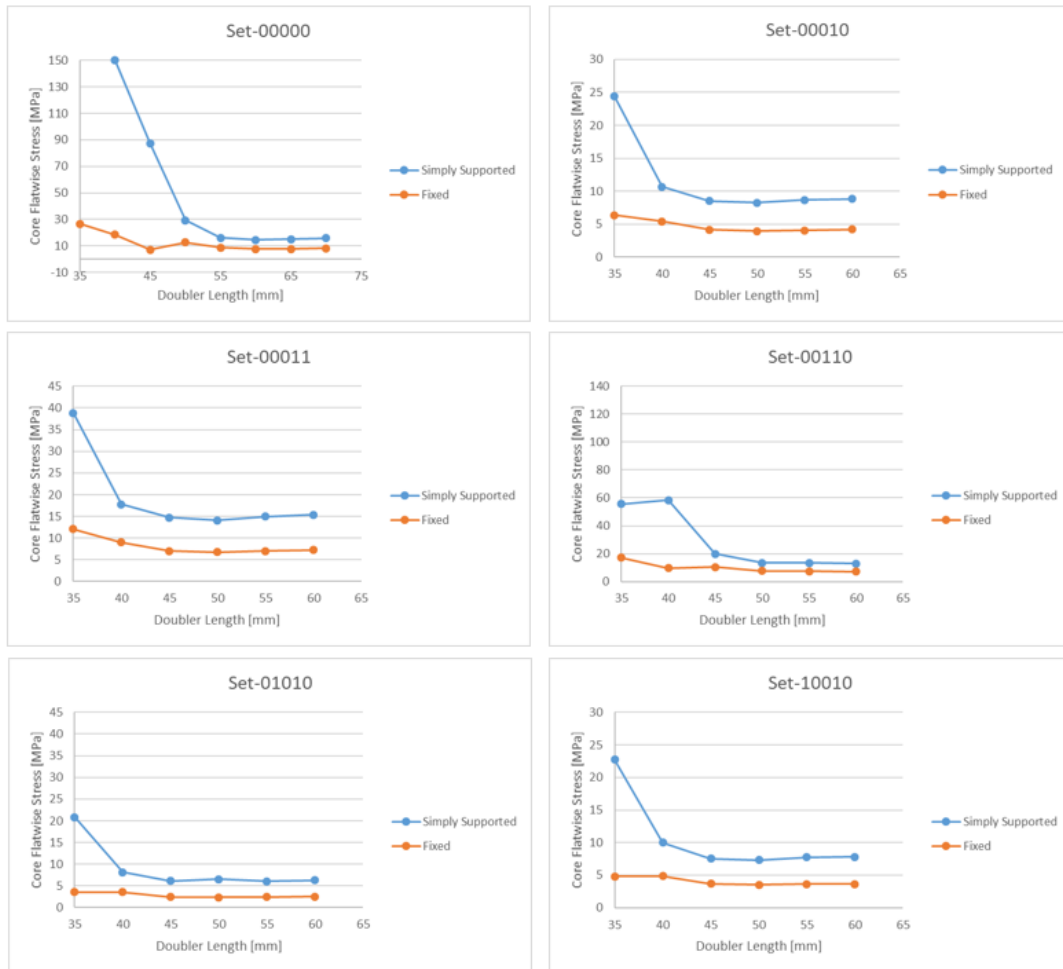


Figure 4.24. Comparison of Fixed and Simply Supported Boundary Conditions

According to Figure 4.24, core flatwise tension stress peaks around the ramp starting region for simply supported case. Also, for the fixed boundary condition, core flatwise tension stress is lower for different sets compared to the simply supported boundary condition. According to this argument, to reduce the core flatwise tension stress the connection of the sandwich structures to adjacent parts must be designed accordingly in addition to the geometry and material specification in service.

### 4.6.3. Minimum Doubler Length of Design of Experiment Sets for Fixed Boundary Conditions

In Table 4.4, doubler span length for which core flatwise tension stress drops below the core flatwise tension allowable is given. For the designs such that core flatwise tension stress is always higher than the allowable is indicated by “N/A” in these tables. For these cases, to reduce the core flatwise stress, design change other than the doubler span length is required.

Table 4.4. *Minimum Doubler Length of Sets for Fixed Boundary Condition*

	SET-00000	SET-00010	SET-00100	SET-00110
Minimum Doubler Length	60	35	N/A	60
	SET-10000	SET-10010	SET-10100	SET-10110
Minimum Doubler Length	60	35	N/A	55
	SET-01000	SET-01010	SET-01100	SET-01110
Minimum Doubler Length	55	35	N/A	50
	SET-11000	SET-11010	SET-11100	SET-11110
Minimum Doubler Length	45	35	N/A	40
	SET-00001	SET-00011	SET-00101	SET-00111
Minimum Doubler Length	N/A	45	N/A	N/A
	SET-10001	SET-10011	SET-10101	SET-10111
Minimum Doubler Length	N/A	40	N/A	N/A
	SET-01001	SET-01011	SET-01101	SET-01111
Minimum Doubler Length	60	35	N/A	55
	SET-11001	SET-11011	SET-11101	SET-11111
Minimum Doubler Length	55	35	N/A	55

Within the scope of these design of experiment sets, smaller core angle with higher core thickness is required to redesigned. For the rest of the sets, change in parameters affect core flatwise tension results differently.

## CHAPTER 5

### DISCUSSION AND CONCLUSION

This thesis determined minimum doubler length of tapered sandwich structures with metallic facings and honeycomb. Analyses are conducted in ABAQUS via Python.

The main point while determination of the minimum doubler length is to avoid any unpredictable failure around ramp-down region. Unpredictable failure can be explained as, the failure occurs at a load below the expected load calculated by considering failure types defined in the literature. These failure loads are explained in Chapter 2 in detail. To be able to calculate and apply the critical load under which a failure in core or facings is faced with, sandwich beam theory is used. Beam theory is applicable for the geometries with the width less than three times of the span length.

The model developed and used in the analyses of this study is verified by the test results conducted in [14] and [33]. The test given in [14], used to correlate sandwich structure without ramp-down region. This correlation is necessary, because there are fewer uncertainties in this test compared to the test conducted in [33]. The effects of uncertainties in [33] is aimed to be understood by using the correlation study done with the test results presented. Effects of bolt preload and friction coefficient between the parts in contact are investigated and their effects are determined to be negligible. During the correlation study, glass that cover the ramp-down region of the sandwich structure is modelled. Effects of mesh size on the core flatwise stress results are analyzed. Firstly, mesh sensitivity study of the finite element model including glass is done. Results of these analyses show that the mesh convergence cannot be ensured when the glass is included into the finite element model. Therefore, glass is omitted from the further analyses, and mesh convergence study is repeated. According to results of these analyses, mesh size of each component in the assembly is determined.

Since the mesh convergence is supplied when glass is not included into finite element model, the load vs. displacement results of the model without glass is compared to the test results. This comparison shows that glass is necessary to represent the overall stiffness of the sandwich structure. However, to be sure of the accuracy of the core flatwise tension stress results, glass is not modeled in this thesis study. Based on the sandwich panel modeling techniques comparison given in [4], equivalent core modeling with solid facings and doubler is decided to be used. A new simplified finite element model is created to use in this thesis in consideration of these results. In this simplified model, adjacent parts are cancelled, and the glass is excluded. In order to understand the effects of connection type of the sandwich structures to adjacent parts two different finite element models are created with fixed and simply supported boundary conditions. The results of these two different boundary conditions are compared and it is seen that, the maximum core flatwise tension stress is higher for fixed boundary condition compared to the simply supported boundary condition under equal loading.

Effects of facing thickness, doubler thickness, core thickness, core material and ramp angle on maximum core flatwise tension stress are examined for varying doubler span length. To cover all combinations of these parameters thirty-two different finite element models with fixed boundary condition are created via Python code. For simply supported boundary condition six of these combinations are selected such that effects of all parameters can be investigated separately. The results of the analyses are presented in the form of “Core Flatwise Stress vs Doubler Length” graphs. These graphs indicate that, core flatwise tension stress decreases with increasing doubler length. At some point, core flatwise stress does not decrease and becomes stable. The doubler length at this point is optimum because it creates the minimum core flatwise tension stress and keeps the weight of the sandwich structure minimum. The optimum doubler length changes by changing sandwich designs. For some designs, the stress level at which core flatwise tension stress converges is higher than the core tension allowable. For these cases design of the sandwich structure must be changed. The most



distinct recommended design change is the use of lower ramp angle with thinner cores. Also, comparison of the results of finite element analyses with fixed and simply supported boundary conditions show that, core flatwise stress level is higher for simply supported boundary condition compared to the fixed ended case. Therefore, to reduce the core flatwise tension stress and prevent an unpredictable failure, connection type of the sandwich construction to adjacent parts may be changed in addition to design change.

These results explained under this title are acceptable for the sandwich construction designs given in this thesis. The design of experiment used in this study is created in consideration of the specimen geometry used in the test conducted by Turkish Aerospace. Within the scope of these results for specified sandwich designs, lighter sandwich structures are aimed to be designed without any unpredictable failure around the ramp down region.

Scope and the accuracy presented in this thesis could increase with further investigations. To lookout for future works can be summarized as follows,

- In this study materials of facings and doubler are both aluminum. Core material is also selected as two different alloys of aluminum. Sandwich structures with different materials and material combinations could be modeled in further studies.
- In order to provide the mesh convergence, glass is excluded from the finite element model in this thesis. Glass may be included into the model to simulate the sandwich structures used in the industry with higher accuracy.
- In real life usage of sandwich structure, potting compound is also used in the ramp-down region. Effect of potting compound on the doubler span length and core flatwise tension stress may be investigated.



## REFERENCES

- [1] Akiwate, S. B., & Shinde, V. D. 2017. Experimental investigation of bending behavior of aluminum alloy honeycomb sandwich structure using four point bending Tests. *International Journal for Innovative Research in Science & Technology*, 4(1).
  
- [2] Allen, H. G. 1969. *Analysis and design of structural sandwich panels*.
  
- [3] ASTM C393/C 393M-06, Standard test method core shear properties of sandwich constructions by beam flexure.
  
- [4] Aydıncak, I. 2007. Investigation of design and analyses principles of honeycomb structures (MS Thesis). METU.
  
- [5] Bitzer, T. 1997. *Honeycomb technology: Materials, Design, Manufacturing, Applications and Testing*.
  
- [6] Bruhn, E. F. 1997. *Analysis and design of flight vehicle structures*. Tri-State Offset Company.
  
- [7] Christensen, A. L., Brett, T. S., James, S. P., & Venkataraman, S. 2013. Testing of sandwich composite edge closeouts with functionally graded honeycomb cores. 54th AIAA/ASME/ASCE/AHS/ASC Structures, Structural Dynamics, and Materials Conference.
  
- [8] Crump, D., Dulieu-Barton, J., & Savage, J. 2009. The manufacturing procedure for aerospace secondary sandwich structure panels. *Journal of Sandwich Structures & Materials*, 12(4).

- [9] Crupi, V., Epasto, G., Guglielmino, E., Mozafari, H., & Najafian, S. 2014. Computed tomography-based reconstruction and finite element modelling of honeycomb sandwiches under low-velocity impacts. *Journal of Sandwich Structures & Materials*, 16(4).
- [10] Dassault Systèmes. 2014. Abaqus analysis user's manuel. Retrieved from Dassault Systèmes: Abaqus Version 6.14.
- [11] Feichtinger, K. A. 1989. Test methods and performance of structural core materials. *Journal of Reinforced Plastics and Composites*, 8(4).
- [12] Fogarty, J. H. 2009. Honeycomb core and the myths of moisture ingression. *Applied Composite Materials*, 17(3).
- [13] Fuller, D. D. Coefficients of friction. <https://web.mit.edu/8.13/8.13c/references-fall/aip/aip-handbook-section2d.pdf>
- [14] Giglio, M., Gilioli, A., & Manes, A. 2012. Numerical investigation of a three point bending test on sandwich panels with aluminum skins and Nomex™ honeycomb core. *Computational Materials Science*, 56.
- [15] Grediac, M. 1993. A finite element study of the transverse shear in honeycomb cores. *International Journal of Solids and Structures*, 30(13).
- [16] Hexcel Corporation. 2016. Aramid fiber/phenolic resin honeycomb. [https://www.hexcel.com/user\\_area/content\\_media/raw/HexWeb\\_HRH10\\_DataSheet\\_us\(1\).pdf](https://www.hexcel.com/user_area/content_media/raw/HexWeb_HRH10_DataSheet_us(1).pdf)
- [17] Hexcel Corporation., Honeycomb attributes and properties handbook.

- [18] Karpanan, K., Brendan, O., & Fegghi, M. 2006. Experimental and finite element analysis of preloaded bolted joints under impact loading. 47th AIAA/ASME/ASCE/AHS/ASC Structures, Structural Dynamics, and Materials Conference.
- [19] Kassapoglou, C. 1996. Stress determination and core failure analysis in sandwich ramp-down structures under bending loads. *Key Engineering Materials*.
- [20] Lister, J. M. 2014. Study the effects of core orientation and different face thicknesses on mechanical behavior of honeycomb sandwich structures under three point bending (MS Thesis). California Polytechnic State University.
- [21] Liu, Q., & Zhao, Y. 2007. Effect of soft honeycomb core on flexural vibration of sandwich panel using low order and high order shear deformation models. *Journal of Sandwich Structures & Materials*, 9(1).
- [22] Löffelmann, F. 2017. Stress distribution investigation at the tapered sandwich endings. *Transactions on Aerospace Research*, 2017(4).
- [23] Masters, I., & Evans, K. 1996. Models for the elastic deformation of honeycombs. *Composite Structures*, 35(4).
- [24] MMPDS-08: Metallic material properties development and standardization. Washington, D.C: Federal Aviation Administration, 2013.
- [25] Nast, E. 1997. On honeycomb-type core moduli. 38th Structures, Structural Dynamics, and Materials Conference.
- [26] Niu, C. 1997. Airframe stress analysis and sizing. Hong Kong: Conmilit Press.
- [27] Paris, I. L. 2009. Characterization of composites sandwich ramp failure under tensile loading. 17th International Conference on Composite Material, Edinburgh.

- [28] Petras, A. 1998. Design of sandwich structures. Ph. D. Thesis, Robinson College, Cambridge.
- [29] Rodrigues, D. S., Silva, J., & Amico, S. 2017. Analysis of sandwich beams using high-order beam theory assisted by software. Proceedings of the 6th International Symposium on Solid Mechanics.
- [30] Shi, G., & Tong, P. 1995. Equivalent transverse shear stiffness of honeycomb cores. *International Journal of Solids and Structures*, 32(10).
- [31] Soltani, S. A., Keshavanarayana, S., Krishnamaraja, M. T., & Bhasin, A. 2014. Study of honeycomb core shear-compression properties during autoclave processing.
- [32] Strength of Sandwich Structures. (n.d.).  
<http://www.mse.mtu.edu/~drjohn/my4150/sandwich/sp2.html>
- [33] Turkish Aerospace In-Company Test Document
- [34] Wagschal, K. R., & Venkataraman, S. 2013. Numerical investigation of tapered sandwich closeouts with isotropic functionally graded cores. 54th AIAA/ASME/ASCE/AHS/ASC Structures, Structural Dynamics, and Materials Conference.
- [35] Zhang, J., & Ashby, M. F. 1992. The out-of-plane properties of honeycombs. *International Journal of Mechanical Science*, 34.

## APPENDICES

### A. RESULTS OF PARAMETRIC STUDY

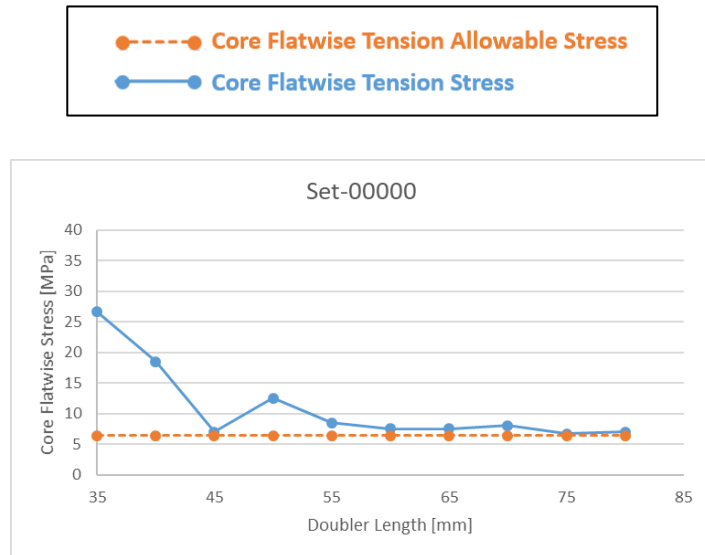


Figure A.1. Core Flatwise Stress vs Doubler Length of Set-00000

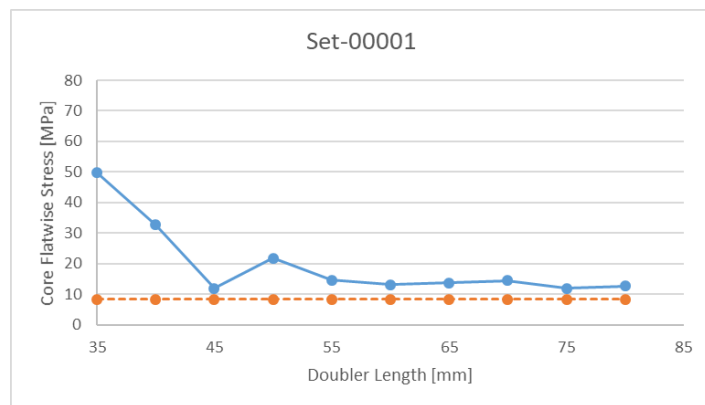


Figure A.2. Core Flatwise Stress vs Doubler Length of Set-00001

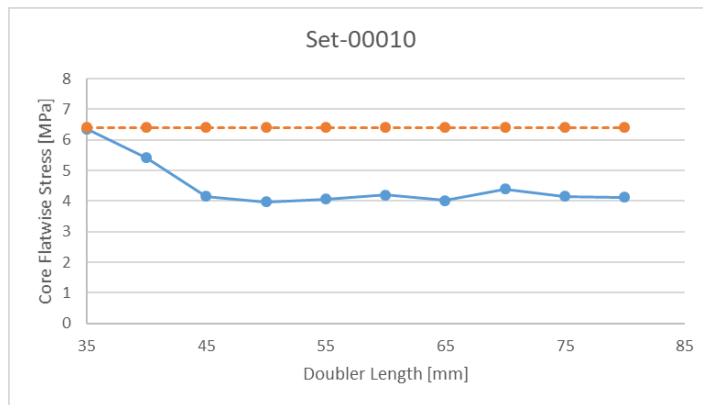


Figure A.3. Core Flatwise Stress vs Doubler Length of Set-00010

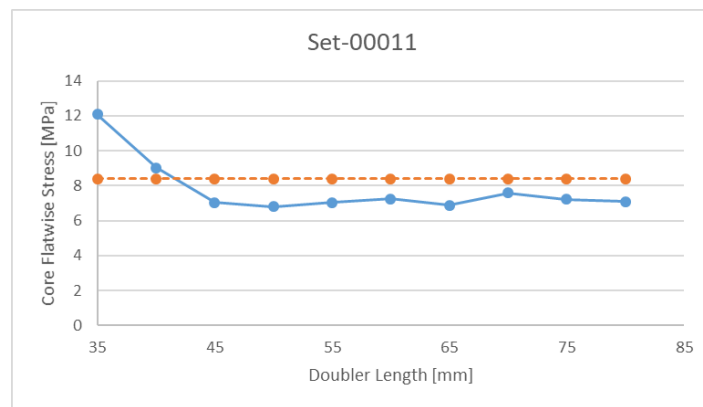


Figure A.4. Core Flatwise Stress vs Doubler Length of Set-00011

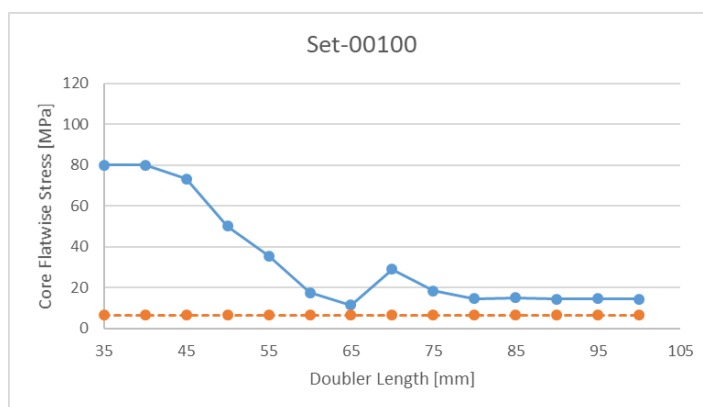


Figure A.5. Core Flatwise Stress vs Doubler Length of Set-00100



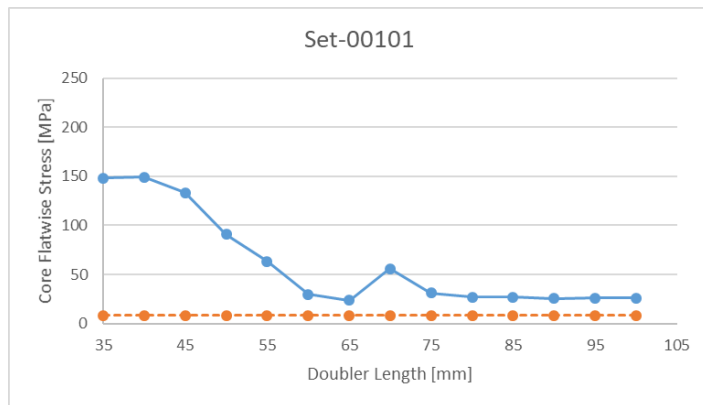


Figure A.6. Core Flatwise Stress vs Doubler Length of Set-00101

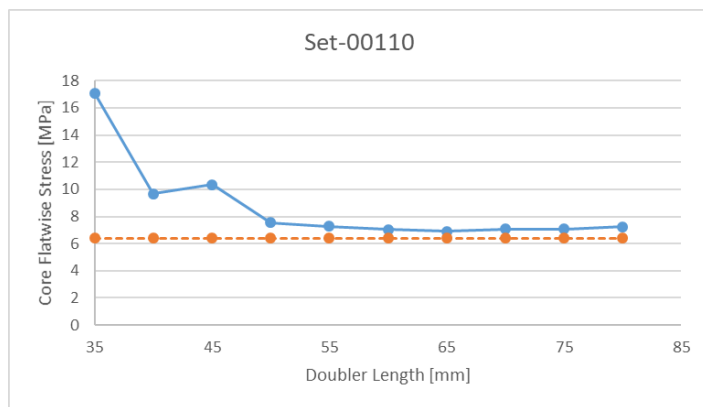


Figure A.7. Core Flatwise Stress vs Doubler Length of Set-00110

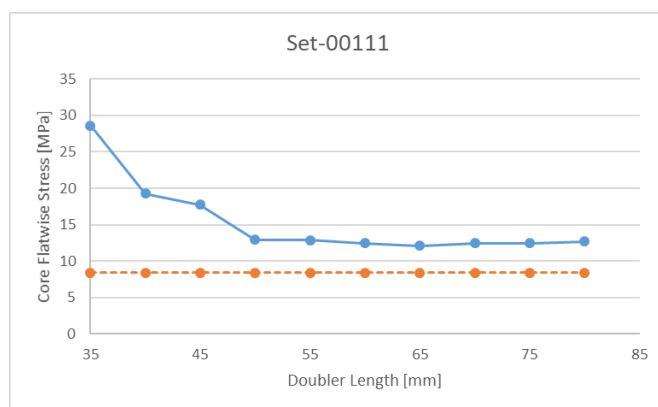


Figure A.8. Core Flatwise Stress vs Doubler Length of Set-00111

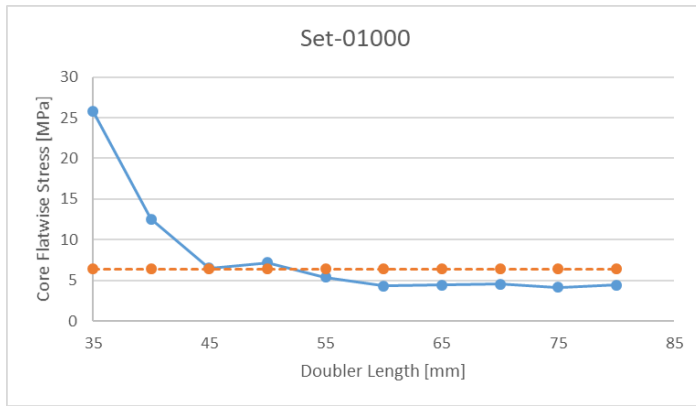


Figure A.9. Core Flatwise Stress vs Doubler Length of Set-01000

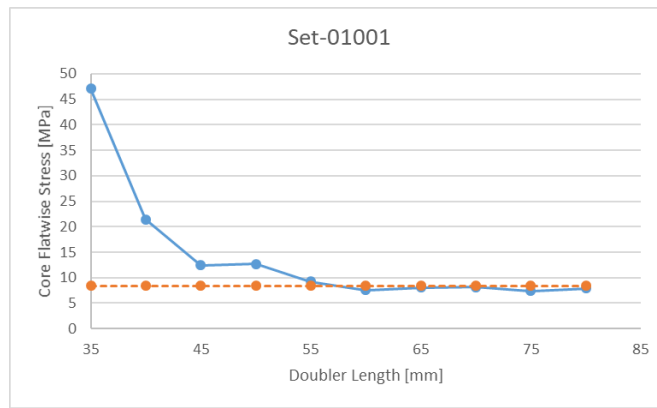


Figure A.10. Core Flatwise Stress vs Doubler Length of Set-01001

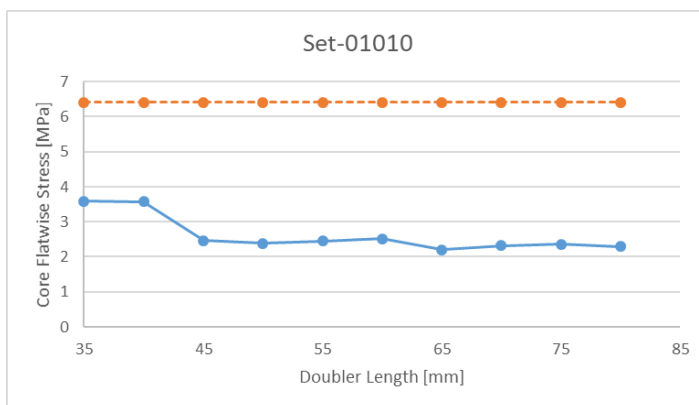


Figure A.11. Core Flatwise Stress vs Doubler Length of Set-01010

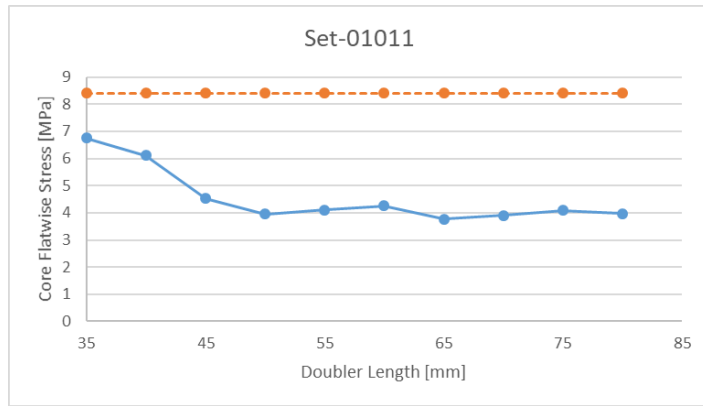


Figure A.12. Core Flatwise Stress vs Doubler Length of Set-01011

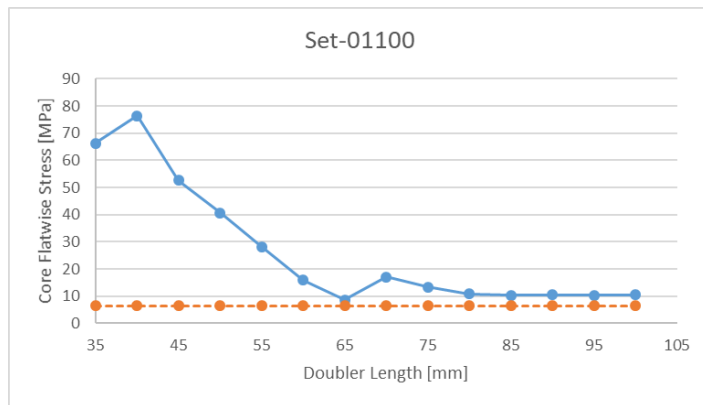


Figure A.13. Core Flatwise Stress vs Doubler Length of Set-01100

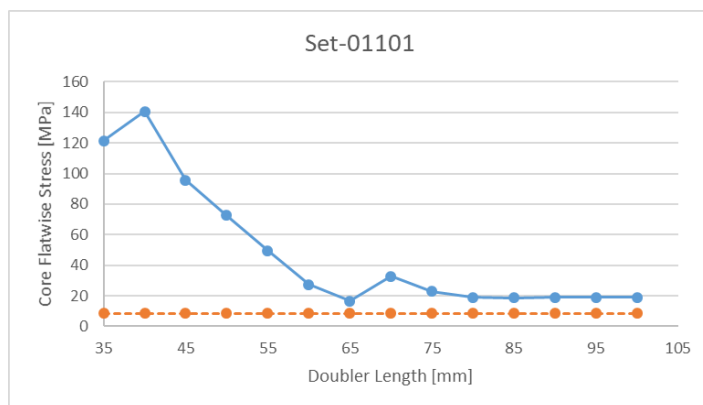


Figure A.14. Core Flatwise Stress vs Doubler Length of Set-01101

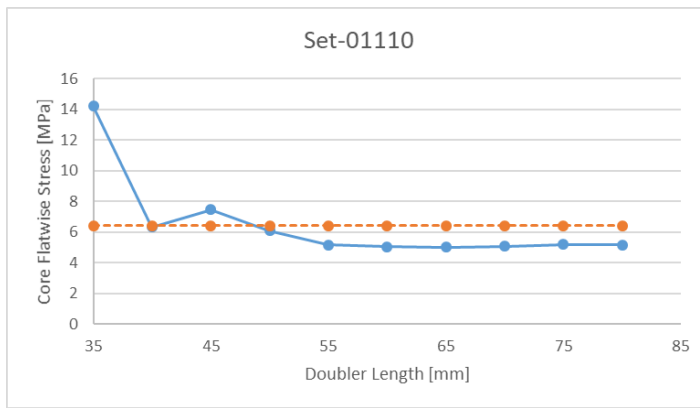


Figure A.15. Core Flatwise Stress vs Doubler Length of Set-01110

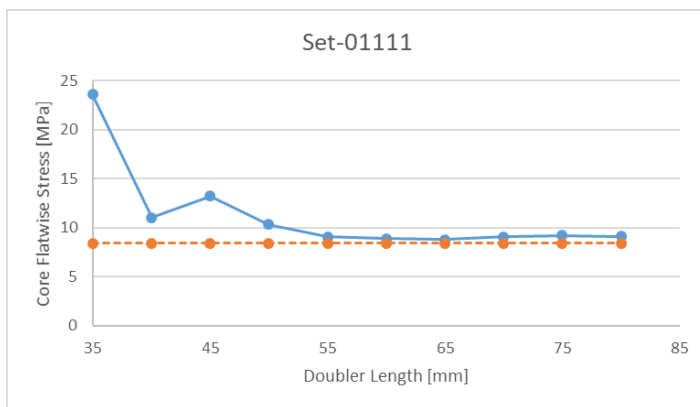


Figure A.16. Core Flatwise Stress vs Doubler Length of Set-01111

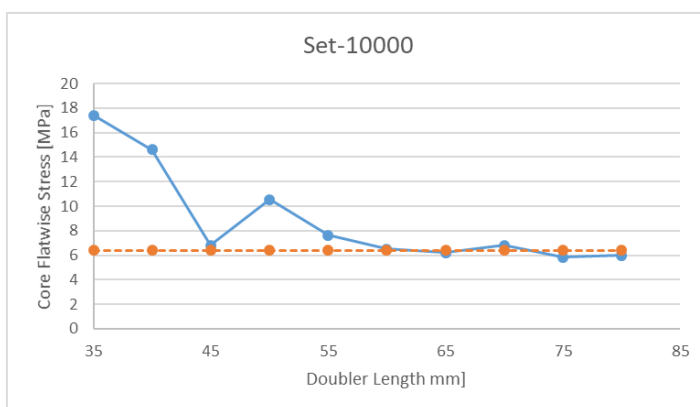


Figure A.17. Core Flatwise Stress vs Doubler Length of Set-10000

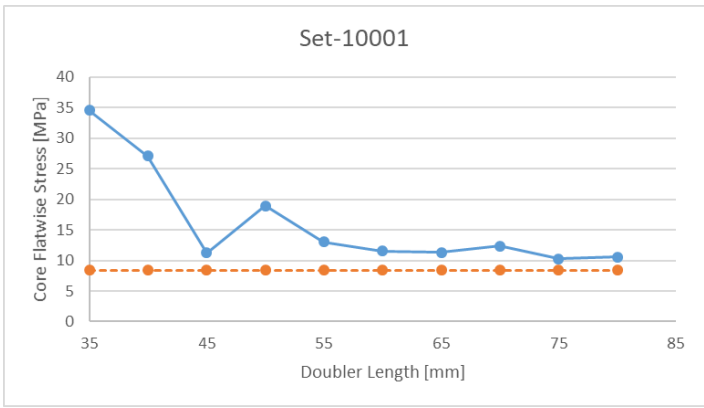


Figure A.18. Core Flatwise Stress vs Doubler Length of Set-10001

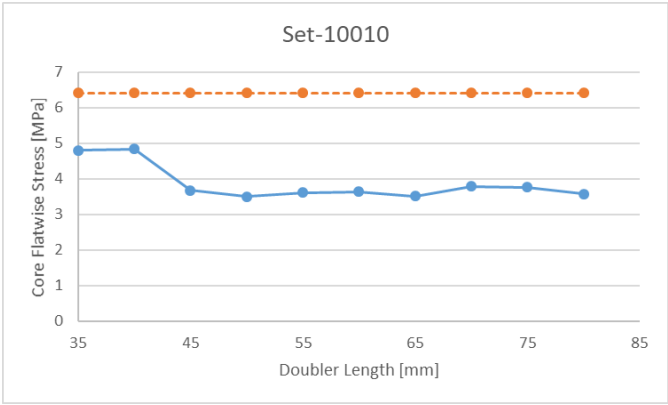


Figure A.19. Core Flatwise Stress vs Doubler Length of Set-10010

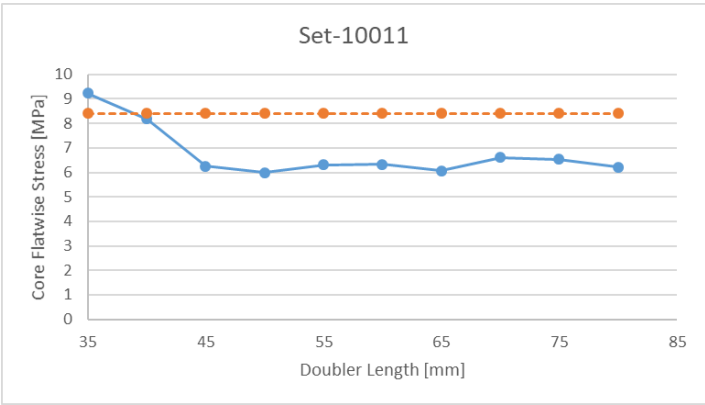


Figure A.20. Core Flatwise Stress vs Doubler Length of Set-10011

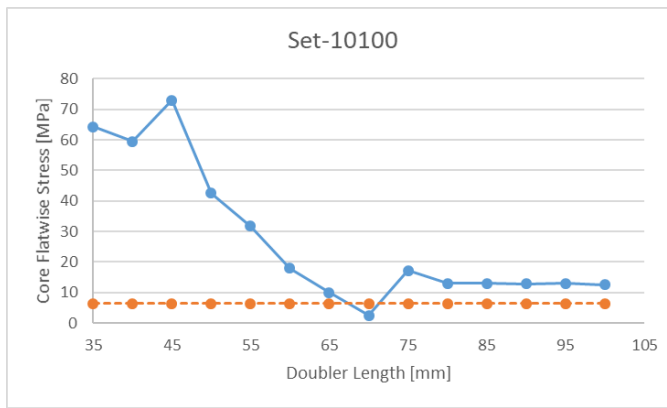


Figure A.21. Core Flatwise Stress vs Doubler Length of Set-10100

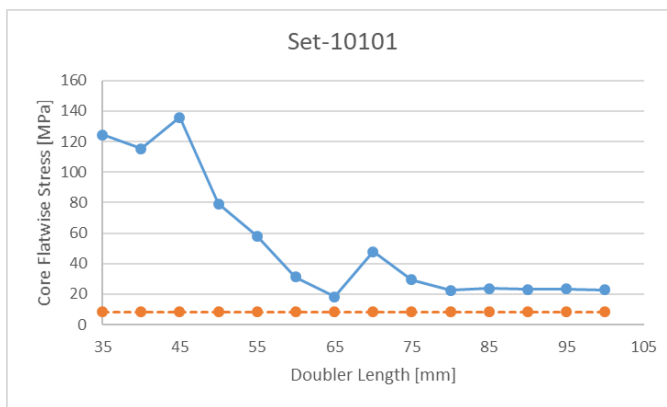


Figure A.22. Core Flatwise Stress vs Doubler Length of Set-10101

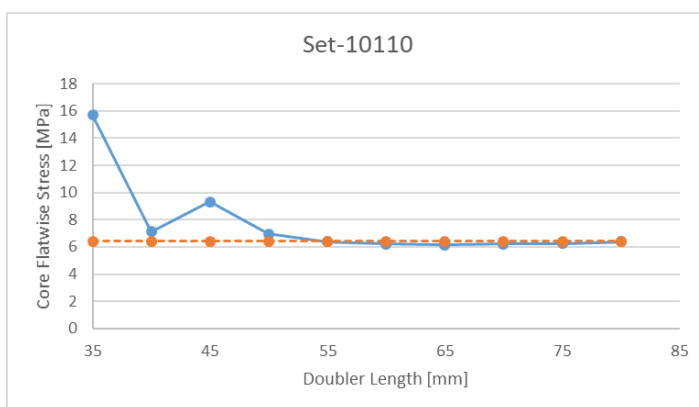


Figure A.23. Core Flatwise Stress vs Doubler Length of Set-10110

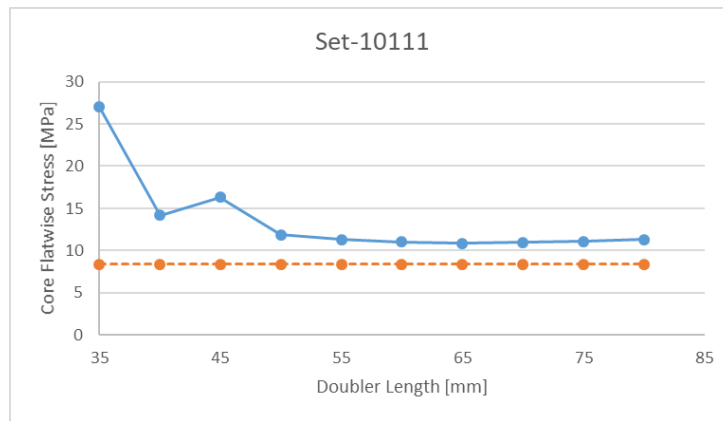


Figure A.24. Core Flatwise Stress vs Doubler Length of Set-10111

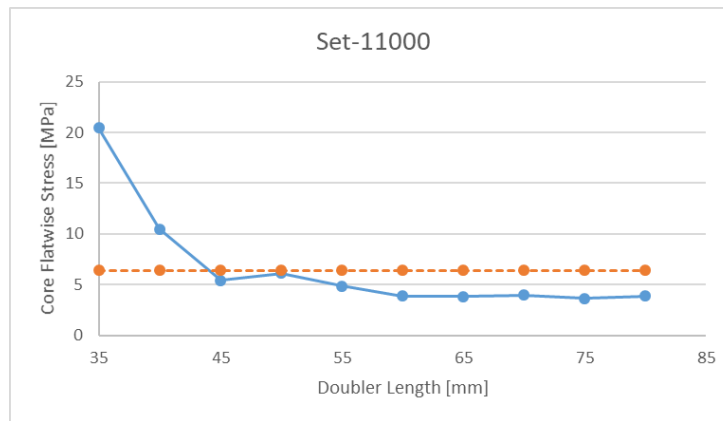


Figure A.25. Core Flatwise Stress vs Doubler Length of Set-11000

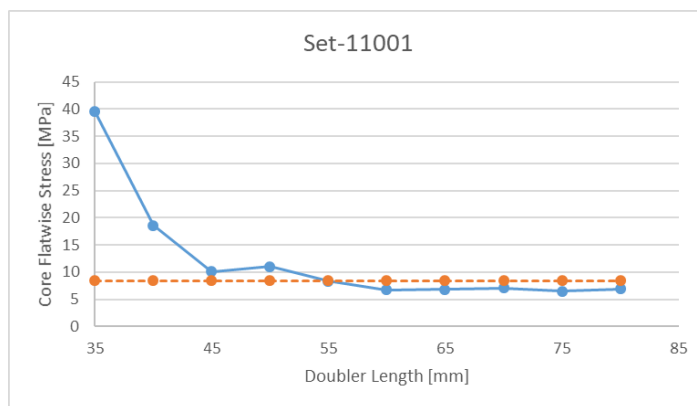


Figure A.26. Core Flatwise Stress vs Doubler Length of Set-11001

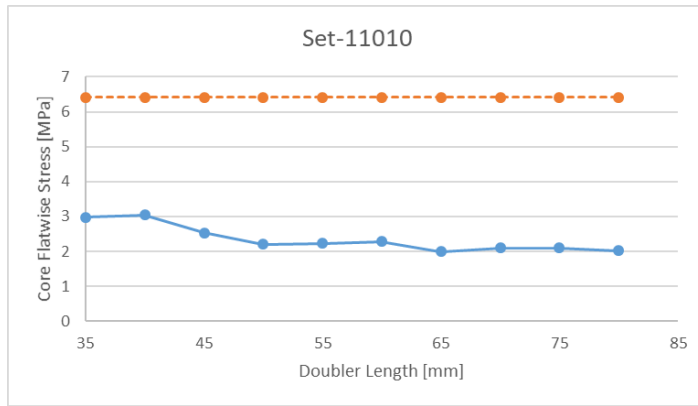


Figure A.27. Core Flatwise Stress vs Doubler Length of Set-11010

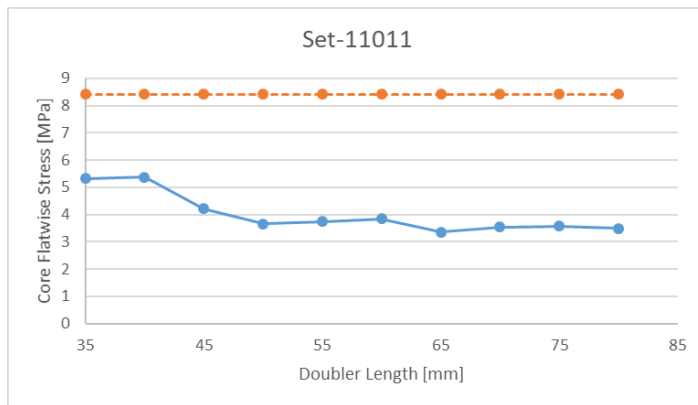


Figure A.28. Core Flatwise Stress vs Doubler Length of Set-11011

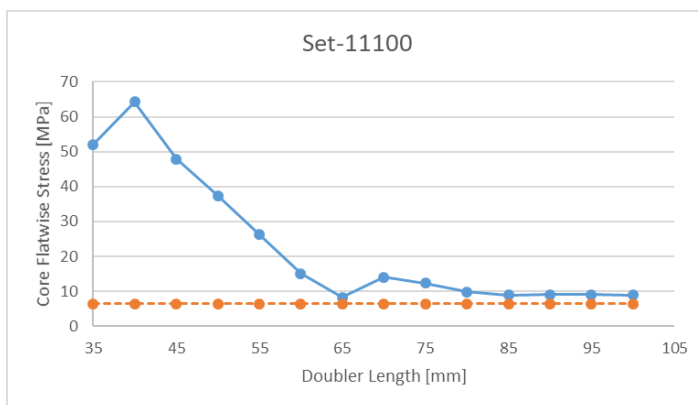


Figure A.29. Core Flatwise Stress vs Doubler Length of Set-11100



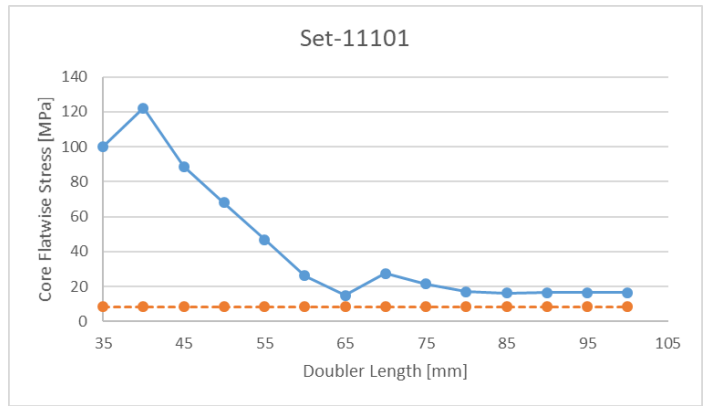


Figure A.30. Core Flatwise Stress vs Doubler Length of Set-11101

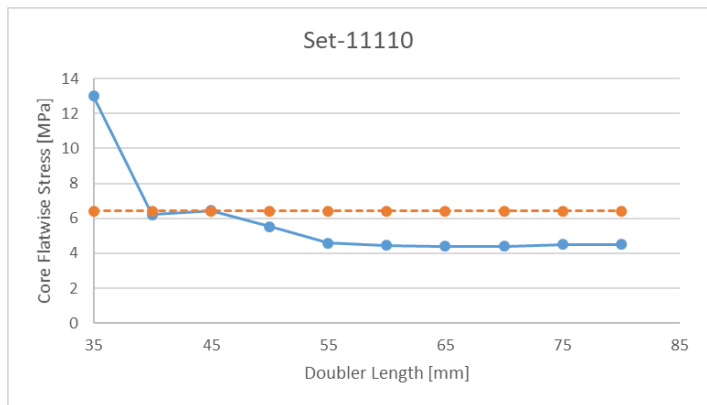


Figure A.31. Core Flatwise Stress vs Doubler Length of Set-11110

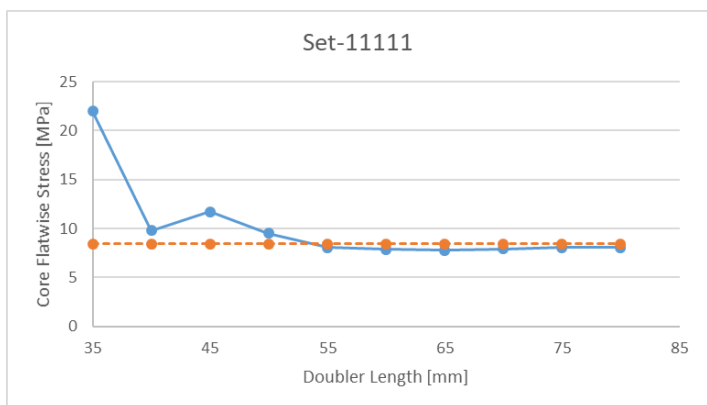


Figure A.32. Core Flatwise Stress vs Doubler Length of Set-11111



## B. SCRIPT FOR FIXED BOUNDARY CONDITION

```
from abaqus import *
from abaqusConstants import *
from caeModules import *
from driverUtils import executeOnCaeStartup
from part import *
from material import *
from section import *
from assembly import *
from step import *
from interaction import *
from load import *
from mesh import *
from optimization import *
from job import *
from sketch import *
from visualization import *
from connectorBehavior import *
import math
import time

#-----#

#INPUTS#

#Geometric Inputs
leff = 210 # effective span length between constraints, mm
b = 70 #width, mm
l1 = 22 #length of the region w/o core, mm
l2 = 27 #distance between the support and the core, mm
l = leff+2*l1 # total span length, mm
upperfacethickness = [0.4,0.6] #upper face thickness, mm
lowerfacethickness = [0.4,0.6] #lower face thickness, mm
doublerthickness = [1,2] #doubler thickness, mm
corethickness = [12.7,25.4] # core thickness, mm
ramp_angle_array = [30,60] #ramp angle, degrees
r_indenter = 20 #indenter radius, mm
core_span = l-2*l2 #total core length, mm

cellsize = 3.2 # core cell size, mm
RibbonDirection = 1

#Materials
#Mechanical Properties
Eu = 72395 # Young's Modulus of the upper face, MPa
El = Eu # Young's Modulus of the lower face, MPa

vu = 0.3 # Poisson's ratio of the upper face
vl = vu # Poisson's ratio of the lower face

E33_array = [670,1034] # Core flatwise modulus, MPa
G13_array = [310,482] # Core shear modulus in ribbon direction, MPa
G23_array = [138,214] # Core shear modulus in transverse direction, MPa

#Allowable Values
Ftransverse_array = [0.76,1.16] # core shear strength in transverse direction, MPa
Fribbon_array = [1.38,1.97] # core shear strength in transverse direction, MPa
S33_allowable_array = [6.41,8.41] #Core flatwise tension allowable, MPa

Fcy1 = 268 # Compressive Yield Strength of the upper face, MPa
Fcy2 = 268 # Compressive Yield Strength of the lower face, MPa

#Materials
upperfacematerial = 'al2024_solid'
```

```

lowerfacematerial = 'al2024_solid'
corematerial = 'core_solid'
indentermaterial = 'steel_solid'

#Mesh Size
coremeshsize = 1.5
indentermeshsize = 8
lowerfacemeshsize = 1.75
upperfacemeshsize = 1.75

for tu in upperfacethickness:
    tu_ind = upperfacethickness.index(tu)
    tl = lowerfacethickness[tu_ind]
    for td in doublerthickness:
        td_ind = doublerthickness.index(td)
        for tc in corethickness:
            tc_ind = corethickness.index(tc)
            for ramp_angle in ramp_angle_array:
                ramp_angle_ind = ramp_angle_array.index(ramp_angle)
                for E33 in E33_array:
                    E33_ind = E33_array.index(E33)
                    G13 = G13_array[E33_ind]
                    G23 = G23_array[E33_ind]
                    Ftransverse=Ftransverse_array[E33_ind]
                    Fribbon=Fribbon_array[E33_ind]
                    S33_allowable=S33_allowable_array[E33_ind]

                #Allowable Load Calculation

                # %Necessary Calculations%
                h = tu/2+tl/2+tc # distance between the facing centroids

                lambda1 = 1-math.pow(vu,2)
                lambda2 = 1-math.pow(vl,2)

                Gc = min(G13,G23)

                #-----#

                # % Intracell Buckling %

                #Compression
                Fc = 2*Eu/lambda1*math.pow((tu/cellsize),2);

                #Shear
                Fs = 0.6*Eu*math.pow((tu/cellsize), (1.5))

                #-----#

                # % Wrinkling %

                if tc<=1.82*tu*math.pow((Eu*E33/math.pow(Gc,2)), (1/3)):
                    Fw = 0.247*math.pow((Eu*E33*Gc), (1/3))+0.078*Gc*tc/tu
                else:
                    Fw = 0.333*math.pow((tu/tc*E33*Eu), (1/2))

                #-----#

                # % Shear Crimping %

                Fsc = math.pow(h,2)*Gc/((tu+tl)*tc)

                #-----#

                # %MAXIMUM LOAD DETERMINATION%

```

```

#For Ends Built-in and Center Load
P_ib = Fc*8*b*tc*0.5*(tu+tl)/leff
P_wr = Fs*8*b*tc*0.5*(tu+tl)/leff
P_sc = Fsc*8*b*tc*0.5*(tu+tl)/leff
P_cs_transverse = Ftransverse*h*b*2
P_cs_ribbon = Fribbon*h*leff*2
comp_vecl = [P_ib, P_wr, P_sc, P_cs_transverse, P_cs_ribbon]
P_critical = min(comp_vecl)

i_count=1

mdb.Model(name='Model-'+str(i_count),modelType=STANDARD_EXPLICIT)

doubler_span = 35 #total doubler length, mm

while doubler_span<81:
    parameterstore=open('PARAMETERS'+Set-'+str(tu_ind)+str(td_ind)\
+str(tc_ind)+str(ramp_angle_ind)+str(E33_ind)+'_UL_'\
+str(doubler_span)+'.txt', "a+")

    core_doubler = doubler_span-12
    #-----#
    #Upperface and Doubler Geometry#
    s = mdb.models['Model-'+str(i_count)].ConstrainedSketch\
(name='__profile__', sheetSize=200.0)
    g, v, d, c = s.geometry, s.vertices, s.dimensions, s.constraints
    s.setPrimaryObject(option=STANDALONE)
    s.Spot(point=(0.0, 0.0))
    s.FixedConstraint(entity=v[0])
    s.Line(point1=(0.0, 0.0), point2=(0.0, 1.25))
    s.VerticalConstraint(entity=g[2], addUndoState=False)
    s.Line(point1=(0.0, 1.25), point2=(-17.5, 1.25))
    s.HorizontalConstraint(entity=g[3], addUndoState=False)
    s.PerpendicularConstraint(entity1=g[2], entity2=g[3],\
addUndoState=False)
    s.Line(point1=(-17.5, 1.25), point2=(-17.5, -1.25))
    s.VerticalConstraint(entity=g[4], addUndoState=False)
    s.PerpendicularConstraint(entity1=g[3], entity2=g[4], \
addUndoState=False)
    s.Line(point1=(-17.5, -1.25), point2=(51.25, -1.25))
    s.HorizontalConstraint(entity=g[5], addUndoState=False)
    s.PerpendicularConstraint(entity1=g[4], entity2=g[5],\
addUndoState=False)
    s.Line(point1=(51.25, -1.25), point2=(51.25, 1.25))
    s.VerticalConstraint(entity=g[6], addUndoState=False)
    s.PerpendicularConstraint(entity1=g[5], entity2=g[6],\
addUndoState=False)
    s.Line(point1=(51.25, 1.25), point2=(36.25, 1.25))
    s.HorizontalConstraint(entity=g[7], addUndoState=False)
    s.PerpendicularConstraint(entity1=g[6], entity2=g[7],\
addUndoState=False)
    s.Line(point1=(36.25, 1.25), point2=(36.25, 0.0))
    s.VerticalConstraint(entity=g[8], addUndoState=False)
    s.PerpendicularConstraint(entity1=g[7], entity2=g[8],\
addUndoState=False)
    s.Line(point1=(36.25, 0.0), point2=(0.0, 0.0))
    s.HorizontalConstraint(entity=g[9], addUndoState=False)
    s.PerpendicularConstraint(entity1=g[8], entity2=g[9],\
addUndoState=False)
    s.ObliqueDimension(vertex1=v[4], vertex2=v[5],\
textPoint=(-14.9218101501465,-4.77973556518555),\
value=1)
    s.DistanceDimension(entity1=g[9], entity2=g[5], \
textPoint=(5.05195045471191,-0.771825790405273),\
value=tu)
    s.DistanceDimension(entity1=g[3], entity2=g[5], \

```

```

textPoint=(-34.7716369628906, 0.383661270141602),\
value=tu+td)
s.DistanceDimension(entity1=g[7], entity2=g[5],\
textPoint=(40.1471405029297, 0.383661270141602),\
value=tu+td)
s.ObliqueDimension(vertex1=v[2], vertex2=v[3],\
textPoint=(-39.1848068237305,3.53499412536621),\
value=doubler_span)
s.ObliqueDimension(vertex1=v[6], vertex2=v[7],\
textPoint=(108.235977172852,5.95101451873779),\
value=doubler_span)

p = mdb.models['Model-'+str(i_count)].Part(name='upperface',\
dimensionality=THREE_D, type=DEFORMABLE_BODY)
p = mdb.models['Model-'+str(i_count)].parts['upperface']
p.BaseSolidExtrude(sketch=s, depth=b)
s.unsetPrimaryObject()
p = mdb.models['Model-'+str(i_count)].parts['upperface']

#partition1
p = mdb.models['Model-'+str(i_count)].parts['upperface']
f, e, d = p.faces, p.edges, p.datums
t = p.MakeSketchTransform(sketchPlane=f[3], sketchUpEdge=e[8],\
sketchPlaneSide=SIDE1, origin=(0, -tu, b/2))
s = mdb.models['Model-'+str(i_count)].ConstrainedSketch\
(name='__profile__',sheetSize=526.93, gridSpacing=13.17,\
transform=t)
g, v, dl, c = s.geometry, s.vertices, s.dimensions,\
s.constraints
s.setPrimaryObject(option=SUPERIMPOSE)
p = mdb.models['Model-'+str(i_count)].parts['upperface']
p.projectReferencesOntoSketch(sketch=s, \
filter=COPLANAR_EDGES)

s.Line(point1=(0, b/2), point2=(0, -b/2))
s.VerticalConstraint(entity=g[6], addUndoState=False)
s.Line(point1=(0-2*doubler_span+1, -b/2), point2=(0-2*doubler_span+1, b/2))
s.VerticalConstraint(entity=g[7], addUndoState=False)
s.Line(point1=(11-doubler_span, b/2), \
point2=(11-doubler_span, -b/2))
s.VerticalConstraint(entity=g[8], addUndoState=False)
s.Line(point1=(11-doubler_span+leff, -b/2), \
point2=(11-doubler_span+leff, b/2))
s.VerticalConstraint(entity=g[9], addUndoState=False)
p = mdb.models['Model-'+str(i_count)].parts['upperface']
f = p.faces
pickedFaces = f.getSequenceFromMask(mask=('[#8 ]', ), )
e1, d2 = p.edges, p.datums
p.PartitionFaceBySketch(sketchUpEdge=e1[8],\
faces=pickedFaces, sketch=s)
s.unsetPrimaryObject()
del mdb.models['Model-'+str(i_count)].sketches['__profile__']
p = mdb.models['Model-'+str(i_count)].parts['upperface']
c = p.cells
pickedCells = c.getSequenceFromMask(mask=('[#1 ]', ), )
e, v1, d = p.edges, p.vertices, p.datums
p.PartitionCellByPlanePointNormal(point=v1[9],\
normal=e[24], cells=pickedCells)
p = mdb.models['Model-'+str(i_count)].parts['upperface']
c = p.cells
pickedCells = c.getSequenceFromMask(mask=('[#2 ]', ), )
e1, v2, d2 = p.edges, p.vertices, p.datums
p.PartitionCellByPlanePointNormal(point=v2[19],\
normal=e1[25], cells=pickedCells)
p = mdb.models['Model-'+str(i_count)].parts['upperface']
c = p.cells
pickedCells = c.getSequenceFromMask(mask=('[#4 ]', ), )
e, v1, d = p.edges, p.vertices, p.datums

```

```

p.PartitionCellByPlanePointNormal (point=v1[20],\
normal=e[30], cells=pickedCells)
p = mdb.models['Model-'+str(i_count)].parts['upperface']
c = p.cells
pickedCells = c.getSequenceFromMask(mask=('[#1 ]', ), )
e1, v2, d2 = p.edges, p.vertices, p.datums
p.PartitionCellByPlanePointNormal (point=v2[20],\
normal=e1[34], cells=pickedCells)

a = mdb.models['Model-'+str(i_count)].rootAssembly
a.DatumCsysByDefault (CARTESIAN)
p = mdb.models['Model-'+str(i_count)].parts['upperface']
a.Instance (name='upperface-1', part=p, dependent=ON)

#Core Geometry#
s1 = mdb.models['Model-'+str(i_count)].\
ConstrainedSketch(name='_profile_', sheetSize=200.0)
g, v, d, c = s1.geometry, s1.vertices, s1.dimensions,\
s1.constraints
s1.setPrimaryObject (option=STANDALONE)
s1.Spot (point=(0.0, 0.0))
s1.FixedConstraint (entity=v[0])
s1.Line (point1=(0.0, 0.0), point2=(0.0, 2.5))
s1.VerticalConstraint (entity=g[2], addUndoState=False)
s1.Line (point1=(0.0, 2.5), point2=(-27.5, 2.5))
s1.HorizontalConstraint (entity=g[3], addUndoState=False)
s1.PerpendicularConstraint (entity1=g[2], entity2=g[3], \
addUndoState=False)
s1.Line (point1=(-27.5, 2.5), point2=(-8.75, 21.25))
s1.Line (point1=(-8.75, 21.25), point2=(48.75, 21.25))
s1.HorizontalConstraint (entity=g[5], addUndoState=False)
s1.Line (point1=(48.75, 21.25), point2=(62.5, 2.5))
s1.Line (point1=(62.5, 2.5), point2=(43.75, 2.5))
s1.HorizontalConstraint (entity=g[7], addUndoState=False)
s1.Line (point1=(43.75, 2.5), point2=(43.75, 0.0))
s1.VerticalConstraint (entity=g[8], addUndoState=False)
s1.PerpendicularConstraint (entity1=g[7], entity2=g[8], \
addUndoState=False)
s1.Line (point1=(43.75, 0.0), point2=(0.0, 0.0))
s1.HorizontalConstraint (entity=g[9], addUndoState=False)
s1.PerpendicularConstraint (entity1=g[8], entity2=g[9], \
addUndoState=False)
s1.AngularDimension (line1=g[4], line2=g[3], \
textPoint=(-15.9243221282959, 6.78413534164429), value=ramp_angle)
s1.AngularDimension (line1=g[6], line2=g[7], \
textPoint=(56.1013412475586, 6.55285787582397), value=ramp_angle)
s1.DistanceDimension (entity1=g[9], entity2=g[5], \
textPoint=(18.3919734954834, 15.4184970855713), value=tc)
s1.HorizontalDimension (vertex1=v[7], vertex2=v[6], \
textPoint=(62.3476791381836, -3.23788666725159), value=core_doubler)
s1.ObliqueDimension (vertex1=v[2], vertex2=v[3], \
textPoint=(-7.75010108947754, 0.385461449623108), value=core_doubler)
s1.HorizontalDimension (vertex1=v[3], vertex2=v[6], \
textPoint=(58.9546051025391, -7.86343622207642), value=core_span)
s1.ObliqueDimension (vertex1=v[2], vertex2=v[0], \
textPoint=(2.99417114257813, 0.0), value=td)
s1.DistanceDimension (entity1=g[7], entity2=g[9], \
textPoint=(143.669281005859, 0.470926284790039), value=td)
p = mdb.models['Model-'+str(i_count)].Part (name='core', \
dimensionality=THREE_D, type=DEFORMABLE_BODY)
p = mdb.models['Model-'+str(i_count)].parts['core']
p.BaseSolidExtrude (sketch=s1, depth=b)
s1.unsetPrimaryObject ()
p = mdb.models['Model-'+str(i_count)].parts['core']
a.DatumCsysByDefault (CARTESIAN)

```

```

a = mdb.models['Model-'+str(i_count)].rootAssembly
p = mdb.models['Model-'+str(i_count)].parts['core']
a.Instance(name='core-1', part=p, dependent=ON)

#Lowerface Geometry#
s2 = mdb.models['Model-'+str(i_count)].ConstrainedSketch\
(name='__profile__', sheetSize=200.0)
g, v, d, c = s2.geometry, s2.vertices, s2.dimensions,\
s2.constraints
s2.setPrimaryObject(option=STANDALONE)
s2.Spot(point=((tc-td)/tan(degreeToRadian(ramp_angle))\
+l2-doubler_span, tc))
s2.FixedConstraint(entity=v[0])
s2.Line(point1=((tc-td)/tan(degreeToRadian(ramp_angle))\
+l2-doubler_span, tc),\
point2=((tc-td)/tan(degreeToRadian(ramp_angle))+l2\
-doubler_span, tc+tl))
s2.VerticalConstraint(entity=g[2], addUndoState=False)
s2.Line(point1=((tc-td)/tan(degreeToRadian(ramp_angle))\
+l2-doubler_span, tc+tl),\
point2=(core_span-(tc-td)/tan(degreeToRadian(ramp_angle))\
-doubler span+l2,tc+tl))
s2.HorizontalConstraint(entity=g[3], addUndoState=False)
s2.PerpendicularConstraint(entity1=g[2], entity2=g[3],\
addUndoState=False)
s2.Line(point1=(core_span-(tc-td)/tan(degreeToRadian(ramp_angle))\
-doubler_span+l2,\
tc+tl), point2=(core_span-(tc-td)/tan(degreeToRadian(ramp_angle))\
-doubler_span+l2,tc))
s2.Line(point1=(core_span-(tc-td)/tan(degreeToRadian(ramp_angle))\
-doubler_span+l2,tc)\
, point2=((tc-td)/tan(degreeToRadian(ramp_angle))+l2-doubler_span, tc))
s2.HorizontalConstraint(entity=g[5], addUndoState=False)
p = mdb.models['Model-'+str(i_count)].Part(name='lowerface',\
dimensionality=THREE_D, type=DEFORMABLE_BODY)
p = mdb.models['Model-'+str(i_count)].parts['lowerface']
p.BaseSolidExtrude(sketch=s2, depth=b)
s2.unsetPrimaryObject()
p = mdb.models['Model-'+str(i_count)].parts['lowerface']
session.viewports['Viewport: 1'].setValues(displayedObject=p)
del mdb.models['Model-'+str(i_count)].sketches['__profile__']
a = mdb.models['Model-'+str(i_count)].rootAssembly
a = mdb.models['Model-'+str(i_count)].rootAssembly
a.DatumCsysByDefault(CARTESIAN)
p = mdb.models['Model-'+str(i_count)].parts['lowerface']
a.Instance(name='lowerface-1', part=p, dependent=ON)
p = mdb.models['Model-'+str(i_count)].parts['lowerface']
a.Instance(name='lowerface-1', part=p, dependent=ON)

#indenter Geometry#
s = mdb.models['Model-'+str(i_count)].ConstrainedSketch\
(name='__profile__', sheetSize=200.0)
g, v, d, c = s.geometry, s.vertices, s.dimensions, s.constraints
s.setPrimaryObject(option=STANDALONE)

s.ArcByCenterEnds(center=(0.5*l-doubler_span, -r_indenter-tu),\
point1=(0.5*l-doubler_span\
-r_indenter, -r_indenter-tu), point2=(0.5*l-doubler_span+r_indenter,\
-r_indenter-tu), direction=COUNTERCLOCKWISE)
s.Line(point1=(0.5*l-doubler_span-r_indenter, -r_indenter-tu),\
point2=(0.5*l-doubler_span+r_indenter, -r_indenter-tu))
s.HorizontalConstraint(entity=g[3], addUndoState=False)
p = mdb.models['Model-'+str(i_count)].Part(name='indenter',\
dimensionality=THREE_D, type=DEFORMABLE_BODY)
p = mdb.models['Model-'+str(i_count)].parts['indenter']
p.BaseSolidExtrude(sketch=s, depth=b)

a = mdb.models['Model-'+str(i_count)].rootAssembly

```



```

a = mdb.models['Model-'+str(i_count)].rootAssembly
p = mdb.models['Model-'+str(i_count)].parts['indenter']
a.Instance(name='indenter-1', part=p, dependent=ON)
a.Instance(name='indenter-1', part=p, dependent=ON)
a = mdb.models['Model-'+str(i_count)].rootAssembly
a.rotate(instanceList=('indenter-1', ), axisPoint=(0.5*1
-doubler_span, -r_indenter-tu, 70.0),\
axisDirection=(0.0, 0.0, -70.0), angle=180.0)

#-----#

#Material and Section Assignments
#Material
mdb.models['Model-'+str(i_count)].Material(name='al2024')
mdb.models['Model-'+str(i_count)].materials['al2024'].\
Elastic(table=((Eu, nu), ))
mdb.models['Model-'+str(i_count)].Material(name='core')
mdb.models['Model-'+str(i_count)].materials['core'].\
Elastic(type=ENGINEERING_CONSTANTS,\
table=((0.1, 0.1, E33, 0.0, 0.0, 0.0, 0.01, G13, G23), ))
mdb.models['Model-'+str(i_count)].Material(name='steel')
mdb.models['Model-'+str(i_count)].materials['steel'].\
Elastic(table=((196000.0, 0.3), ))

#Sections
mdb.models['Model-'+str(i_count)].HomogeneousSolidSection\
(name='al2024_solid',\
material='al2024', thickness=None)
mdb.models['Model-'+str(i_count)].HomogeneousSolidSection\
(name='steel_solid', \
material='steel', thickness=None)
mdb.models['Model-'+str(i_count)].HomogeneousSolidSection\
(name='core_solid',\
material='core', thickness=None)

#Section Assignments

#CORE
p = mdb.models['Model-'+str(i_count)].parts['core']
session.viewports['Viewport: 1'].setValues(displayedObject=p)
p = mdb.models['Model-'+str(i_count)].parts['core']
c = p.cells
cells = c.getSequenceFromMask(mask=('[#1 ]', ), )
region = p.Set(cells=cells, name='Set-1')
p = mdb.models['Model-'+str(i_count)].parts['core']
p.SectionAssignment(region=region, sectionName=corematerial,\
offset=0.0, offsetType=MIDDLE_SURFACE, offsetField='', \
thicknessAssignment=FROM_SECTION)
p = mdb.models['Model-'+str(i_count)].parts['core']
c = p.cells
cells = c.getSequenceFromMask(mask=('[#1 ]', ), )
region = regionToolset.Region(cells=cells)
p = mdb.models['Model-'+str(i_count)].parts['core']
s = p.faces
sidelFaces = s.getSequenceFromMask(mask=('[#8 ]', ), )
normalAxisRegion = p.Surface(sidelFaces=sidelFaces, name='Surf-2')
p = mdb.models['Model-'+str(i_count)].parts['core']
e = p.edges
edges = e.getSequenceFromMask(mask=('[#100 ]', ), )
primaryAxisRegion = p.Set(edges=edges, name='Set-4')
mdb.models['Model-'+str(i_count)].parts['core'].\

```

```

MaterialOrientation(region=region,\
orientationType=DISCRETE, axis=AXIS_1, normalAxisDefinition=SURFACE,\
normalAxisRegion=normalAxisRegion, flipNormalDirection=False,\
normalAxisDirection=AXIS_3, primaryAxisDefinition=EDGE, \
primaryAxisRegion=primaryAxisRegion, primaryAxisDirection=AXIS_1, \
flipPrimaryDirection=False, additionalRotationType=ROTATION_NONE,\
angle=0.0, additionalRotationField='', stackDirection=STACK_3)

#indenter
p = mdb.models['Model-'+str(i_count)].parts['indenter']
session.viewports['Viewport: 1'].setValues(displayedObject=p)
p = mdb.models['Model-'+str(i_count)].parts['indenter']
c = p.cells
cells = c.getSequenceFromMask(mask=('[#1 ]', ), )
region = p.Set(cells=cells, name='Set-1')
p = mdb.models['Model-'+str(i_count)].parts['indenter']
p.SectionAssignment(region=region, sectionName=indentermaterial,\
offset=0.0,offsetType=MIDDLE_SURFACE, offsetField='',\
thicknessAssignment=FROM_SECTION)

#LOWERFACE
p = mdb.models['Model-'+str(i_count)].parts['lowerface']
session.viewports['Viewport: 1'].setValues(displayedObject=p)
p = mdb.models['Model-'+str(i_count)].parts['lowerface']
c = p.cells
cells = c.getSequenceFromMask(mask=('[#1 ]', ), )
region = p.Set(cells=cells, name='Set-1')
p = mdb.models['Model-'+str(i_count)].parts['lowerface']
p.SectionAssignment(region=region, sectionName=lowerfacematerial,\
offset=0.0, offsetType=MIDDLE_SURFACE, offsetField='', \
thicknessAssignment=FROM_SECTION)

#UPPERFACE
p = mdb.models['Model-'+str(i_count)].parts['upperface']
session.viewports['Viewport: 1'].setValues(displayedObject=p)
p = mdb.models['Model-'+str(i_count)].parts['upperface']
c = p.cells
cells = c.getSequenceFromMask(mask=('[#1f ]', ), )
region = p.Set(cells=cells, name='Set-1')
p = mdb.models['Model-'+str(i_count)].parts['upperface']
p.SectionAssignment(region=region, sectionName=upperfacematerial, \
offset=0.0, offsetType=MIDDLE_SURFACE, offsetField='', \
thicknessAssignment=FROM_SECTION)

#-----#

#STEP
mdb.models['Model-'+str(i_count)].StaticStep(name='Step-1', \
previous='Initial',maxNumInc=1000, initialInc=0.01, minInc=1e-08)

#-----#

#TIE_CONSTRAINTS

#Upperface-Doubler-Core
a = mdb.models['Model-'+str(i_count)].rootAssembly
s1 = a.instances['upperface-1'].faces
sidelFaces1 = s1.getSequenceFromMask(mask=('[#2002004 ]', ), )
region1=a.Surface(sidelFaces=sidelFaces1, name='m_Surf-10')

a = mdb.models['Model-'+str(i_count)].rootAssembly
s1 = a.instances['core-1'].faces
sidelFaces1 = s1.getSequenceFromMask(mask=('[#a2 ]', ), )
region2=a.Surface(sidelFaces=sidelFaces1, name='s_Surf-12')
mdb.models['Model-'+str(i_count)].Tie(name='Constraint-1', \
master=region1, slave=region2,\
positionToleranceMethod=COMPUTED, adjust=OFF, tieRotations=ON,\
thickness=ON)

```

```

#Lowerface-Core
a = mdb.models['Model-'+str(i_count)].rootAssembly
s1 = a.instances['lowerface-1'].faces
sidelFaces1 = s1.getSequenceFromMask(mask=('[#8 ]', ), )
region1=a.Surface(sidelFaces=sidelFaces1, name='m_Surf-3')
a = mdb.models['Model-'+str(i_count)].rootAssembly
s1 = a.instances['core-1'].faces
sidelFaces1 = s1.getSequenceFromMask(mask=('[#8 ]', ), )
region2=a.Surface(sidelFaces=sidelFaces1, name='s_Surf-3')
mdb.models['Model-'+str(i_count)].Tie(name='Constraint-2',\
master=region1, slave=region2, \
positionToleranceMethod=COMPUTED, adjust=OFF, tieRotations=ON,\
thickness=ON)

#-----#

#MESH

#core
p = mdb.models['Model-'+str(i_count)].parts['core']
session.viewports['Viewport: 1'].setValues(displayedObject=p)
p = mdb.models['Model-'+str(i_count)].parts['core']
p.seedPart(size=coremeshsize, deviationFactor=0.1, \
minSizeFactor=0.1)
p = mdb.models['Model-'+str(i_count)].parts['core']
p.generateMesh()

#indenter
p = mdb.models['Model-'+str(i_count)].parts['indenter']
session.viewports['Viewport: 1'].setValues(displayedObject=p)
p = mdb.models['Model-'+str(i_count)].parts['indenter']
p.seedPart(size=indentermeshsize, deviationFactor=0.1, \
minSizeFactor=0.1)
p = mdb.models['Model-'+str(i_count)].parts['indenter']
c = p.cells
pickedRegions = c.getSequenceFromMask(mask=('[#1 ]', ), )
p.setMeshControls(regions=pickedRegions, algorithm=MEDIAL_AXIS)
p = mdb.models['Model-'+str(i_count)].parts['indenter']
p.generateMesh()

#lowerface
p = mdb.models['Model-'+str(i_count)].parts['lowerface']
session.viewports['Viewport: 1'].setValues(displayedObject=p)
p = mdb.models['Model-'+str(i_count)].parts['lowerface']
p.seedPart(size=lowerfacemeshsize, deviationFactor=0.1, \
minSizeFactor=0.1)
p = mdb.models['Model-'+str(i_count)].parts['lowerface']
p.generateMesh()

#upperface
p = mdb.models['Model-'+str(i_count)].parts['upperface']
session.viewports['Viewport: 1'].setValues(displayedObject=p)
p = mdb.models['Model-'+str(i_count)].parts['upperface']
p.seedPart(size=upperfacemeshsize, deviationFactor=0.1, \
minSizeFactor=0.1)
p = mdb.models['Model-'+str(i_count)].parts['upperface']
c = p.cells
pickedRegions = c.getSequenceFromMask(mask=('[#1f ]', ), )
p.setMeshControls(regions=pickedRegions, technique=SWEEP, \
algorithm=MEDIAL_AXIS)
p = mdb.models['Model-'+str(i_count)].parts['upperface']
p.generateMesh()

#-----#

#CONTACT_DEFINITIONS

```

```

#Interaction Definition
mdb.models['Model-'+str(i_count)].ContactProperty('IntProp-1')
mdb.models['Model-'+str(i_count)].interactionProperties\
['IntProp-1'].TangentialBehavior(formulation=PENALTY, \
directionality=ISOTROPIC, slipRateDependency=OFF, \
pressureDependency=OFF, temperatureDependency=OFF,dependencies=0, table=((\
0.5, ), ), shearStressLimit=None, maximumElasticSlip=FRACTION, \
fraction=0.005, elasticSlipStiffness=None)
mdb.models['Model-'+str(i_count)].interactionProperties['IntProp-1'].\
NormalBehavior(pressureOverclosure=HARD, allowSeparation=ON,\
constraintEnforcementMethod=DEFAULT)

#indenter-to-upperface
a = mdb.models['Model-'+str(i_count)].rootAssembly
s1 = a.instances['indenter-1'].faces
sidelFaces1 = s1.getSequenceFromMask(mask=('[#1 ]', ), )
region1=a.Surface(sidelFaces=sidelFaces1, name='m_Surf-11')
a = mdb.models['Model-'+str(i_count)].rootAssembly
s1 = a.instances['upperface-1'].faces
sidelFaces1 = s1.getSequenceFromMask(mask=('[#10000 ]', ), )
region2=a.Surface(sidelFaces=sidelFaces1, name='s_Surf-11')
mdb.models['Model-'+str(i_count)].SurfaceToSurfaceContactStd(name='Int-1',\
createStepName='Initial', master=region1, slave=region2, sliding=FINITE,\
thickness=ON, interactionProperty='IntProp-1', surfaceSmoothing=AUTOMATIC,\
adjustMethod=OVERCLOSED, initialClearance=OMIT, datumAxis=None,\
clearanceRegion=None, tied=OFF)

#-----#

#BOUNDARY CONDITION

a = mdb.models['Model-'+str(i_count)].rootAssembly
f1 = a.instances['upperface-1'].faces
faces1 = f1.getSequenceFromMask(mask=('[#8a4000 ]', ), )
region = a.Set(faces=faces1, name='Set-3')
mdb.models['Model-'+str(i_count)].EncastreBC(name='encastre', \
createStepName='Initial',region=region, localCsys=None)

a = mdb.models['Model-'+str(i_count)].rootAssembly
f1 = a.instances['indenter-1'].faces
faces1 = f1.getSequenceFromMask(mask=('[#c ]', ), )
region = a.Set(faces=faces1, name='Set-2')
mdb.models['Model-'+str(i_count)].DisplacementBC(name='indenter', \
createStepName='Initial', region=region, u1=SET, u2=UNSET, \
u3=SET, ur1=UNSET, ur2=UNSET, ur3=UNSET, \
amplitude=UNSET, distributionType=UNIFORM, fieldName='', localCsys=None)

#-----#

#LOAD

a = mdb.models['Model-'+str(i_count)].rootAssembly
s1 = a.instances['indenter-1'].faces
sidelFaces1 = s1.getSequenceFromMask(mask=('[#2 ]', ), )
region = a.Surface(sidelFaces=sidelFaces1, name='Surf-31')
mdb.models['Model-'+str(i_count)].Pressure(name='Load-1',\
createStepName='Step-1', region=region, distributionType=TOTAL_FORCE,\
field='', magnitude=P_critical, amplitude=UNSET)

#-----#

#JOB
mdb.Job(name='Set-'+str(tu_ind)+str(td_ind)+str(tc_ind)+\
str(ramp_angle_ind)+str(E33_ind)+'_UL_'\
+str(doubler_span), model='Model-'+str(i_count), description='', \
type=ANALYSIS,atTime=None, waitMinutes=0, waitHours=0,\
queue=None, memory=90, memoryUnits=PERCENTAGE, \

```

```

getMemoryFromAnalysis=True, explicitPrecision=SINGLE, \
nodalOutputPrecision=SINGLE, echoPrint=OFF, modelPrint=OFF, \
contactPrint=OFF, historyPrint=OFF, userSubroutine='', \
scratch='', resultsFormat=ODB, multiprocessingMode=DEFAULT, \
numCpus=4,numDomains=4, numGPUs=0)

mdb.jobs['Set-'+str(tu_ind)+str(td_ind)+str(tc_ind)\
+str(ramp_angle_ind)+str(E33_ind)+'_UL_'+str(doubler_span)].submit()

mdb.jobs['Set-'+str(tu_ind)+str(td_ind)+str(tc_ind)\
+str(ramp_angle_ind)+str(E33_ind)+'_UL_'+str(doubler_span)].\
waitForCompletion()

#-----#

#READ FIELD OUTPUT

from odbAccess import *

o1 = session.openOdb(name='C:\Temp\Set-'+str(tu_ind)+\
str(td_ind)+str(tc_ind)+str(ramp_angle_ind)+str(E33_ind)+\
'_UL_'+str(doubler_span)+'.odb')
session.viewports['Viewport: 1'].setValues(displayedObject=o1)

odb = session.odbs['C:\Temp\Set-'+str(tu_ind)+str(td_ind)+str(tc_ind)\
+str(ramp_angle_ind)+str(E33_ind)+'_UL_'+str(doubler_span)+'.odb']
lastFrame = odb.steps['Step-1'].frames[-1]
session.fieldReportOptions.setValues(printXYData=OFF, printMinMax=ON)
session.writeFieldReport(fileName='CORE_S33'+str(tu_ind)+\
str(td_ind)+str(tc_ind)+str(ramp_angle_ind)\
+str(E33_ind)+'_UL_'+str(doubler_span)+'.rpt', append=ON,\
sortItem='Element Label', odb=odb, step=0, frame=lastFrame,
outputPosition=INTEGRATION_POINT, variable=((('S',\
INTEGRATION_POINT, ((COMPONENT, 'S33'), )), ))

core_S33_lines_UL = []

filepath = 'CORE_S33'+str(tu_ind)+str(td_ind)+str(tc_ind)\
+str(ramp_angle_ind)+str(E33_ind)+'_UL_'+str(doubler_span)+'.rpt'
with open(filepath) as fp:
    line = fp.readline()
    cnt = 1
    while line:
        core_S33_lines_UL.append("Line {}: {}".format(cnt, line.strip()))
        line = fp.readline()
        cnt += 1

    wo_space = core_S33_lines_UL[23].replace(" ", "")
    onlynumber = wo_space.replace("Line24:Maximum", "")
    S33_core_UL = float(onlynumber)
    parameterstore.write("Doubler Span %d\r\n" % (doubler_span))
    parameterstore.write("Core Stress %d\r\n" % (S33_core_UL))
    parameterstore.close()
    doubler_span=doubler_span+5
    i_count = i_count+1
    mdb.Model(name='Model-'+str(i_count), modelType=STANDARD_EXPLICIT)

mdb.saveAs(pathName='C:/Temp/'+str(tu_ind)+str(td_ind)+str(tc_ind)\
+str(ramp_angle_ind)+str(E33_ind)+'_UL')

modelindex = 1
while modelindex<i_count:
    del mdb.models['Model-'+str(modelindex)]
    modelindex = modelindex+1

```



## C. SCRIPT FOR SIMPLY SUPPORTED BOUNDARY CONDITION

```
from abaqus import *
from abaqusConstants import *
from caeModules import *
from driverUtils import executeOnCaeStartup
from part import *
from material import *
from section import *
from assembly import *
from step import *
from interaction import *
from load import *
from mesh import *
from optimization import *
from job import *
from sketch import *
from visualization import *
from connectorBehavior import *
import math
import time

#-----#

#INPUTS#

#Geometric Inputs
leff = 210 # effective span length between constraints, mm
b = 70 #width, mm
l1 = 22 #length of the region w/o core, mm
l2 = 27 #distance between the support and the core, mm
l = leff+2*l1 # total span length, mm
upperfacethickness = [0.4,0.6] #upper face thickness, mm
lowerfacethickness = [0.4,0.6] #lower face thickness, mm
doublerthickness = [1,2] #doubler thickness, mm
corethickness = [12.7,25.4] # core thickness, mm
ramp_angle_array = [30,60] #ramp angle, degrees
r_indenter = 20 #indenter radius, mm
core_span = l-2*l2 #total core length, mm

cellsize = 3.2 # core cell size, mm
RibbonDirection = 1

#Materials
#Mechanical Properties
Eu = 72395 # Young's Modulus of the upper face, MPa
El = Eu # Young's Modulus of the lower face, MPa

vu = 0.3 # Poisson's ratio of the upper face
vl = vu # Poisson's ratio of the lower face

E33_array = [670,1034] # Core flatwise modulus, MPa
G13_array = [310,482] # Core shear modulus in ribbon direction, MPa
G23_array = [138,214] # Core shear modulus in transverse direction, MPa

#Allowable Values
Ftransverse_array = [0.76,1.16] # core shear strength in transverse direction, MPa
Fribbon_array = [1.38,1.97] # core shear strength in transverse direction, MPa
S33_allowable_array = [6.41,8.41] #Core flatwise tension allowable, MPa

Fcy1 = 268 # Compressive Yield Strength of the upper face, MPa
Fcy2 = 268 # Compressive Yield Strength of the lower face, MPa

#Materials
upperfacematerial = 'al2024_solid'
```

```

lowerfacematerial = 'al2024_solid'
corematerial = 'core_solid'
indentermaterial = 'steel_solid'

#Mesh Size
coremeshsize = 1.5
indentermeshsize = 8
lowerfacemeshsize = 1.75
upperfacemeshsize = 1.75

for tu in upperfacethickness:
    tu_ind = upperfacethickness.index(tu)
    tl = lowerfacethickness[tu_ind]
    for td in doublerthickness:
        td_ind = doublerthickness.index(td)
        for tc in corethickness:
            tc_ind = corethickness.index(tc)
            for ramp_angle in ramp_angle_array:
                ramp_angle_ind = ramp_angle_array.index(ramp_angle)
                for E33 in E33_array:
                    E33_ind = E33_array.index(E33)
                    G13 = G13_array[E33_ind]
                    G23 = G23_array[E33_ind]
                    Ftransverse=Ftransverse_array[E33_ind]
                    Fribbon=Fribbon_array[E33_ind]
                    S33_allowable=S33_allowable_array[E33_ind]

                #Allowable Load Calculation

                # %Necessary Calculations%
                h = tu/2+tl/2+tc # distance between the facing centroids

                lambda1 = 1-math.pow(vu,2)
                lambda2 = 1-math.pow(vl,2)

                Gc = min(G13,G23)

                #-----#

                # % Intracell Buckling %

                #Compression
                Fc = 2*Eu/lambda1*math.pow((tu/cellsize),2);

                #Shear
                Fs = 0.6*Eu*math.pow((tu/cellsize), (1.5))

                #-----#

                # % Wrinkling %

                if tc<=1.82*tu*math.pow((Eu*E33/math.pow(Gc,2)), (1/3)):
                    Fw = 0.247*math.pow((Eu*E33*Gc), (1/3))+0.078*Gc*tc/tu
                else:
                    Fw = 0.333*math.pow((tu/tc*E33*Eu), (1/2))

                #-----#

                # % Shear Crimping %

                Fsc = math.pow(h,2)*Gc/((tu+tl)*tc)

                #-----#

                # %MAXIMUM LOAD DETERMINATION%

                #For Ends Built-in and Center Load
                P_ib = Fc*8*b*tc*0.5*(tu+tl)/leff

```



```

P_wr = Fs*8*b*tc*0.5*(tu+tl)/leff
P_sc = Fsc*8*b*tc*0.5*(tu+tl)/leff
P_cs_transverse = Ftransverse*h*b*2
P_cs_ribbon = Fribbon*h*leff*2
comp_vec1 = [P_ib, P_wr, P_sc, P_cs_transverse, P_cs_ribbon]
P_critical = min(comp_vec1)

i_count=1

mdb.Model(name='Model-'+str(i_count),modelType=STANDARD_EXPLICIT)

doubler_span = 35 #total doubler length, mm

while doubler_span<81:
    parameterstore=open('PARAMETERS'+str(i_count)+'Set-'+str(tu_ind)+str(td_ind)\
+str(tc_ind)+str(ramp_angle_ind)+str(E33_ind)+'_UL'\
+str(doubler_span)+'.txt', "a+")

    core_doubler = doubler_span-12
    #-----#
    #Upperface and Doubler Geometry#
    s = mdb.models['Model-'+str(i_count)].ConstrainedSketch\
(name='__profile__', sheetSize=200.0)
    g, v, d, c = s.geometry, s.vertices, s.dimensions, s.constraints
    s.setPrimaryObject(option=STANDALONE)
    s.Spot(point=(0.0, 0.0))
    s.FixedConstraint(entity=v[0])
    s.Line(point1=(0.0, 0.0), point2=(0.0, 1.25))
    s.VerticalConstraint(entity=g[2], addUndoState=False)
    s.Line(point1=(0.0, 1.25), point2=(-17.5, 1.25))
    s.HorizontalConstraint(entity=g[3], addUndoState=False)
    s.PerpendicularConstraint(entity1=g[2], entity2=g[3],\
addUndoState=False)
    s.Line(point1=(-17.5, 1.25), point2=(-17.5, -1.25))
    s.VerticalConstraint(entity=g[4], addUndoState=False)
    s.PerpendicularConstraint(entity1=g[3], entity2=g[4], \
addUndoState=False)
    s.Line(point1=(-17.5, -1.25), point2=(51.25, -1.25))
    s.HorizontalConstraint(entity=g[5], addUndoState=False)
    s.PerpendicularConstraint(entity1=g[4], entity2=g[5],\
addUndoState=False)
    s.Line(point1=(51.25, -1.25), point2=(51.25, 1.25))
    s.VerticalConstraint(entity=g[6], addUndoState=False)
    s.PerpendicularConstraint(entity1=g[5], entity2=g[6],\
addUndoState=False)
    s.Line(point1=(51.25, 1.25), point2=(36.25, 1.25))
    s.HorizontalConstraint(entity=g[7], addUndoState=False)
    s.PerpendicularConstraint(entity1=g[6], entity2=g[7],\
addUndoState=False)
    s.Line(point1=(36.25, 1.25), point2=(36.25, 0.0))
    s.VerticalConstraint(entity=g[8], addUndoState=False)
    s.PerpendicularConstraint(entity1=g[7], entity2=g[8],\
addUndoState=False)
    s.Line(point1=(36.25, 0.0), point2=(0.0, 0.0))
    s.HorizontalConstraint(entity=g[9], addUndoState=False)
    s.PerpendicularConstraint(entity1=g[8], entity2=g[9],\
addUndoState=False)
    s.ObliqueDimension(vertex1=v[4], vertex2=v[5],\
textPoint=(-14.9218101501465,-4.77973556518555),\
value=1)
    s.DistanceDimension(entity1=g[9], entity2=g[5], \
textPoint=(5.05195045471191,-0.771825790405273),\
value=tu)
    s.DistanceDimension(entity1=g[3], entity2=g[5],\
textPoint=(-34.7716369628906, 0.383661270141602),\
value=tu+td)

```

```

s.DistanceDimension(entity1=g[7], entity2=g[5],\
textPoint=(40.1471405029297, 0.383661270141602),\
value=tu+td)
s.ObliqueDimension(vertex1=v[2], vertex2=v[3],\
textPoint=(-39.1848068237305,3.53499412536621),\
value=doubler_span)
s.ObliqueDimension(vertex1=v[6], vertex2=v[7],\
textPoint=(108.235977172852,5.95101451873779),\
value=doubler_span)

p = mdb.models['Model-'+str(i_count)].Part(name='upperface',\
dimensionality=THREE_D, type=DEFORMABLE_BODY)
p = mdb.models['Model-'+str(i_count)].parts['upperface']
p.BaseSolidExtrude(sketch=s, depth=b)
s.unsetPrimaryObject()
p = mdb.models['Model-'+str(i_count)].parts['upperface']

#partition1
p = mdb.models['Model-'+str(i_count)].parts['upperface']
f, e, d = p.faces, p.edges, p.datums
t = p.MakeSketchTransform(sketchPlane=f[3], sketchUpEdge=e[8],\
sketchPlaneSide=SIDE1, origin=(0, -tu, b/2))
s = mdb.models['Model-'+str(i_count)].ConstrainedSketch(\
(name='__profile__',sheetSize=526.93, gridSpacing=13.17,\
transform=t)
g, v, dl, c = s.geometry, s.vertices, s.dimensions,\
s.constraints
s.setPrimaryObject(option=SUPERIMPOSE)
p = mdb.models['Model-'+str(i_count)].parts['upperface']
p.projectReferencesOntoSketch(sketch=s, \
filter=COPLANAR_EDGES)

s.Line(point1=(0, b/2), point2=(0, -b/2))
s.VerticalConstraint(entity=g[6], addUndoState=False)
s.Line(point1=(0-2*doubler_span+1, -b/2), point2=(0-2*doubler_span+1, b/2))
s.VerticalConstraint(entity=g[7], addUndoState=False)
s.Line(point1=(11-doubler_span, b/2), \
point2=(11-doubler_span, -b/2))
s.VerticalConstraint(entity=g[8], addUndoState=False)
s.Line(point1=(11-doubler_span+leff, -b/2), \
point2=(11-doubler_span+leff, b/2))
s.VerticalConstraint(entity=g[9], addUndoState=False)
p = mdb.models['Model-'+str(i_count)].parts['upperface']
f = p.faces
pickedFaces = f.getSequenceFromMask(mask=('[#8 ]', ), )
e1, d2 = p.edges, p.datums
p.PartitionFaceBySketch(sketchUpEdge=e1[8],\
faces=pickedFaces, sketch=s)
s.unsetPrimaryObject()
del mdb.models['Model-'+str(i_count)].sketches['__profile__']
p = mdb.models['Model-'+str(i_count)].parts['upperface']
c = p.cells
pickedCells = c.getSequenceFromMask(mask=('[#1 ]', ), )
e, v1, d = p.edges, p.vertices, p.datums
p.PartitionCellByPlanePointNormal(point=v1[9],\
normal=e[24], cells=pickedCells)
p = mdb.models['Model-'+str(i_count)].parts['upperface']
c = p.cells
pickedCells = c.getSequenceFromMask(mask=('[#2 ]', ), )
e1, v2, d2 = p.edges, p.vertices, p.datums
p.PartitionCellByPlanePointNormal(point=v2[19],\
normal=e1[25], cells=pickedCells)
p = mdb.models['Model-'+str(i_count)].parts['upperface']
c = p.cells
pickedCells = c.getSequenceFromMask(mask=('[#4 ]', ), )
e, v1, d = p.edges, p.vertices, p.datums
p.PartitionCellByPlanePointNormal(point=v1[20],\
normal=e[30], cells=pickedCells)

```

```

p = mdb.models['Model-'+str(i_count)].parts['upperface']
c = p.cells
pickedCells = c.getSequenceFromMask(mask=('[#1 ]', ), )
e1, v2, d2 = p.edges, p.vertices, p.datums
p.PartitionCellByPlanePointNormal(point=v2[20],\
normal=e1[34], cells=pickedCells)

```

```

a = mdb.models['Model-'+str(i_count)].rootAssembly
a.DatumCsysByDefault(CARTESIAN)
p = mdb.models['Model-'+str(i_count)].parts['upperface']
a.Instance(name='upperface-1', part=p, dependent=ON)

```

#### #Core Geometry#

```

s1 = mdb.models['Model-'+str(i_count)].\
ConstrainedSketch(name='__profile__', sheetSize=200.0)
g, v, d, c = s1.geometry, s1.vertices, s1.dimensions,\
s1.constraints
s1.setPrimaryObject(option=STANDALONE)
s1.Spot(point=(0.0, 0.0))
s1.FixedConstraint(entity=v[0])
s1.Line(point1=(0.0, 0.0), point2=(0.0, 2.5))
s1.VerticalConstraint(entity=g[2], addUndoState=False)
s1.Line(point1=(0.0, 2.5), point2=(-27.5, 2.5))
s1.HorizontalConstraint(entity=g[3], addUndoState=False)
s1.PerpendicularConstraint(entity1=g[2], entity2=g[3], \
addUndoState=False)
s1.Line(point1=(-27.5, 2.5), point2=(-8.75, 21.25))
s1.Line(point1=(-8.75, 21.25), point2=(48.75, 21.25))
s1.HorizontalConstraint(entity=g[5], addUndoState=False)
s1.Line(point1=(48.75, 21.25), point2=(62.5, 2.5))
s1.Line(point1=(62.5, 2.5), point2=(43.75, 2.5))
s1.HorizontalConstraint(entity=g[7], addUndoState=False)
s1.Line(point1=(43.75, 2.5), point2=(43.75, 0.0))
s1.VerticalConstraint(entity=g[8], addUndoState=False)
s1.PerpendicularConstraint(entity1=g[7], entity2=g[8], \
addUndoState=False)
s1.Line(point1=(43.75, 0.0), point2=(0.0, 0.0))
s1.HorizontalConstraint(entity=g[9], addUndoState=False)
s1.PerpendicularConstraint(entity1=g[8], entity2=g[9], \
addUndoState=False)
s1.AngularDimension(line1=g[4], line2=g[3], \
textPoint=(-15.9243221282959, 6.78413534164429), value=ramp_angle)
s1.AngularDimension(line1=g[6], line2=g[7], \
textPoint=(56.1013412475586, 6.55285787582397), value=ramp_angle)
s1.DistanceDimension(entity1=g[9], entity2=g[5], \
textPoint=(18.3919734954834, 15.4184970855713), value=tc)
s1.HorizontalDimension(vertex1=v[7], vertex2=v[6], \
textPoint=(62.3476791381836, -3.23788666725159), value=core_doubler)
s1.ObliqueDimension(vertex1=v[2], vertex2=v[3], \
textPoint=(-7.75010108947754, 0.385461449623108), value=core_doubler)
s1.HorizontalDimension(vertex1=v[3], vertex2=v[6], \
textPoint=(58.9546051025391, -7.86343622207642), value=core_span)
s1.ObliqueDimension(vertex1=v[2], vertex2=v[0], \
textPoint=(2.99417114257813, 0.0), value=td)
s1.DistanceDimension(entity1=g[7], entity2=g[9], \
textPoint=(143.669281005859, 0.470926284790039), value=td)
p = mdb.models['Model-'+str(i_count)].Part(name='core', \
dimensionality=THREE_D, type=DEFORMABLE_BODY)
p = mdb.models['Model-'+str(i_count)].parts['core']
p.BaseSolidExtrude(sketch=s1, depth=b)
s1.unsetPrimaryObject()
p = mdb.models['Model-'+str(i_count)].parts['core']
a.DatumCsysByDefault(CARTESIAN)
a = mdb.models['Model-'+str(i_count)].rootAssembly
p = mdb.models['Model-'+str(i_count)].parts['core']

```

```

a.Instance(name='core-1', part=p, dependent=ON)

#Lowerface Geometry#
s2 = mdb.models['Model-'+str(i_count)].ConstrainedSketch\
(name='__profile__', sheetSize=200.0)
g, v, d, c = s2.geometry, s2.vertices, s2.dimensions,\
s2.constraints
s2.setPrimaryObject(option=STANDALONE)
s2.Spot(point=((tc-td)/tan(degreeToRadian(ramp_angle))\
+l2-doubler_span, tc))
s2.FixedConstraint(entity=v[0])
s2.Line(point1=((tc-td)/tan(degreeToRadian(ramp_angle))\
+l2-doubler_span, tc),\
point2=((tc-td)/tan(degreeToRadian(ramp_angle))+l2\
-doubler_span, tc+tl))
s2.VerticalConstraint(entity=g[2], addUndoState=False)
s2.Line(point1=((tc-td)/tan(degreeToRadian(ramp_angle))\
+l2-doubler_span, tc+tl),\
point2=(core_span-(tc-td)/tan(degreeToRadian(ramp_angle))\
-doubler_span+l2,tc+tl))
s2.HorizontalConstraint(entity=g[3], addUndoState=False)
s2.PerpendicularConstraint(entity1=g[2], entity2=g[3],\
addUndoState=False)
s2.Line(point1=(core_span-(tc-td)/tan(degreeToRadian(ramp_angle))\
-doubler_span+l2,\
tc+tl), point2=(core_span-(tc-td)/tan(degreeToRadian(ramp_angle))\
-doubler_span+l2,tc))
s2.Line(point1=(core_span-(tc-td)/tan(degreeToRadian(ramp_angle))\
-doubler_span+l2,tc)\
, point2=((tc-td)/tan(degreeToRadian(ramp_angle))+l2-doubler_span, tc))
s2.HorizontalConstraint(entity=g[5], addUndoState=False)
p = mdb.models['Model-'+str(i_count)].Part(name='lowerface',\
dimensionality=THREE_D, type=DEFORMABLE_BODY)
p = mdb.models['Model-'+str(i_count)].parts['lowerface']
p.BaseSolidExtrude(sketch=s2, depth=b)
s2.unsetPrimaryObject()
p = mdb.models['Model-'+str(i_count)].parts['lowerface']
session.viewports['Viewport: 1'].setValues(displayedObject=p)
del mdb.models['Model-'+str(i_count)].sketches['__profile__']
a = mdb.models['Model-'+str(i_count)].rootAssembly
a = mdb.models['Model-'+str(i_count)].rootAssembly
a.DatumCsysByDefault(CARTESIAN)
p = mdb.models['Model-'+str(i_count)].parts['lowerface']
a.Instance(name='lowerface-1', part=p, dependent=ON)
p = mdb.models['Model-'+str(i_count)].parts['lowerface']
a.Instance(name='lowerface-1', part=p, dependent=ON)

#indenter Geometry#
s = mdb.models['Model-'+str(i_count)].ConstrainedSketch\
(name='__profile__', sheetSize=200.0)
g, v, d, c = s.geometry, s.vertices, s.dimensions, s.constraints
s.setPrimaryObject(option=STANDALONE)

s.ArcByCenterEnds(center=(0.5*l-doubler_span, -r_indenter-tu),\
point1=(0.5*l-doubler_span\
-r_indenter, -r_indenter-tu), point2=(0.5*l-doubler_span+r_indenter,\
-r_indenter-tu), direction=COUNTERCLOCKWISE)
s.Line(point1=(0.5*l-doubler_span-r_indenter, -r_indenter-tu),\
point2=(0.5*l-doubler_span+r_indenter, -r_indenter-tu))
s.HorizontalConstraint(entity=g[3], addUndoState=False)
p = mdb.models['Model-'+str(i_count)].Part(name='indenter',\
dimensionality=THREE_D, type=DEFORMABLE_BODY)
p = mdb.models['Model-'+str(i_count)].parts['indenter']
p.BaseSolidExtrude(sketch=s, depth=b)

a = mdb.models['Model-'+str(i_count)].rootAssembly

a = mdb.models['Model-'+str(i_count)].rootAssembly

```

```

p = mdb.models['Model-'+str(i_count)].parts['indenter']
a.Instance(name='indenter-1', part=p, dependent=ON)
a.Instance(name='indenter-1', part=p, dependent=ON)
a = mdb.models['Model-'+str(i_count)].rootAssembly
a.rotate(instanceList=('indenter-1', ), axisPoint=(0.5*1
-doubler_span, -r_indenter-tu, 70.0),\
axisDirection=(0.0, 0.0, -70.0), angle=180.0)

#-----#

#Material and Section Assignments
#Material
mdb.models['Model-'+str(i_count)].Material(name='al2024')
mdb.models['Model-'+str(i_count)].materials['al2024'].\
Elastic(table=((Eu, nu), ))
mdb.models['Model-'+str(i_count)].Material(name='core')
mdb.models['Model-'+str(i_count)].materials['core'].\
Elastic(type=ENGINEERING_CONSTANTS,\
table=((0.1, 0.1, E33, 0.0, 0.0, 0.0, 0.01, G13, G23), ))
mdb.models['Model-'+str(i_count)].Material(name='steel')
mdb.models['Model-'+str(i_count)].materials['steel'].\
Elastic(table=((196000.0, 0.3), ))

#Sections
mdb.models['Model-'+str(i_count)].HomogeneousSolidSection\
(name='al2024_solid',\
material='al2024', thickness=None)
mdb.models['Model-'+str(i_count)].HomogeneousSolidSection\
(name='steel_solid', \
material='steel', thickness=None)
mdb.models['Model-'+str(i_count)].HomogeneousSolidSection\
(name='core_solid',\
material='core', thickness=None)

#Section Assignments

#CORE
p = mdb.models['Model-'+str(i_count)].parts['core']
session.viewports['Viewport: 1'].setValues(displayedObject=p)
p = mdb.models['Model-'+str(i_count)].parts['core']
c = p.cells
cells = c.getSequenceFromMask(mask=('#1 ', ), )
region = p.Set(cells=cells, name='Set-1')
p = mdb.models['Model-'+str(i_count)].parts['core']
p.SectionAssignment(region=region, sectionName=corematerial,\
offset=0.0, offsetType=MIDDLE_SURFACE, offsetField='', \
thicknessAssignment=FROM_SECTION)
p = mdb.models['Model-'+str(i_count)].parts['core']
c = p.cells
cells = c.getSequenceFromMask(mask=('#1 ', ), )
region = regionToolset.Region(cells=cells)
p = mdb.models['Model-'+str(i_count)].parts['core']

#Material orientation
p = mdb.models['Model-'+str(i_count)].parts['core']
c = p.cells
cells = c.getSequenceFromMask(mask=('#1 ', ), )
region = regionToolset.Region(cells=cells)
p = mdb.models['Model-'+str(i_count)].parts['core']
s = p.faces
sidelFaces = s.getSequenceFromMask(mask=('#8 ', ), )
normalAxisRegion = p.Surface(sidelFaces=sidelFaces, name='Surf-2')
p = mdb.models['Model-'+str(i_count)].parts['core']
e = p.edges
edges = e.getSequenceFromMask(mask=('#100 ', ), )
primaryAxisRegion = p.Set(edges=edges, name='Set-4')
mdb.models['Model-'+str(i_count)].parts['core'].\
MaterialOrientation(region=region,\

```

```

orientationType=DISCRETE, axis=AXIS_1, normalAxisDefinition=SURFACE,\
normalAxisRegion=normalAxisRegion, flipNormalDirection=False,\
normalAxisDirection=AXIS_3, primaryAxisDefinition=EDGE, \
primaryAxisRegion=primaryAxisRegion, primaryAxisDirection=AXIS_1, \
flipPrimaryDirection=False, additionalRotationType=ROTATION_NONE,\
angle=0.0, additionalRotationField='', stackDirection=STACK_3)

#indenter
p = mdb.models['Model-'+str(i_count)].parts['indenter']
session.viewports['Viewport: 1'].setValues(displayedObject=p)
p = mdb.models['Model-'+str(i_count)].parts['indenter']
c = p.cells
cells = c.getSequenceFromMask(mask=('[#1 ]', ), )
region = p.Set(cells=cells, name='Set-1')
p = mdb.models['Model-'+str(i_count)].parts['indenter']
p.SectionAssignment(region=region, sectionName=indentermaterial,\
offset=0.0, offsetType=MIDDLE_SURFACE, offsetField='', \
thicknessAssignment=FROM_SECTION)

#LOWERFACE
p = mdb.models['Model-'+str(i_count)].parts['lowerface']
session.viewports['Viewport: 1'].setValues(displayedObject=p)
p = mdb.models['Model-'+str(i_count)].parts['lowerface']
c = p.cells
cells = c.getSequenceFromMask(mask=('[#1 ]', ), )
region = p.Set(cells=cells, name='Set-1')
p = mdb.models['Model-'+str(i_count)].parts['lowerface']
p.SectionAssignment(region=region, sectionName=lowerfacematerial,\
offset=0.0, offsetType=MIDDLE_SURFACE, offsetField='', \
thicknessAssignment=FROM_SECTION)

#UPPERFACE
p = mdb.models['Model-'+str(i_count)].parts['upperface']
session.viewports['Viewport: 1'].setValues(displayedObject=p)
p = mdb.models['Model-'+str(i_count)].parts['upperface']
c = p.cells
cells = c.getSequenceFromMask(mask=('[#1f ]', ), )
region = p.Set(cells=cells, name='Set-1')
p = mdb.models['Model-'+str(i_count)].parts['upperface']
p.SectionAssignment(region=region, sectionName=upperfacematerial, \
offset=0.0, offsetType=MIDDLE_SURFACE, offsetField='', \
thicknessAssignment=FROM_SECTION)

#-----#

#STEP
mdb.models['Model-'+str(i_count)].StaticStep(name='Step-1', \
previous='Initial', maxNumInc=1000, initialInc=0.01, minInc=1e-08)

#-----#

#TIE_CONSTRAINTS

#Upperface-Doubler-Core
a = mdb.models['Model-'+str(i_count)].rootAssembly
s1 = a.instances['upperface-1'].faces
sides1Faces1 = s1.getSequenceFromMask(mask=('[#2002004 ]', ), )
region1=a.Surface(sides1Faces=sides1Faces1, name='m_Surf-10')

a = mdb.models['Model-'+str(i_count)].rootAssembly
s1 = a.instances['core-1'].faces
sides1Faces1 = s1.getSequenceFromMask(mask=('[#a2 ]', ), )
region2=a.Surface(sides1Faces=sides1Faces1, name='s_Surf-12')
mdb.models['Model-'+str(i_count)].Tie(name='Constraint-1', \
master=region1, slave=region2,\
positionToleranceMethod=COMPUTED, adjust=OFF, tieRotations=ON,\
thickness=ON)

```

```

#Lowerface-Core
a = mdb.models['Model-'+str(i_count)].rootAssembly
s1 = a.instances['lowerface-1'].faces
sidelFaces1 = s1.getSequenceFromMask(mask=('[#8 ]', ), )
region1=a.Surface(sidelFaces=sidelFaces1, name='m_Surf-3')
a = mdb.models['Model-'+str(i_count)].rootAssembly
s1 = a.instances['core-1'].faces
sidelFaces1 = s1.getSequenceFromMask(mask=('[#8 ]', ), )
region2=a.Surface(sidelFaces=sidelFaces1, name='s_Surf-3')
mdb.models['Model-'+str(i_count)].Tie(name='Constraint-2',\
master=region1, slave=region2, \
positionToleranceMethod=COMPUTED, adjust=OFF, tieRotations=ON,\
thickness=ON)

#-----#

#MESH

#core
p = mdb.models['Model-'+str(i_count)].parts['core']
session.viewports['Viewport: 1'].setValues(displayedObject=p)
p = mdb.models['Model-'+str(i_count)].parts['core']
p.seedPart(size=coremeshsize, deviationFactor=0.1, \
minSizeFactor=0.1)
p = mdb.models['Model-'+str(i_count)].parts['core']
p.generateMesh()

#indenter
p = mdb.models['Model-'+str(i_count)].parts['indenter']
session.viewports['Viewport: 1'].setValues(displayedObject=p)
p = mdb.models['Model-'+str(i_count)].parts['indenter']
p.seedPart(size=indentermeshsize, deviationFactor=0.1,\
minSizeFactor=0.1)
p = mdb.models['Model-'+str(i_count)].parts['indenter']
c = p.cells
pickedRegions = c.getSequenceFromMask(mask=('[#1 ]', ), )
p.setMeshControls(regions=pickedRegions, algorithm=MEDIAL_AXIS)
p = mdb.models['Model-'+str(i_count)].parts['indenter']
p.generateMesh()

#lowerface
p = mdb.models['Model-'+str(i_count)].parts['lowerface']
session.viewports['Viewport: 1'].setValues(displayedObject=p)
p = mdb.models['Model-'+str(i_count)].parts['lowerface']
p.seedPart(size=lowerfacemeshsize, deviationFactor=0.1,\
minSizeFactor=0.1)
p = mdb.models['Model-'+str(i_count)].parts['lowerface']
p.generateMesh()

#upperface
p = mdb.models['Model-'+str(i_count)].parts['upperface']
session.viewports['Viewport: 1'].setValues(displayedObject=p)
p = mdb.models['Model-'+str(i_count)].parts['upperface']
p.seedPart(size=upperfacemeshsize, deviationFactor=0.1,\
minSizeFactor=0.1)
p = mdb.models['Model-'+str(i_count)].parts['upperface']
c = p.cells
pickedRegions = c.getSequenceFromMask(mask=('[#1f ]', ), )
p.setMeshControls(regions=pickedRegions, technique=SWEEP,\
algorithm=MEDIAL_AXIS)
p = mdb.models['Model-'+str(i_count)].parts['upperface']
p.generateMesh()

#-----#

#CONTACT_DEFINITIONS

```

```

#Interaction Definition
mdb.models['Model-'+str(i_count)].ContactProperty('IntProp-1')
mdb.models['Model-'+str(i_count)].interactionProperties\
['IntProp-1'].TangentialBehavior(formulation=PENALTY, \
directionality=ISOTROPIC, slipRateDependency=OFF, \
pressureDependency=OFF, temperatureDependency=OFF,dependencies=0, table=((\
0.5, ), ), shearStressLimit=None, maximumElasticSlip=FRACTION, \
fraction=0.005, elasticSlipStiffness=None)
mdb.models['Model-'+str(i_count)].interactionProperties['IntProp-1'].\
NormalBehavior(pressureOverclosure=HARD, allowSeparation=ON,\
constraintEnforcementMethod=DEFAULT)

#indenter-to-upperface
a = mdb.models['Model-'+str(i_count)].rootAssembly
s1 = a.instances['indenter-1'].faces
side1Faces1 = s1.getSequenceFromMask(mask=('[#1 ]', ), )
region1=a.Surface(side1Faces=side1Faces1, name='m_Surf-11')
a = mdb.models['Model-'+str(i_count)].rootAssembly
s1 = a.instances['upperface-1'].faces
side1Faces1 = s1.getSequenceFromMask(mask=('[#10000 ]', ), )
region2=a.Surface(side1Faces=side1Faces1, name='s_Surf-11')
mdb.models['Model-'+str(i_count)].SurfaceToSurfaceContactStd(name='Int-1',\
createStepName='Initial', master=region1, slave=region2, sliding=FINITE,\
thickness=ON, interactionProperty='IntProp-1', surfaceSmoothing=AUTOMATIC,\
adjustMethod=OVERCLOSED, initialClearance=OMIT, datumAxis=None,\
clearanceRegion=None, tied=OFF)

#-----#

#BOUNDARY CONDITION

a = mdb.models['Model-'+str(i_count)].rootAssembly
e1 = a.instances['upperface-1'].edges
edges1 = e1.getSequenceFromMask(mask=('[#0 #1 ]', ), )
region = a.Set(edges=edges1, name='Set-7')
mdb.models['Model-'+str(i_count)].DisplacementBC(name='fixed_edge',\
createStepName='Initial', region=region, u1=SET, u2=SET, u3=SET, \
url=UNSET, ur2=UNSET, ur3=UNSET, amplitude=UNSET,\
distributionType=UNIFORM, fieldName='', localCsys=None)

a = mdb.models['Model-'+str(i_count)].rootAssembly
e1 = a.instances['upperface-1'].edges
edges1 = e1.getSequenceFromMask(mask=('[#2 ]', ), )
region = a.Set(edges=edges1, name='Set-8')
mdb.models['Model-'+str(i_count)].DisplacementBC(name=\
'y_constraint', createStepName='Initial', \region=region,\
u1=UNSET, u2=SET, u3=UNSET, url1=UNSET, ur2=UNSET, ur3=UNSET,\
amplitude=UNSET, distributionType=UNIFORM, fieldName='', \
localCsys=None)

a = mdb.models['Model-'+str(i_count)].rootAssembly
f1 = a.instances['indenter-1'].faces
faces1 = f1.getSequenceFromMask(mask=('[#c ]', ), )
region = a.Set(faces=faces1, name='Set-2')
mdb.models['Model-'+str(i_count)].DisplacementBC(name='indenter',\
createStepName='Initial', region=region, u1=SET, u2=UNSET, u3=SET, \
url1=UNSET, ur2=UNSET, ur3=UNSET, amplitude=UNSET, distributionType=UNIFORM,\
fieldName='', localCsys=None)

#-----#

#LOAD

a = mdb.models['Model-'+str(i_count)].rootAssembly
s1 = a.instances['indenter-1'].faces
side1Faces1 = s1.getSequenceFromMask(mask=('[#2 ]', ), )
region = a.Surface(side1Faces=side1Faces1, name='Surf-31')

```



```

mdb.models['Model-'+str(i_count)].Pressure(name='Load-1',\
createStepName='Step-1', region=region, distributionType=TOTAL_FORCE,\
field='', magnitude=P_critical, amplitude=UNSET)

#-----#

#JOB
mdb.Job(name='Set-'+str(tu_ind)+str(td_ind)+str(tc_ind)+\
str(ramp_angle_ind)+str(E33_ind)+'_UL_'+\
str(doubler_span), model='Model-'+str(i_count), description='', \
type=ANALYSIS,atTime=None, waitMinutes=0, waitHours=0,\
queue=None, memory=90, memoryUnits=PERCENTAGE, \
getMemoryFromAnalysis=True, explicitPrecision=SINGLE, \
nodalOutputPrecision=SINGLE, echoPrint=OFF, modelPrint=OFF,\
contactPrint=OFF, historyPrint=OFF, userSubroutine='',\
scratch='', resultsFormat=ODB, multiprocessingMode=DEFAULT,\
numCpus=4,numDomains=4, numGPUs=0)

mdb.jobs['Set-'+str(tu_ind)+str(td_ind)+str(tc_ind)\
+str(ramp_angle_ind)+str(E33_ind)+'_UL_'+str(doubler_span)].submit()

mdb.jobs['Set-'+str(tu_ind)+str(td_ind)+str(tc_ind)\
+str(ramp_angle_ind)+str(E33_ind)+'_UL_'+str(doubler_span)].\
waitForCompletion()

#-----#

#READ FIELD OUTPUT

from odbAccess import *

o1 = session.openOdb(name='C:\Temp\Set-'+str(tu_ind)+\
str(td_ind)+str(tc_ind)+str(ramp_angle_ind)+str(E33_ind)+\
'_UL_'+str(doubler_span)+'.odb')
session.viewports['Viewport: 1'].setValues(displayedObject=o1)

odb = session.odbs['C:\Temp\Set-'+str(tu_ind)+str(td_ind)+str(tc_ind)\
+str(ramp_angle_ind)+str(E33_ind)+'_UL_'+str(doubler_span)+'.odb']
lastFrame = odb.steps['Step-1'].frames[-1]
session.fieldReportOptions.setValues(printXYData=OFF, printMinMax=ON)
session.writeFieldReport(fileName='CORE_S33'+str(tu_ind)+\
str(td_ind)+str(tc_ind)+str(ramp_angle_ind)+\
str(E33_ind)+'_UL_'+str(doubler_span)+'.rpt', append=ON,\
sortItem='Element Label', odb=odb, step=0, frame=lastFrame,
outputPosition=INTEGRATION_POINT, variable=((('S',\
INTEGRATION_POINT, ((COMPONENT, 'S33'), )), ))

core_S33_lines_UL = []

filepath = 'CORE_S33'+str(tu_ind)+str(td_ind)+str(tc_ind)\
+str(ramp_angle_ind)+str(E33_ind)+'_UL_'+str(doubler_span)+'.rpt'
with open(filepath) as fp:
    line = fp.readline()
    cnt = 1
    while line:
        core_S33_lines_UL.append("Line {}: {}".format(cnt, line.strip()))
        line = fp.readline()
        cnt += 1

wo_space = core_S33_lines_UL[23].replace(" ", "")
onlynumber = wo_space.replace("Line24:Maximum", "")
S33_core_UL = float(onlynumber)
parameterstore.write("Doubler Span %d\r\n" % (doubler_span))
parameterstore.write("Core Stress %d\r\n" % (S33_core_UL))
parameterstore.close()
doubler_span=doubler_span+5
i_count = i_count+1
mdb.Model(name='Model-'+str(i_count), modelType=STANDARD_EXPLICIT)

```

```
mdb.saveAs(pathName='C:/Temp/'+ 'Set-'+str(tu_ind)+str(td_ind)+str(tc_ind)\
+str(ramp_angle_ind)+str(E33_ind)+'_UL')

modelindex = 1
while modelindex<i_count:
    del mdb.models['Model-'+str(modelindex)]
    modelindex = modelindex
```